REPORT No. 119

THE PRESSURE DISTRIBUTION OVER THE HORIZONTAL TAIL SURFACES OF AN AIRPLANE—II

NATIONAL ADVISORY COMMITTEE
FOR AERONAUTICS

WASHINGTON
GOVERNMENT PRINTING OFFICE
1921

REPORT No. 119

THE PRESSURE DISTRIBUTION OVER THE HORIZONTAL TAIL SURFACES OF AN AIRPLANE—II

By F. H. NORTON and D. L. BACON
Langley Memorial Aeronautical Laboratory
Langley Field, Va.

59752—21——1

ADDITIONAL COPIES

OF THIS PUBLICATION MAY BE PROCURED FROM
THE SUPERINTENDENT OF DOCUMENTS
GOVERNMENT PRINTING OFFICE
WASHINGTON, D. C.
AT

10 CENTS PER COPY

REPORT No. 119.

THE PRESSURE DISTRIBUTION OVER THE HORIZONTAL TAIL SURFACES OF AN AIRPLANE—II.

By F. H. Norton and D. L. Bacon.

SUMMARY.

This investigation was undertaken by the aerodynamic staff of the National Advisory Committee for Aeronautics at Langley Field in order to determine whether the results obtained upon model tail surfaces can be used to accurately predict loads upon the full-sized tail; and also to find the distribution of load when large elevator angles are used, as the loads from such angles can not be obtained readily in free flight. The method consisted in using a metal horizontal tail surface inside of which small air passages, connecting with a series of holes in the surface, led the pressure off from the tail in rubber tubes. In this way the pressure at each of these holes was measured by a manometer at several angles of attack and several elevator settings. The results show that the model tests give a loading which is equivalent to the loading under similar conditions in the full-sized airplane and that the manner of distribution is quite similar in the two cases when there is no slip stream.

INTRODUCTION.

The only work which has previously been done on the pressure distribution on model tail surfaces is given in the first two references below, the remaining references applying only to the forces on model tails. The scope of the present investigation comprises the determination of the distribution of the pressure over two separate tail planes, models of the tail planes used in National Advisory Committee for Aeronautics Report No. 118. The tail planes were tested on a fifteenth scale model of the JN4H, and runs were made at various angles of attack and elevator angles to cover all conditions that might occur in flight.

References:

"The Distribution of Pressure Over a Tail Plane." Bulletin of the Airplane Engineering Division, December, 1919.

"Experiments on the Effect of Altering the Position of the Hinges of the Elevators for the B.E.2C Aeroplane." British Advisory R. & M. No. 254.

"Pressure Distribution Over the Tail Plane of B2C, Part I," R. & M. No. 661.

"Flossendruckmessungen." Technische Berichte, vol. 1, No. 6, October, 1917.

"Systematishe Versuche an Leitwerkmodellen." Technische Berichte, vol. 1, No. 5, August, 1917.

APPARATUS AND METHODS.

A model was constructed in the usual manner with aluminum wings and wooden fuselage, the scale being one-fifteenth in order to make the size of the tail plane sufficient to allow large air passages. This model was supported in the center of the tunnel on a spindle from the N. P. L. balance so that it could be easily rotated to any angle of attack. As the forces on the model were considerable, the upper wing tip was firmly supported by three wires running to the side of the tunnel, but still allowing free rotation.

The tail planes, figures 1 and 2, were made of brass by Mr. Carl Selig, instrument maker at the Massachusetts Institute of Technology. The sections were one-fifteenth that given for the tail surfaces in Part I within 0.003 inch. Figure 3 shows their method of construction, which consisted of soldering together two plates which had already been grooved for the air passages. In order to prevent this solder from closing up the air passages aluminum wires were placed in them during the soldering. This soldering was so well done that there was

no leakage between the adjacent passages in any case. In order to save time it was desired to take a number of readings simultaneously, so that a separate connection was made to each air passage by means of fine rubber tubes about 1 millimeter in diameter leading to the multiple manometer as shown in figure 4.

The multiple manometer used for reading the pressures in this investigation is shown in figure 5 and consists simply of a reservoir of large area which is adjustable vertically, and a series of inclined tubes each having its corresponding scale. The two outside tubes are connected back to the reservoir so that they will read at all times the level in it, thus giving a pair of zero readings with which to compare the various heads.

When ready to make a test all of the holes in the tail plane were covered by strips of tissue paper which had been coated with paraffin. These strips of paper were applied over each row of holes with a hot iron, making a very smooth and tight joint without danger of plugging the air passages, a trouble that was encountered in previous tests. The whole system was then tested out for tightness by applying a small pressure to the reservoir in the gauge, and if this pressure was held it was proof that there were no leaks. After this test the strip of paper was removed from a single row of holes and the tunnel was run at a steady speed of 40 miles per hour. The pressures on the tail were compared with the static pressure in the tunnel by connecting a static head, which was placed near the model in the tunnel, to the reservoir of the manometer.

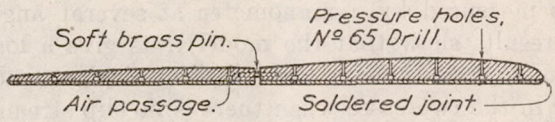

Fig.3. METHOD OF CONSTRUCTING TAIL SURFACES.

The readings of pressure obtained were converted into vertical inches of water, and the plotting of the results carried out in exactly the same way as for Part I, excepting that the scale in this case was somewhat increased because the pressures read were considerably smaller than those obtained on the full-sized tail plane. It was not thought worth while to determine the position of the center of pressure on the model tail plane, as it was easier to find the moment about the center of gravity of the machine mechanically than it was to find it by the integrated pressures.

PRECISION OF RESULTS.

The heads of water as computed may be considered precise to 0.005 of an inch and the areas measured with a precision of 0.01 of a square inch, which is the same as for the full-flight tests. These model tests, however, do not have the errors which were inevitable in the full-flight tests due to varying atmospheric conditions, so that the evenness of the results from the model tests may be considered quite superior to those obtained in free flight, and this is evident by the smoothness and regularity of the load curves.

SCOPE OF THE TESTS.

Two horizontal tail surfaces were used in this investigation, being one-fifteenth scale models of those used in Part I. Each tail was tested at the following angles of attack of the tail plane of the airplane: $-2°$, $4°$, $10°$, $16°$, $20°$. At each angle of attack the elevator was placed at $-15°$, $-5°$, $0°$, $+5°$, $+15°$, $+25°$, all in respect to the tail plane. It should be noted that in this report a positive elevator angle is taken when the trailing edge is pulled up. In order to determine the effect on the model of closing the crack between the elevator and tail plane the pressure distribution was taken along one row of holes. In the same way the effect of giving the tail plane a more positive angle of $2°$ was determined.

DISCUSSION OF RESULTS.

In figures 6 to 65 are shown the distribution of pressure over the two tail planes under various conditions of angle of attack and elevator setting. The most prominent characteristic evident on the JN4H tail is the region of marked down load at the outer leading edge for small angles of

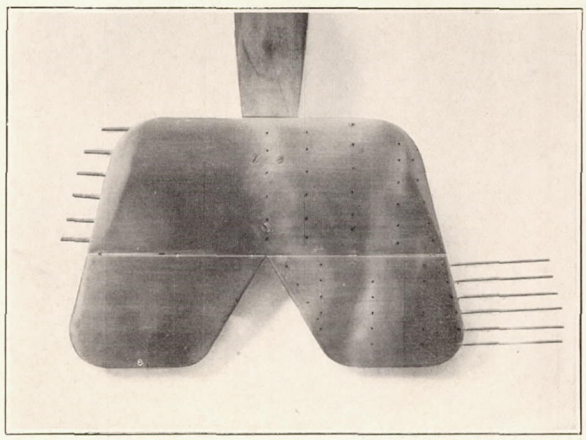

FIG. 1.—MODEL OF JN4H TAIL SURFACE.

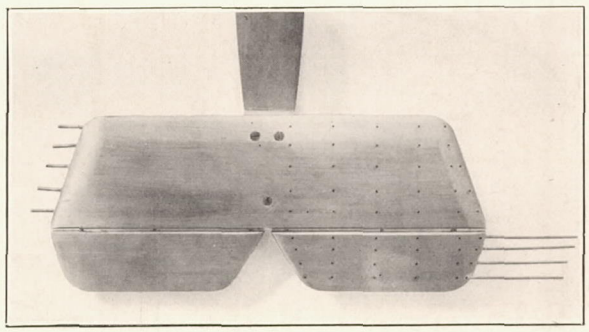

FIG. 2.—MODEL OF SPECIAL TAIL SURFACE.

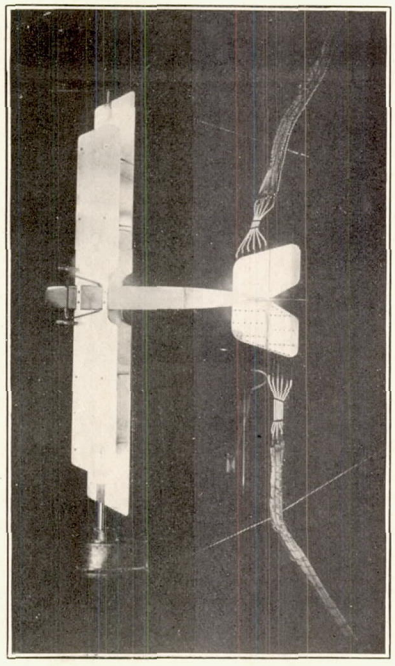

FIG. 4.—PRESSURE DISTRIBUTION MODEL SET UP IN THE TUNNEL.

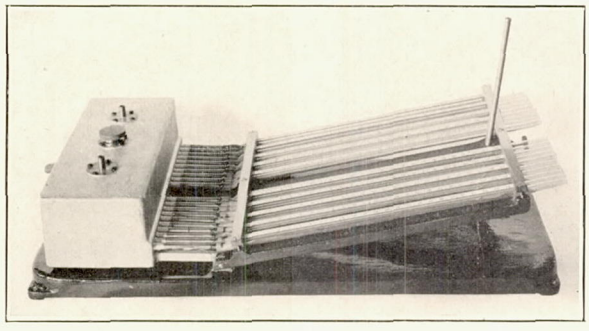

FIG. 5.—MULTIPLE MANOMETER FOR MEASURING PRESSURES ON THE TAIL.

attack and especially when the elevator is pulled up, a region of down load at the outer edge of the elevator due to the positive rake of that member. On the other hand, when the elevator is pulled down there is a sharp up load at the outer edge of the whole tail plane. In contrast to this, the special tail plane does not show a very high loading at the outer tip and the general distribution is more even along the span.

Turning now to figures 66 to 77, which show the load on the tail in cubic inches of water along the chord, it is seen that there are two distinct regions of high load, the first region being at the leading edge and the second just behind the hinge. It will be seen that the region at the leading edge varies mainly with the angle of attack while the region on the elevator varies mainly with the elevator setting, although each one is slightly affected by the other. The region of high loading on the elevator is much more concentrated and pronounced on the special tail plane than it is on the other.

By making the assumption that an airplane will retain its velocity for an instant after pulling up the elevator sharply, we may compute the loads that will arise on the full-scale tail plane in accelerated flight. For example, from figure 81 the load on the model tail at 0° attack and 0° elevator is 1 cubic inch. As this corresponds to 100 miles per hour full scale, the load on the tail will be 51 pounds, or about 1 pound per square foot, which checks very well with the value actually obtained in full flight of 0.97 pound. If the elevator is pulled up to 25° while the same speed is maintained the load, from the model curves, is increased nine times or to 459 pounds, which gives a loading of 9 pounds per square foot. The load encountered here is not large, even for the severity of the conditions, and it is interesting to compare it with the load factor of 5.5 for the wings as determined under identical conditions.[1]

A run was made on the JN4H horizontal tail surface with the crack between the elevator and tail plane closed up with wax, and another run was made on the same tail surface with the tail plane angle changed by 2°. As these changes, however, made no appreciable effect upon the distribution of pressure it was not thought worth while to include the curves of the results.

STABILIZING AND CONTROLLING PROPERTIES OF THE TAIL SURFACES.

In figures 78 and 79 there are plotted the loads on the tail plane of the two tail surfaces for various angles of attack and for various elevator settings. An evident fact is that the force on the special tail plane when the elevator is set at +5° crosses the curve for zero elevator at high angles and the force with the elevator down −5° is also very close to the force when the elevator is at zero. This all confirms what has been found in full flight, that the controlling effect of this tail surface is very poor. This is probably due to the fact that the tail is so thick and the elevator so small that a small movement of the elevator does not influence the flow passing over the forward tail plane surfaces. This leads to the conclusion that a tail should not be made of such a thick section, although more tests should be made before this statement can be considered conclusive.

In figure 80 there is plotted the force on the elevator alone for various angles of attack and elevator settings. It is evident that the force on the special tail surface varies slightly with the angle of attack; the force, however, seems to be almost exactly proportional to the angle of the elevator. On the JN4H tail, however, the force changes quite markedly with the angle of attack and changes even more than for the special tail when the elevator angle is changed.

In figures 81 and 82 there are plotted the curves for the total load on the tail surface, which is simply the summation of the previous curves. It will be noted that the slope of the curves for the special tail is considerably greater than for the JN4H tail, the former giving, as would be expected from its greater aspect ratio, about 13 per cent greater force than the other for a given change in angle of attack. A change in angle of attack of the whole surface of 1° has about the same effect on the total loading as a change of 1½° of the elevator.

In figure 83 there are plotted the pitching moments of the complete airplane for each tail plane and also for the wing cell, and the wing cell plus the fuselage and landing gear. All of these moments were taken about a center of gravity position which was 38 per cent back on the

[1] Accelerations in Flight. N. A. C. A. Report No. 99.

mean chord, which is about the standard position for the full-sized airplane. It will be seen that the moment curves for the wing cell alone are unstable up to about 16°, beyond which they are stable, which is typical of a biplane of this type. The curve of moments for the wing cell with the fuselage and chassis attached lies remarkably close to that of the wing cell alone, showing that these members have an inappreciable effect on the total moment of the airplane. Turning to the moment curves for the complete airplane it at first seems rather surprising that they all show a region of instability at angles lower than 4°. If it is remembered, however, that the models were tested under conditions of locked controls, it will be seen that the stability is almost identical with the full-flight tests. This brings up the question of why an airlpane is more stable with free than with locked controls under certain conditions. This does not seem reasonable, as in the latter case the effective tail area is much greater. A possible explanation is that the weight of the elevator itself changes the configuration of the tail-plane section. At any rate, all wind-tunnel models should be tested with both free and locked elevators, the free elevators having a weight proportional to the full-scale ones.

It was found by the British [2] in model and free-flight tests on elevators that the efficiency of the latter was greatly increased by the use of a negative rake. The reason for this, which was not clear at that time, is shown by a study of the pressure distribution on the two tails. The JN4H tail (positive rake) shows a very high loading along its outer edge due to its action as a leading edge. The other tail, however, with a negative rake shows that this load is transferred to the tail plaine, so for a given controlling effect there is much less load on the movable portion.

COMPARISON OF FULL-FLIGHT TESTS WITH MODEL TESTS.

The principal reason for conducting these model tests was to determine whether the loads on the full-sized tail plane could be accurately predicted from the results obtained on the model. Unfortunately, however, there are few cases where a direct comparison may be made. First, because of the slip stream on the full-sized airplane, and, second, because the elevator angle is not known to better than 1° at high speeds, and perhaps not better than 3° at the very low speeds on the full-sized airplane. In figures 84 and 85 there are plotted for comparison the model and full-flight tests to equivalent scales; that is, the model tests have been multiplied by the ratio of the speeds squared. These conditions were chosen because there was no slip stream in the free-flight case. A careful examination of these figures will show that the agreement between the two cases is quite disappointing. While the tendencies of the curves are the same in a great many cases it is quite evident that the assymetry of the full-flight tests even when there is no appreciable slip stream is quite large. The lack of agreement of the pressures on the elevator may be due to the fact that the elevator setting was not exactly the same in both cases.

Probably a better comparison can be had between the model and full scale by comparing the total load, as has been done for the two tail planes in figure 86. The full-scale results were taken when there was no slip stream. The corresponding curves show a fairly good agreement except at low speeds with the JN4H tail, where the elevator was turned to a large angle. The discrepancies that do occur can readily be accounted for by the lack of agreement between the elevator setting in corresponding cases. As the normal movement of the elevator in flight is only a few degrees, an error of one degree will greatly affect the loading.

CONCLUSIONS.

Within the error of comparison, the model tests will give the tail load experienced on the full-sized airplane in steady flight and without slip stream. The stability of the model compares closely with that of the full-sized airplane if care is taken to make the conditions identical. The results emphasize the desirability of using a tail surface of high aspect ratio, of not too thick a section, and with negatively raked tips. If the comparison is assumed to hold good between model and full size for accelerated flight, the tail load on a JN4H with standard tail would amount to 9 pounds per square foot when suddenly pulling out of a 100 mile per hour dive.

[2] British Advisory Committee. R. & M. 409, T. 825, T. 1115.

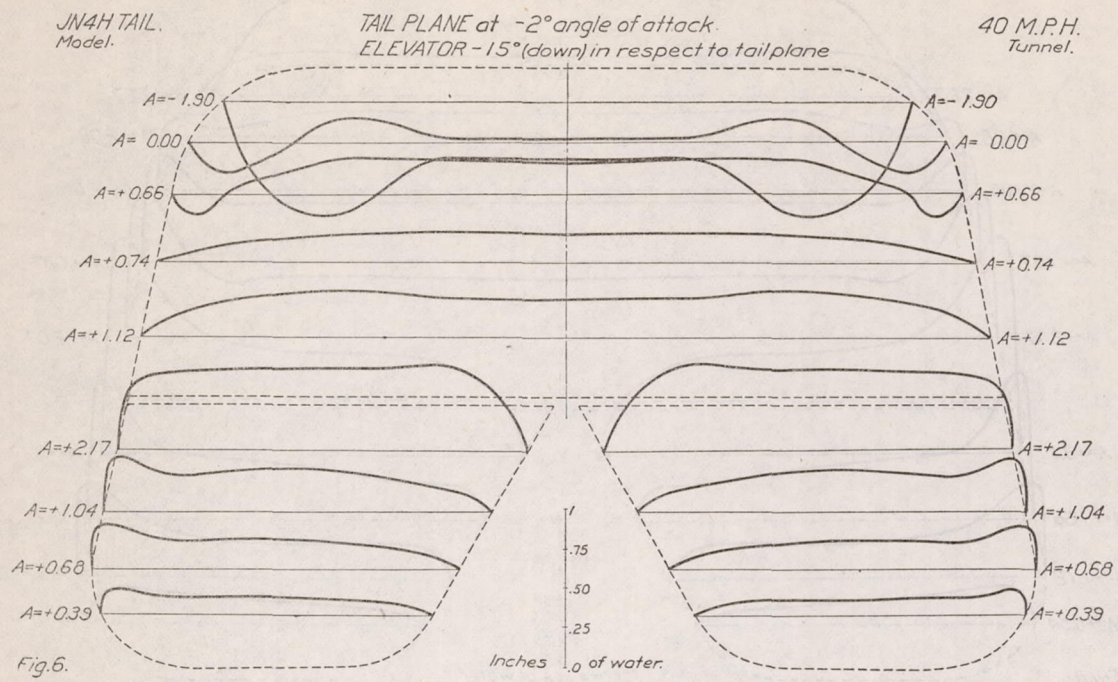
JN4H TAIL.
Model.
TAIL PLANE at -2° angle of attack.
ELEVATOR - 15° (down) in respect to tail plane
40 M.P.H.
Tunnel.
A=- 1.90
A= 0.00
A=+0.66
A=+0.74
A=+1.12
A=+2.17
A=+1.04
A=+0.68
A=+0.39
1
.75
.50
.25
.0
Inches of water.

Fig. 6.

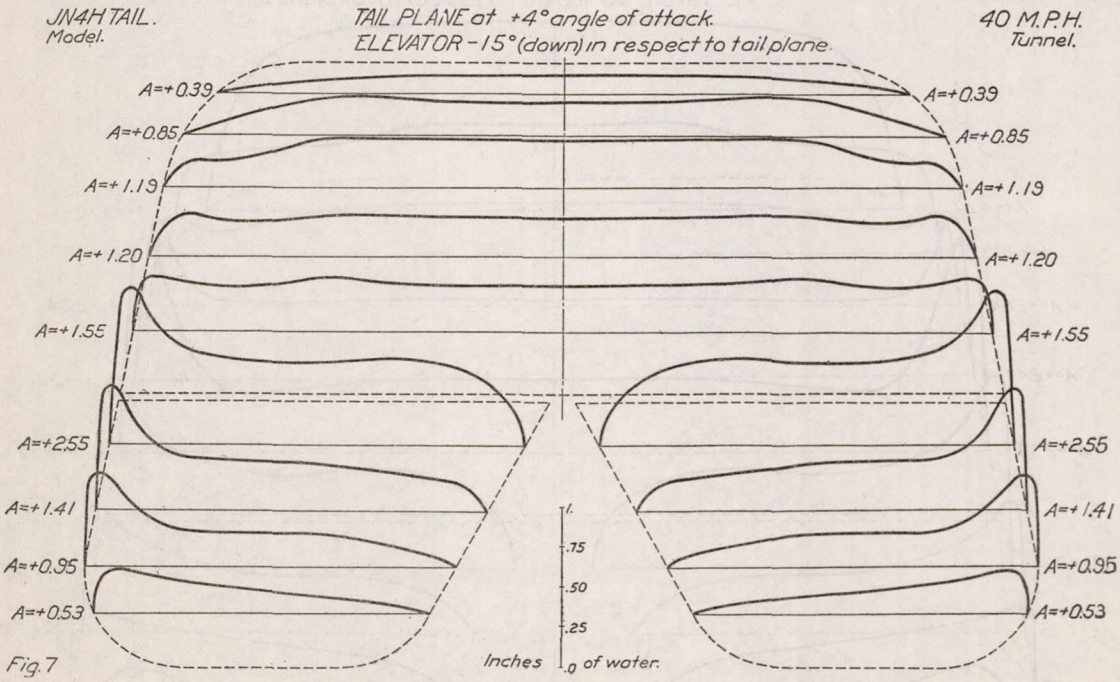
JN4H TAIL.
Model.
TAIL PLANE at +4° angle of attack.
ELEVATOR - 15° (down) in respect to tail plane.
40 M.P.H.
Tunnel.
A=+0.39
A=+0.85
A=+1.19
A=+1.20
A=+1.55
A=+2.55
A=+1.41
A=+0.95
A=+0.53
1
.75
.50
.25
.0
Inches of water.

Fig. 7

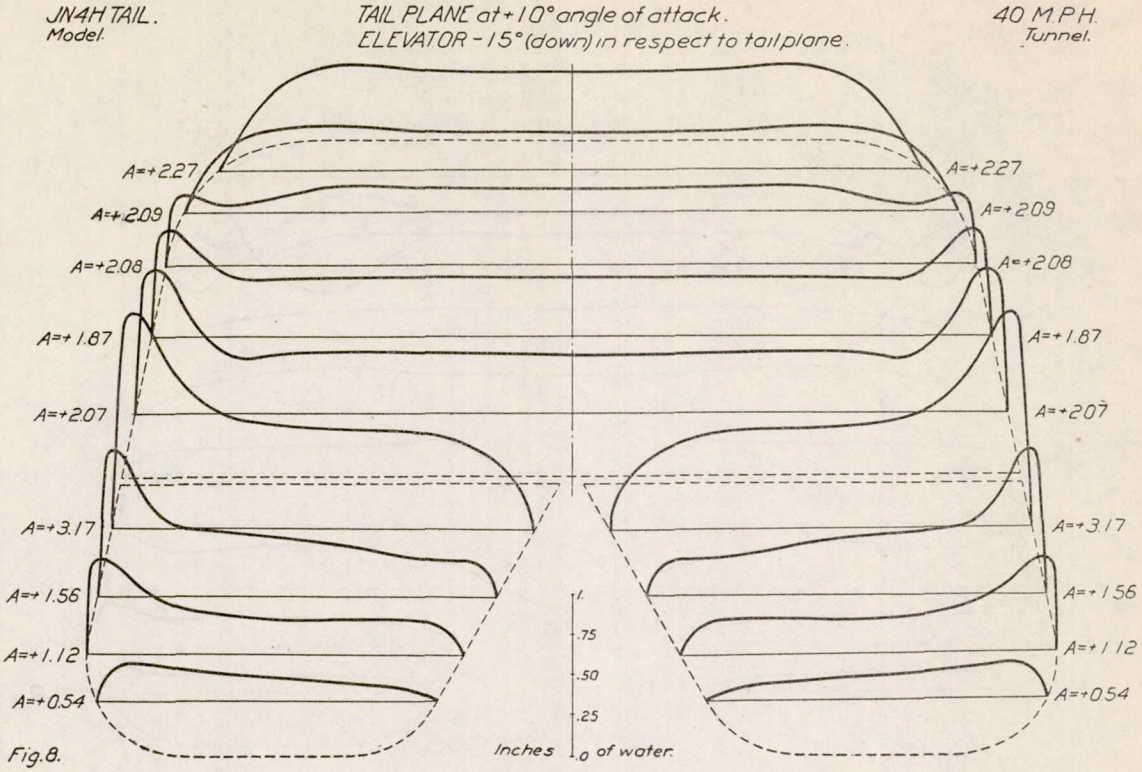
JN4H TAIL.
Model.
TAIL PLANE at +10° angle of attack.
ELEVATOR - 15° (down) in respect to tail plane.
40 M.P.H.
Tunnel.
A=+2.27
A=+2.09
A=+2.08
A=+1.87
A=+2.07
A=+3.17
A=+1.56
A=+1.12
A=+0.54
1.
.75
.50
.25
0
Inches of water.

Fig. 8.

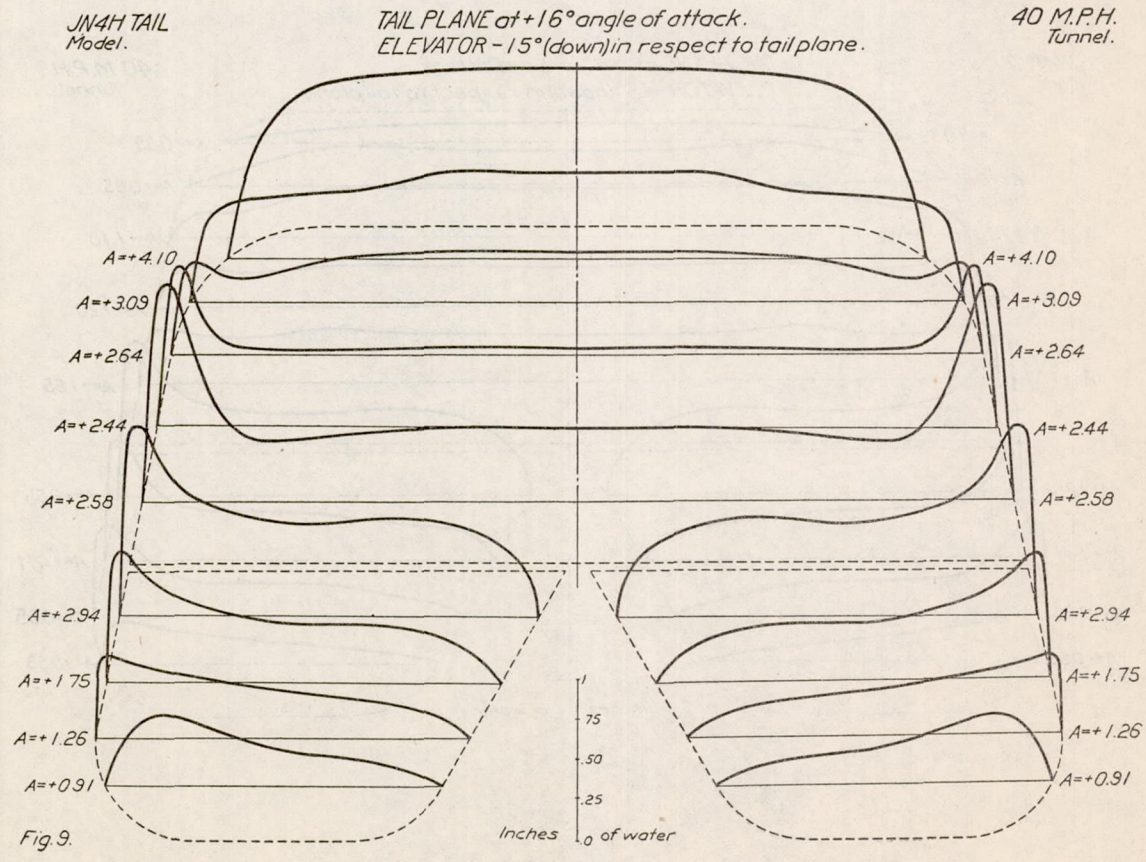
JN4H TAIL
Model.
TAIL PLANE at +16° angle of attack.
ELEVATOR - 15° (down) in respect to tail plane.
40 M.P.H.
Tunnel.
A=+4.10
A=+3.09
A=+2.64
A=+2.44
A=+2.58
A=+2.94
A=+1.75
A=+1.26
A=+0.91
1
.75
.50
.25
0
Inches of water

Fig. 9.

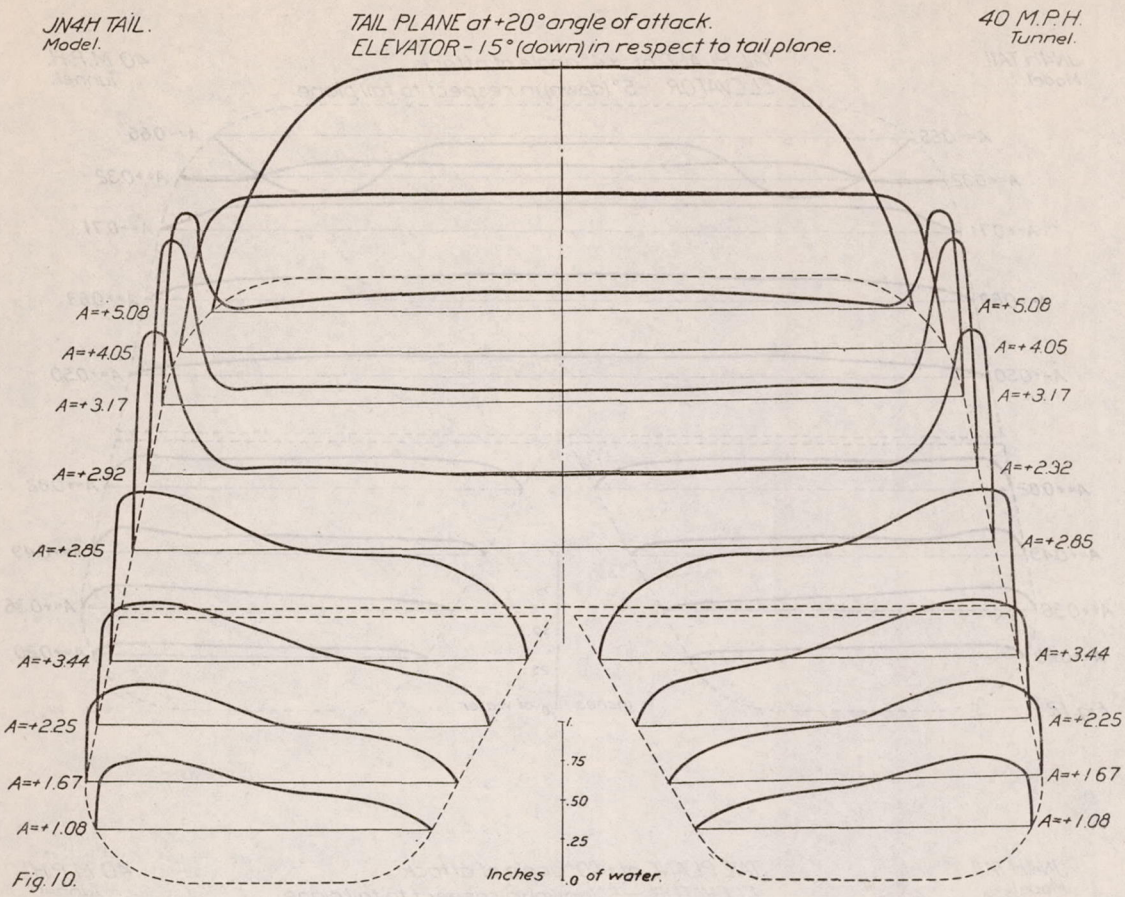
JN4H TAIL.
Model.
TAIL PLANE at +20° angle of attack.
ELEVATOR - 15° (down) in respect to tail plane.
40 M.P.H.
Tunnel.
A=+5.08
A=+4.05
A=+3.17
A=+2.92
A=+2.85
A=+3.44
A=+2.25
A=+1.67
A=+1.08
1.
.75
.50
.25
0
Inches of water.

Fig. 10.

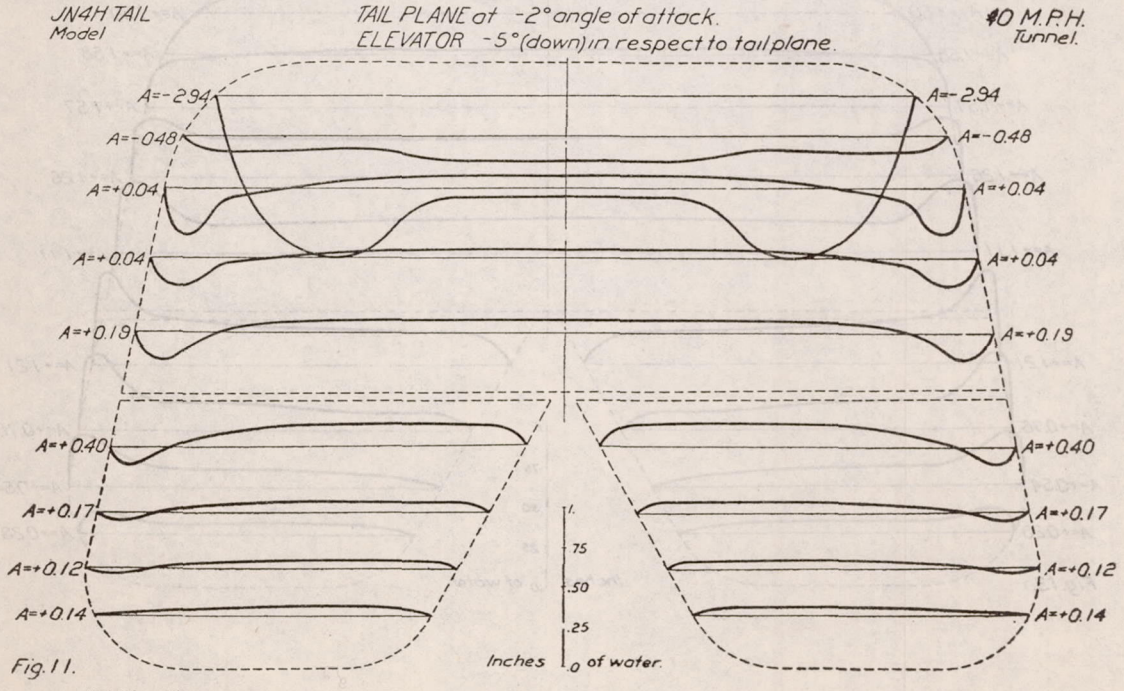
JN4H TAIL
Model
TAIL PLANE at -2° angle of attack.
ELEVATOR -5° (down) in respect to tail plane.
40 M.P.H.
Tunnel.
A=-2.94
A=-0.48
A=+0.04
A=+0.04
A=+0.19
A=+0.40
A=+0.17
A=+0.12
A=+0.14
1.
.75
.50
.25
0
Inches of water.

Fig. 11.

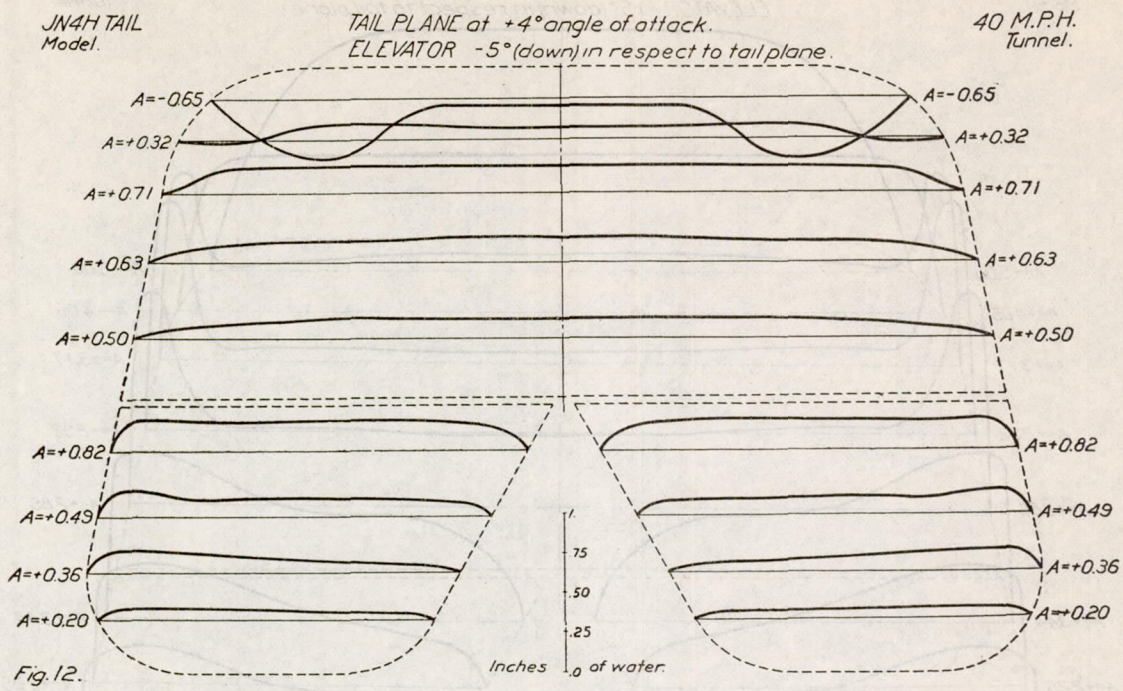
JN4H TAIL
Model.
TAIL PLANE at +4° angle of attack.
ELEVATOR -5° (down) in respect to tail plane.
40 M.P.H.
Tunnel.
A=-0.65
A=+0.32
A=+0.71
A=+0.63
A=+0.50
A=+0.82
A=+0.49
A=+0.36
A=+0.20
1.
.75
.50
.25
.0
Inches of water.

Fig. 12.

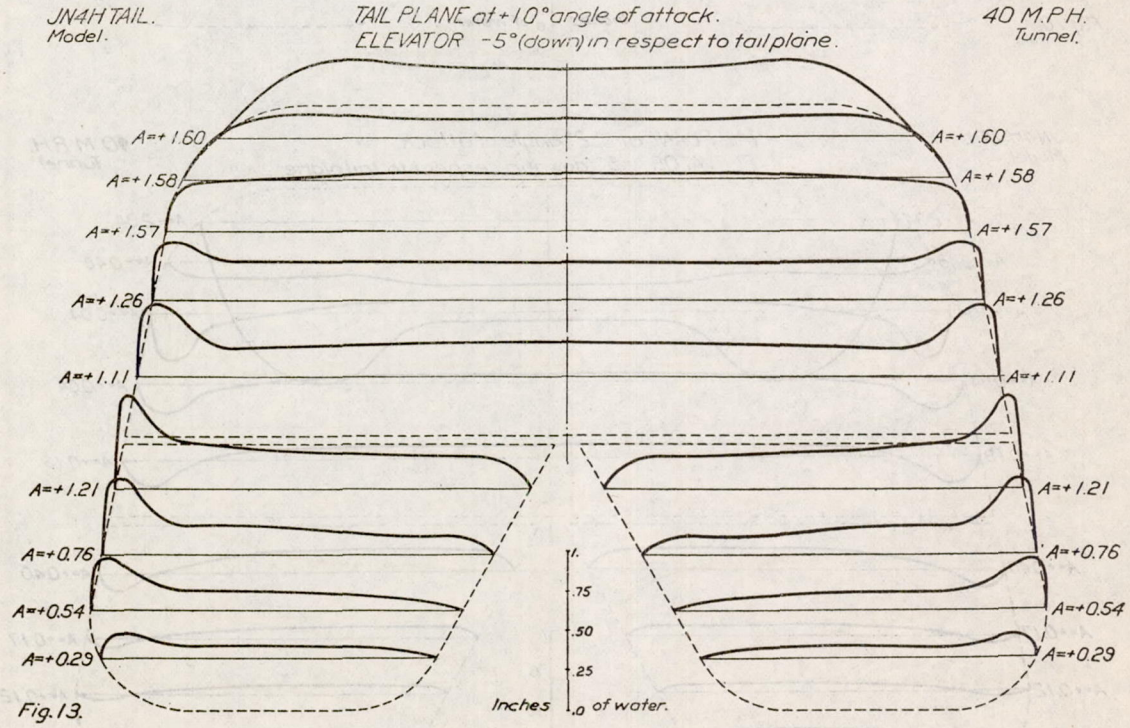
JN4H TAIL.
Model.
TAIL PLANE at +10° angle of attack.
ELEVATOR -5° (down) in respect to tail plane.
40 M.P.H.
Tunnel.
A=+1.60
A=+1.58
A=+1.57
A=+1.26
A=+1.11
A=+1.21
A=+0.76
A=+0.54
A=+0.29
1.
.75
.50
.25
.0
Inches of water.

Fig. 13.

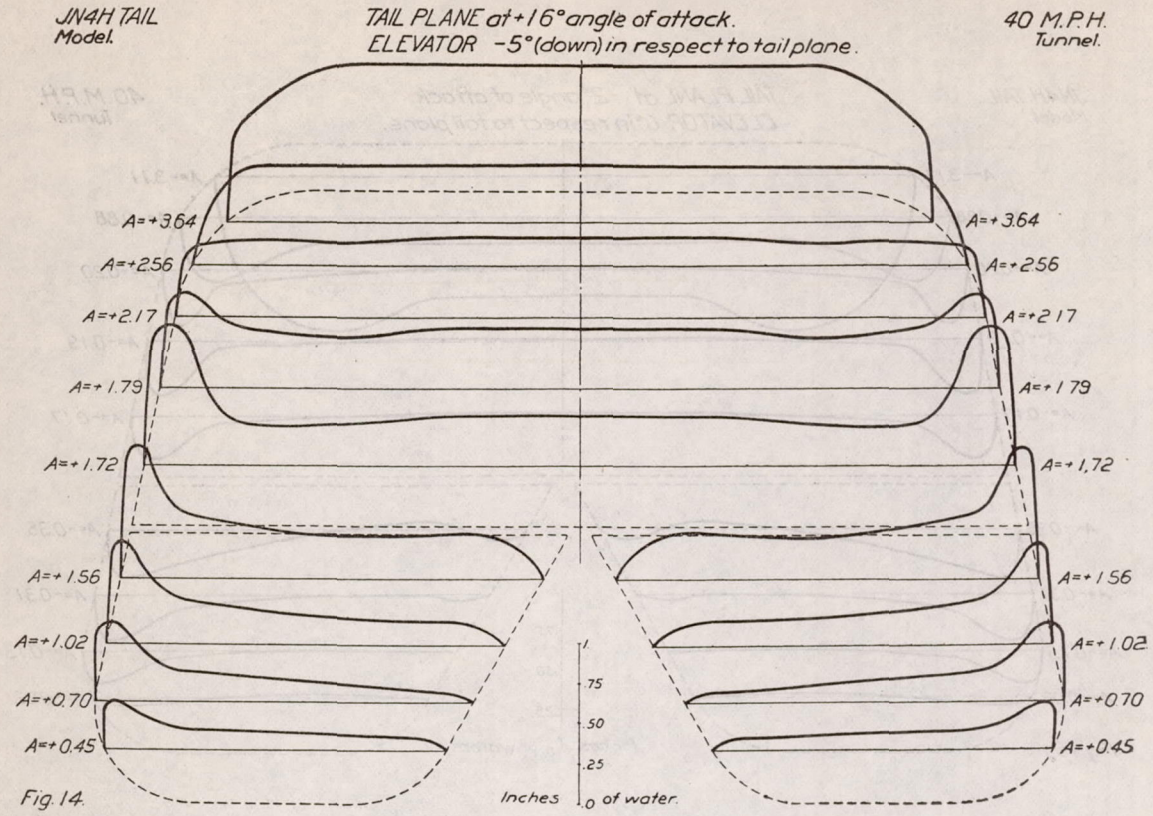
JN4H TAIL
Model.
TAIL PLANE at +16° angle of attack.
ELEVATOR -5° (down) in respect to tail plane.
40 M.P.H.
Tunnel.
A=+3.64
A=+2.56
A=+2.17
A=+1.79
A=+1.72
A=+1.56
A=+1.02
A=+0.70
A=+0.45
1
.75
.50
.25
0
Inches of water.

Fig. 14.

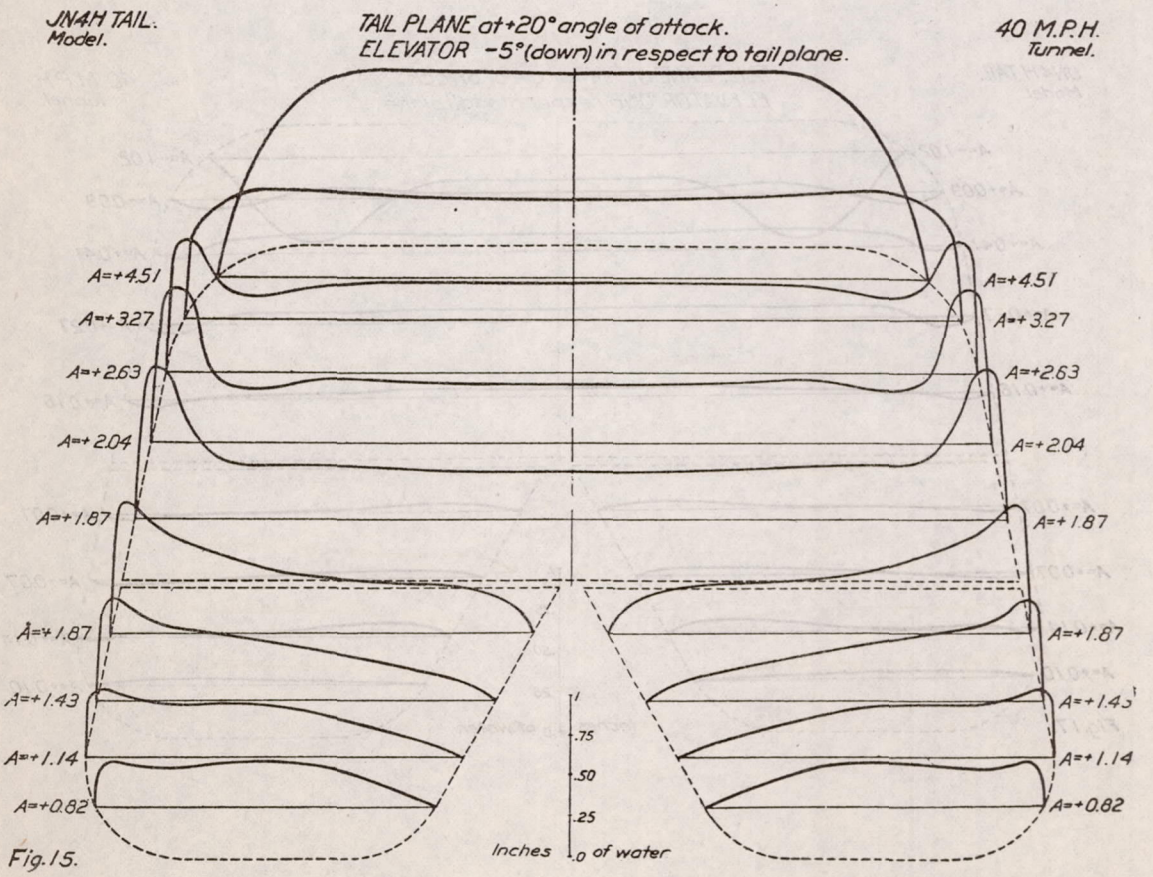
JN4H TAIL.
Model.
TAIL PLANE at +20° angle of attack.
ELEVATOR -5° (down) in respect to tail plane.
40 M.P.H.
Tunnel.
A=+4.51
A=+3.27
A=+2.63
A=+2.04
A=+1.87
A=+1.87
A=+1.43
A=+1.14
A=+0.82
1
.75
.50
.25
0
Inches of water.

Fig. 15.

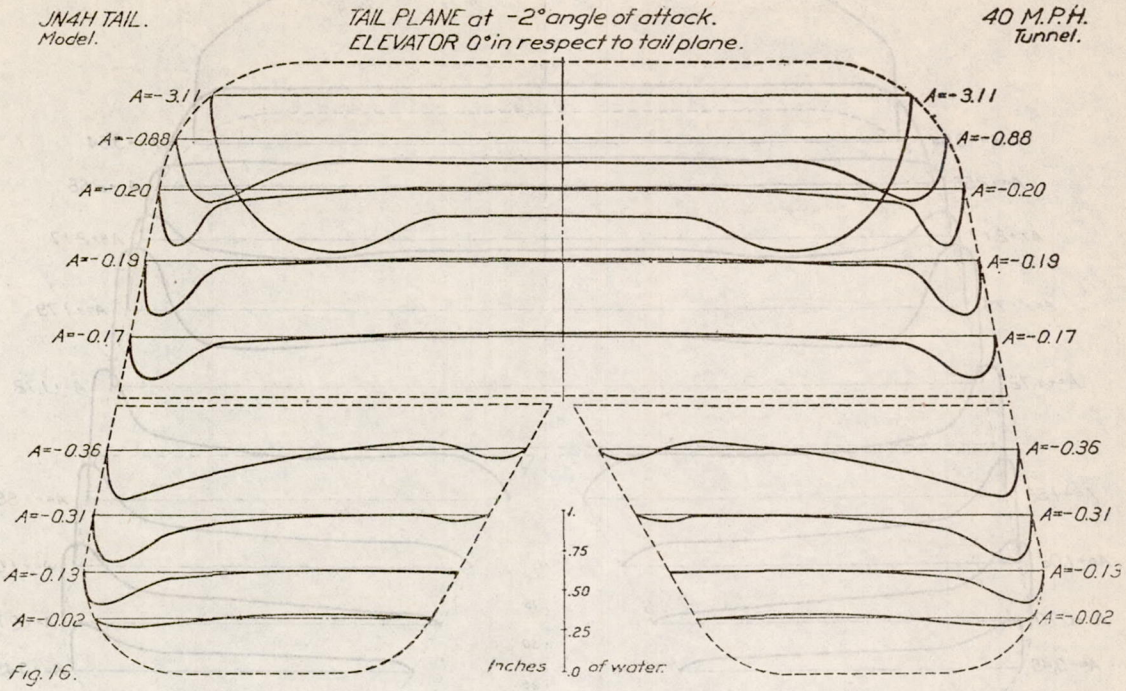
JN4H TAIL.
Model.
TAIL PLANE at -2° angle of attack.
ELEVATOR 0° in respect to tail plane.
40 M.P.H.
Tunnel.
A=-3.11
A=-0.88
A=-0.20
A=-0.19
A=-0.17
A=-0.36
A=-0.31
A=-0.13
A=-0.02
1.
.75
.50
.25
.0
Inches of water.

Fig. 16.

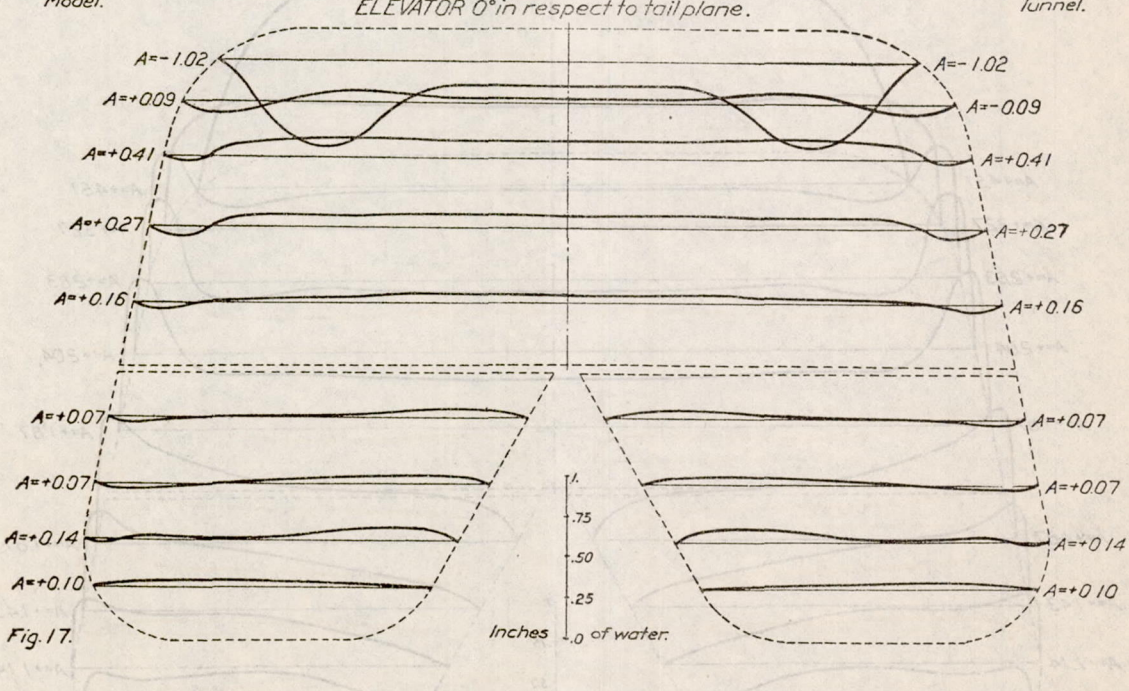
JN4H TAIL.
Model.
TAIL PLANE at +4° angle of attack.
ELEVATOR 0° in respect to tail plane.
40 M.P.H.
Tunnel.
A=-1.02
A=+0.09
A=+0.41
A=+0.27
A=+0.16
A=+0.07
A=+0.07
A=+0.14
A=+0.10
1.
.75
.50
.25
.0
Inches of water.

Fig. 17.

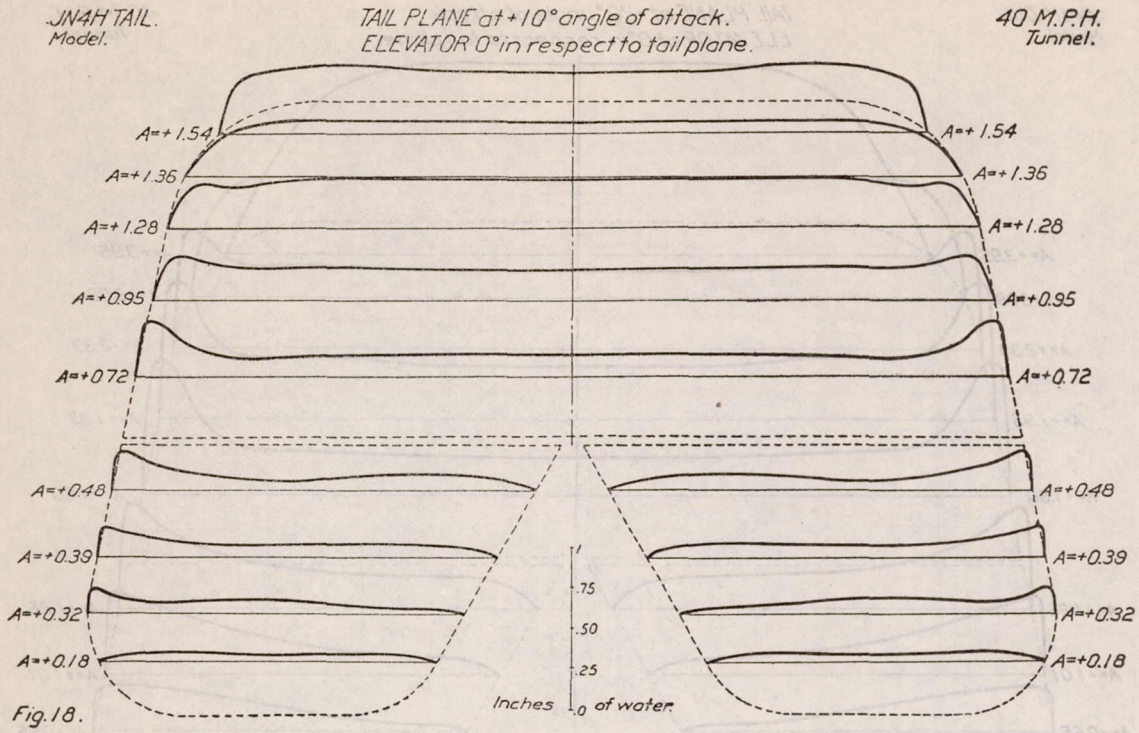
JN4H TAIL.
Model.
TAIL PLANE at +10° angle of attack.
ELEVATOR 0° in respect to tail plane.
40 M.P.H.
Tunnel.
A=+1.54
A=+1.36
A=+1.28
A=+0.95
A=+0.72
A=+0.48
A=+0.39
A=+0.32
A=+0.18
1
.75
.50
.25
0
Inches of water.

Fig. 18.

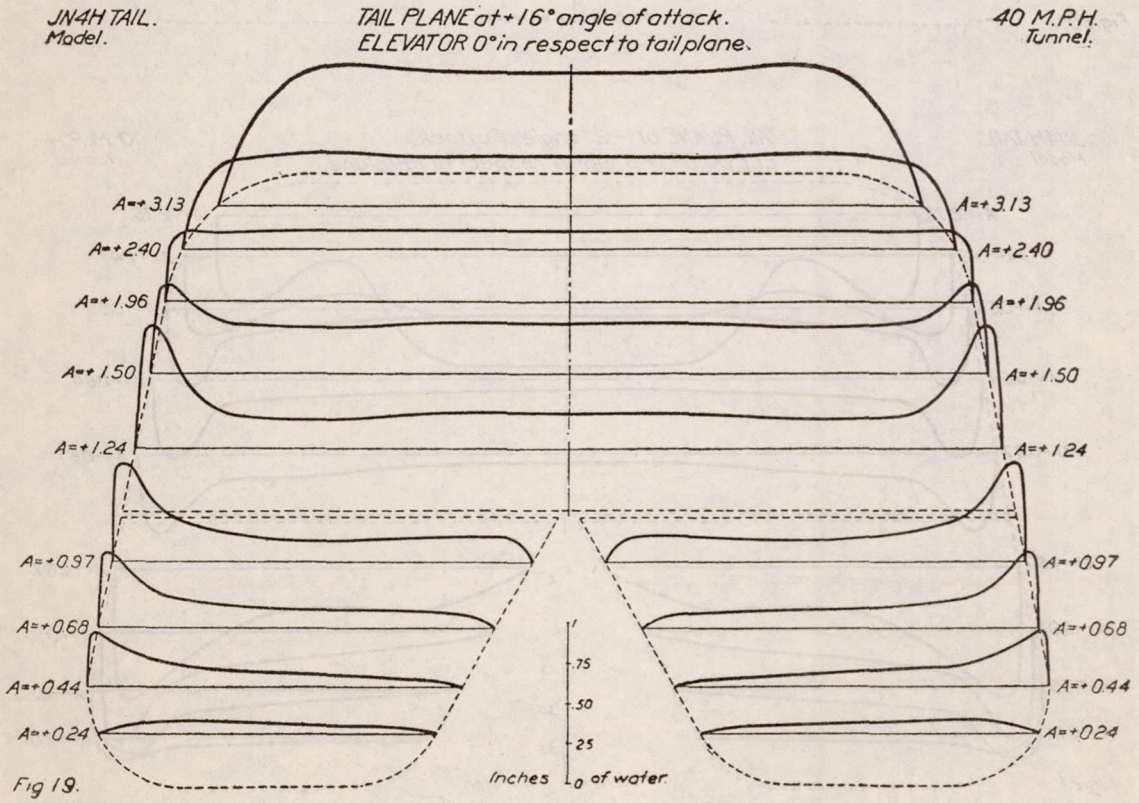
JN4H TAIL.
Model.
TAIL PLANE at +16° angle of attack.
ELEVATOR 0° in respect to tail plane.
40 M.P.H.
Tunnel.
A=+3.13
A=+2.40
A=+1.96
A=+1.50
A=+1.24
A=+0.97
A=+0.68
A=+0.44
A=+0.24
1
.75
.50
.25
0
Inches of water.

Fig 19.

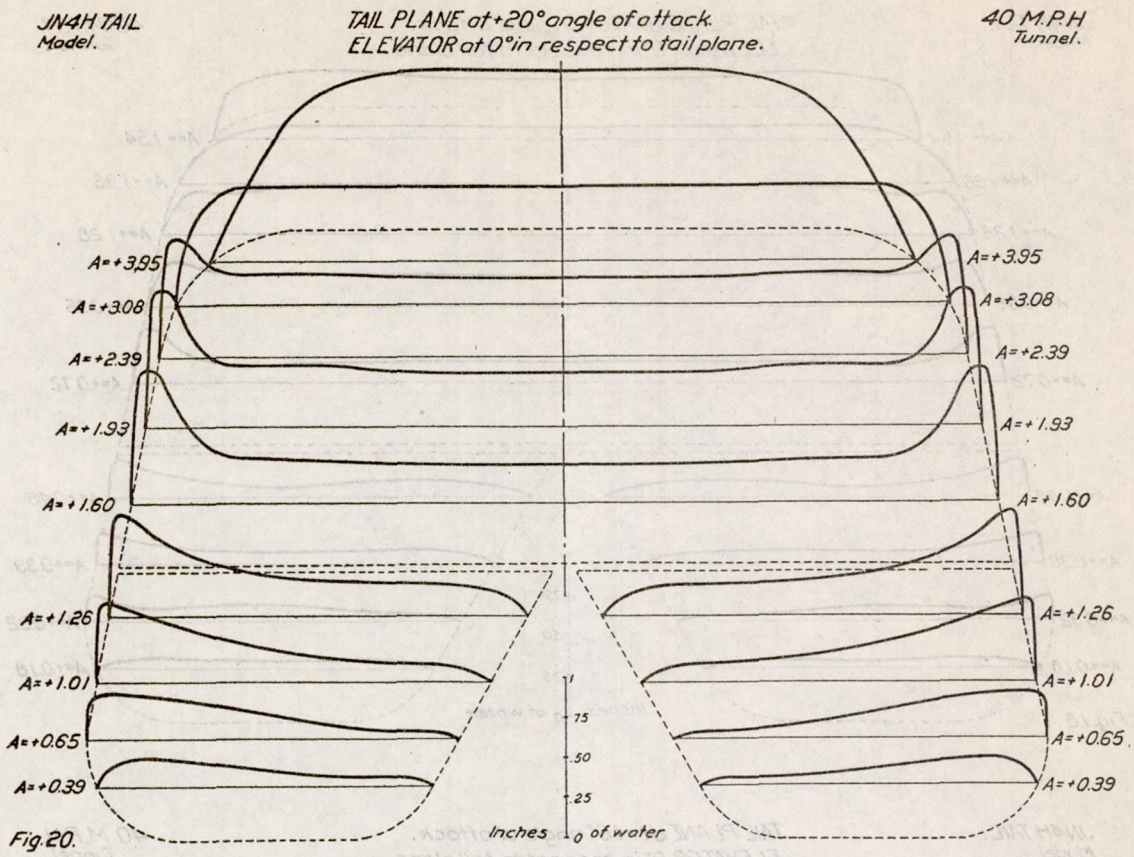
JN4H TAIL
Model.
TAIL PLANE at +20° angle of attack.
ELEVATOR at 0° in respect to tail plane.
40 M.P.H
Tunnel.
A=+3.95
A=+3.08
A=+2.39
A=+1.93
A=+1.60
A=+1.26
A=+1.01
A=+0.65
A=+0.39
1
.75
.50
.25
0
Inches of water.

Fig. 20.

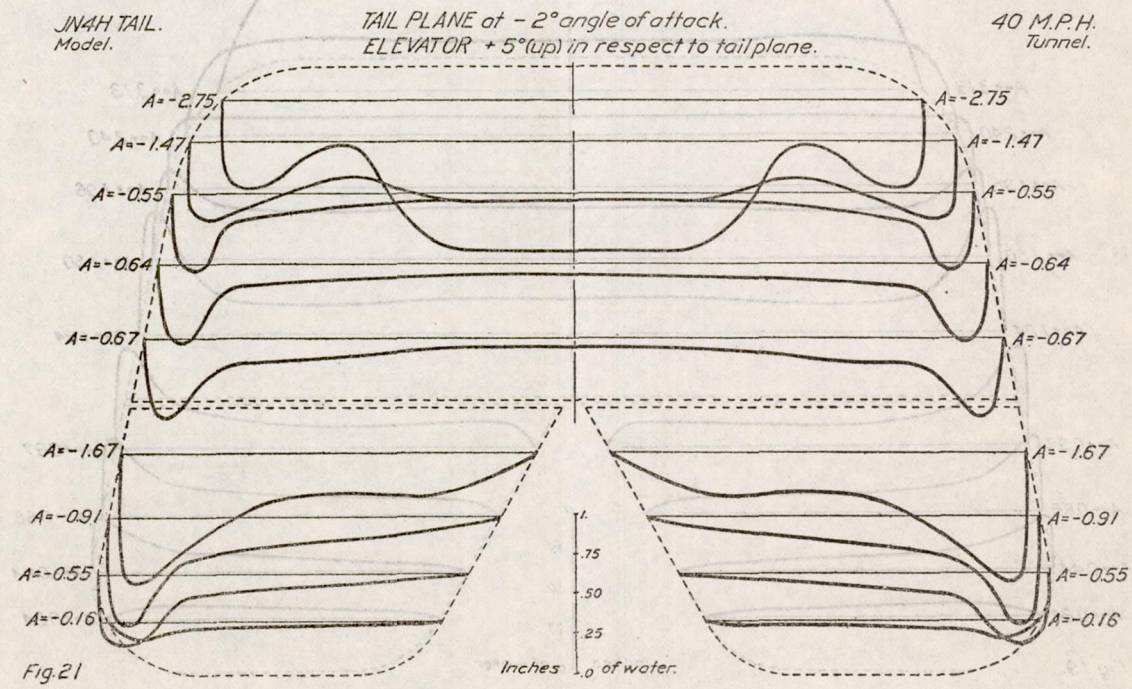
JN4H TAIL.
Model.
TAIL PLANE at −2° angle of attack.
ELEVATOR +5° (up) in respect to tail plane.
40 M.P.H.
Tunnel.
A=-2.75
A=-1.47
A=-0.55
A=-0.64
A=-0.67
A=-1.67
A=-0.91
A=-0.55
A=-0.16
1.
.75
.50
.25
.0
Inches of water.

Fig. 21

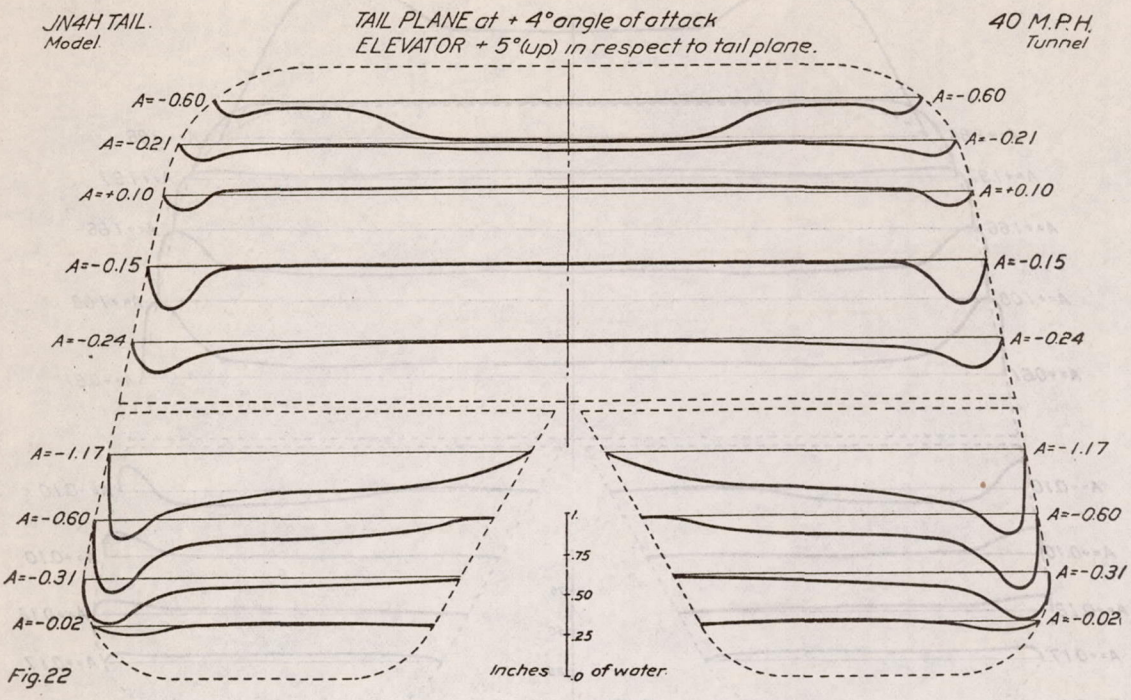
JN4H TAIL.
Model.
TAIL PLANE at + 4° angle of attack
ELEVATOR + 5° (up) in respect to tail plane.
40 M.P.H.
Tunnel
A=-0.60
A=-0.21
A=+0.10
A=-0.15
A=-0.24
A=-1.17
A=-0.60
A=-0.31
A=-0.02
1.
.75
.50
.25
0
Inches of water.

Fig. 22

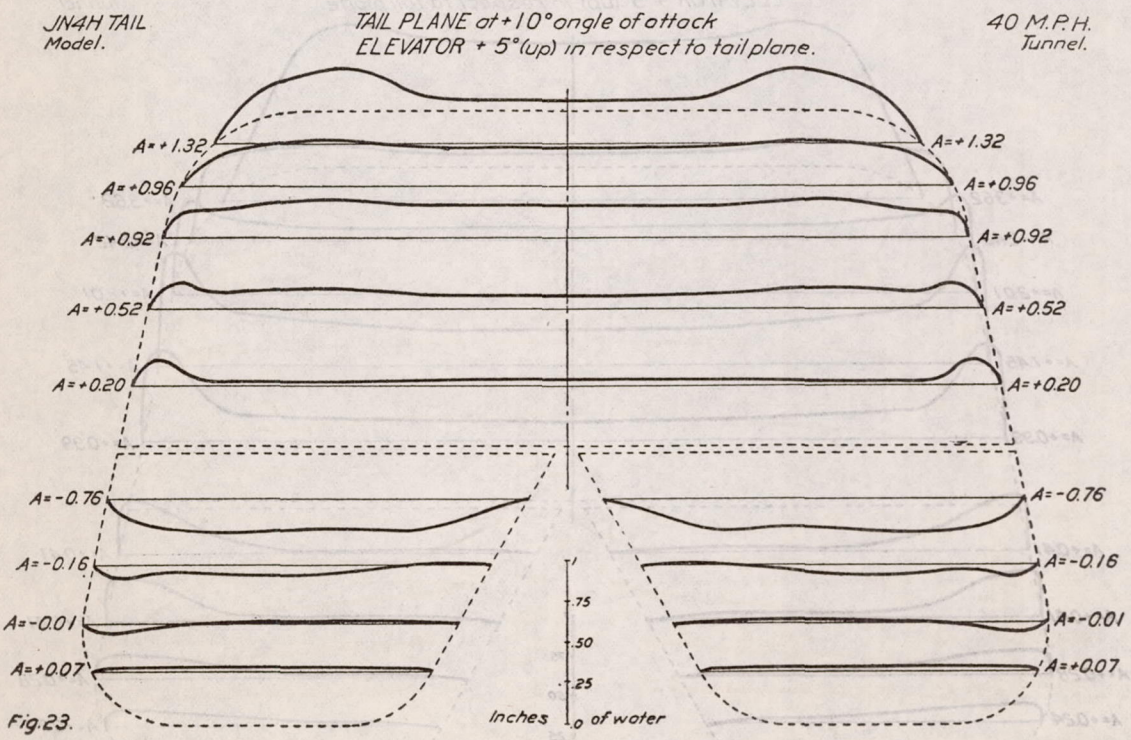
JN4H TAIL
Model.
TAIL PLANE at + 10° angle of attack
ELEVATOR + 5° (up) in respect to tail plane.
40 M.P.H.
Tunnel.
A=+1.32
A=+0.96
A=+0.92
A=+0.52
A=+0.20
A=-0.76
A=-0.16
A=-0.01
A=+0.07
1
.75
.50
.25
0
Inches of water

Fig. 23.

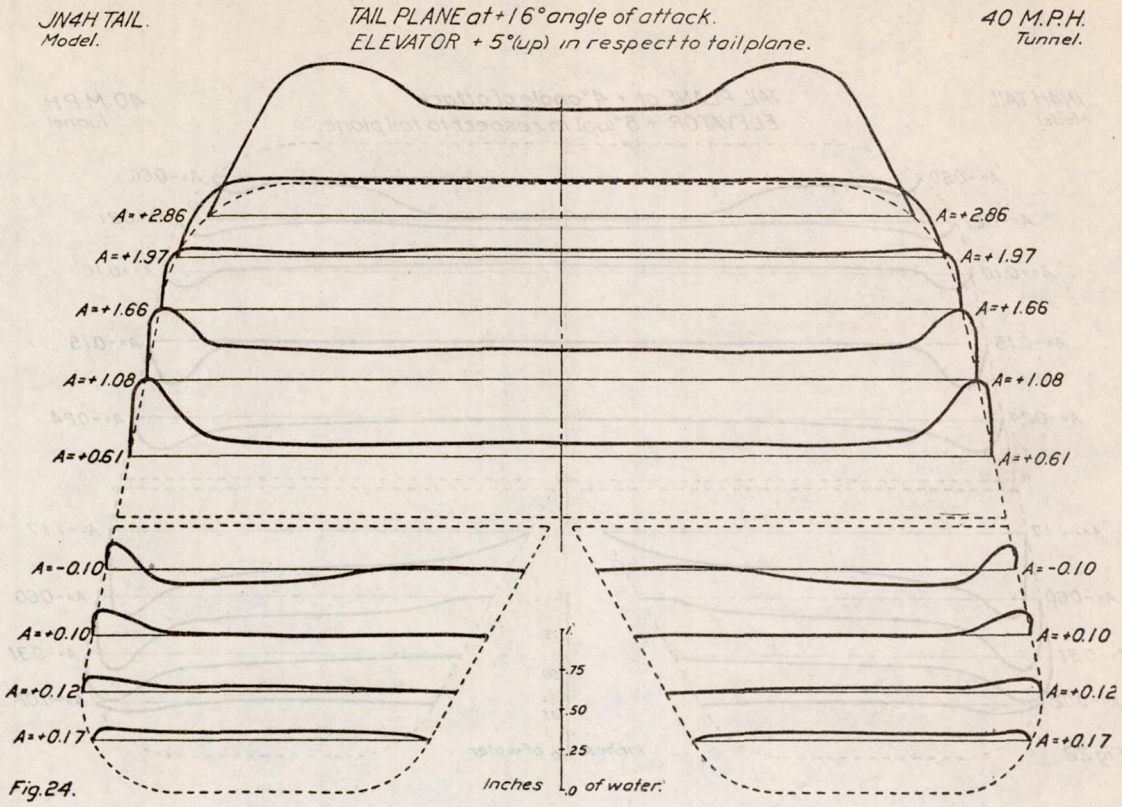
JN4H TAIL.
Model.
TAIL PLANE at +16° angle of attack.
ELEVATOR + 5° (up) in respect to tail plane.
40 M.P.H.
Tunnel.
A = +2.86
A = +1.97
A = +1.66
A = +1.08
A = +0.61
A = -0.10
A = +0.10
A = +0.12
A = +0.17
1
.75
.50
.25
.0
Inches of water.

Fig. 24.

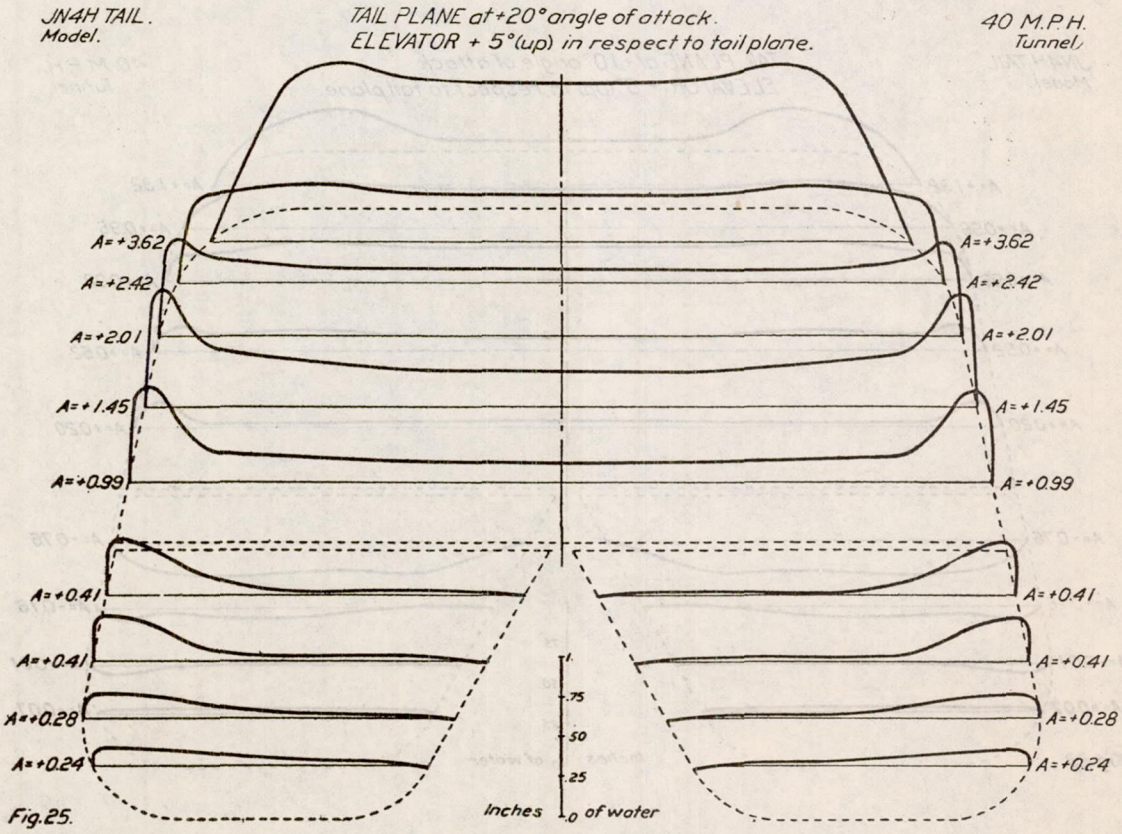
JN4H TAIL.
Model.
TAIL PLANE at +20° angle of attack.
ELEVATOR + 5° (up) in respect to tail plane.
40 M.P.H.
Tunnel.
A = +3.62
A = +2.42
A = +2.01
A = +1.45
A = +0.99
A = +0.41
A = +0.41
A = +0.28
A = +0.24
1
.75
.50
.25
.0
Inches of water

Fig. 25.

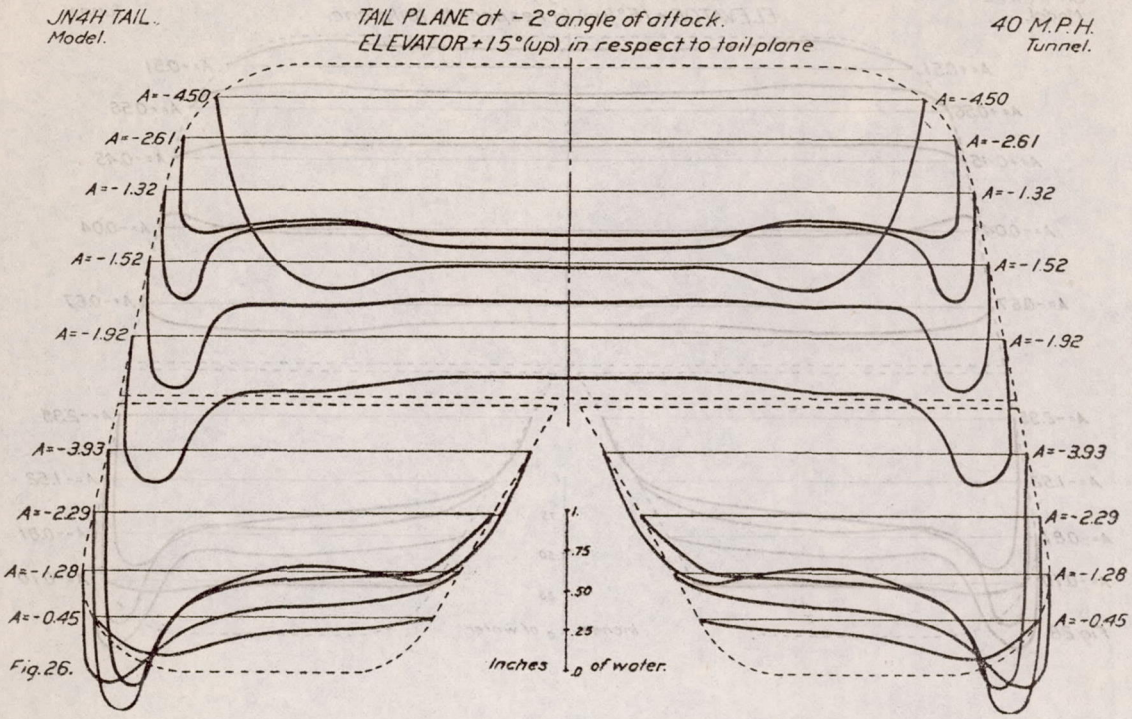
JN4H TAIL.
Model.
TAIL PLANE at - 2° angle of attack.
ELEVATOR + 15° (up) in respect to tail plane
40 M.P.H.
Tunnel.
A=-4.50
A=-2.61
A=-1.32
A=-1.52
A=-1.92
A=-3.93
A=-2.29
A=-1.28
A=-0.45
1.
.75
.50
.25
0
Inches of water.

Fig. 26.

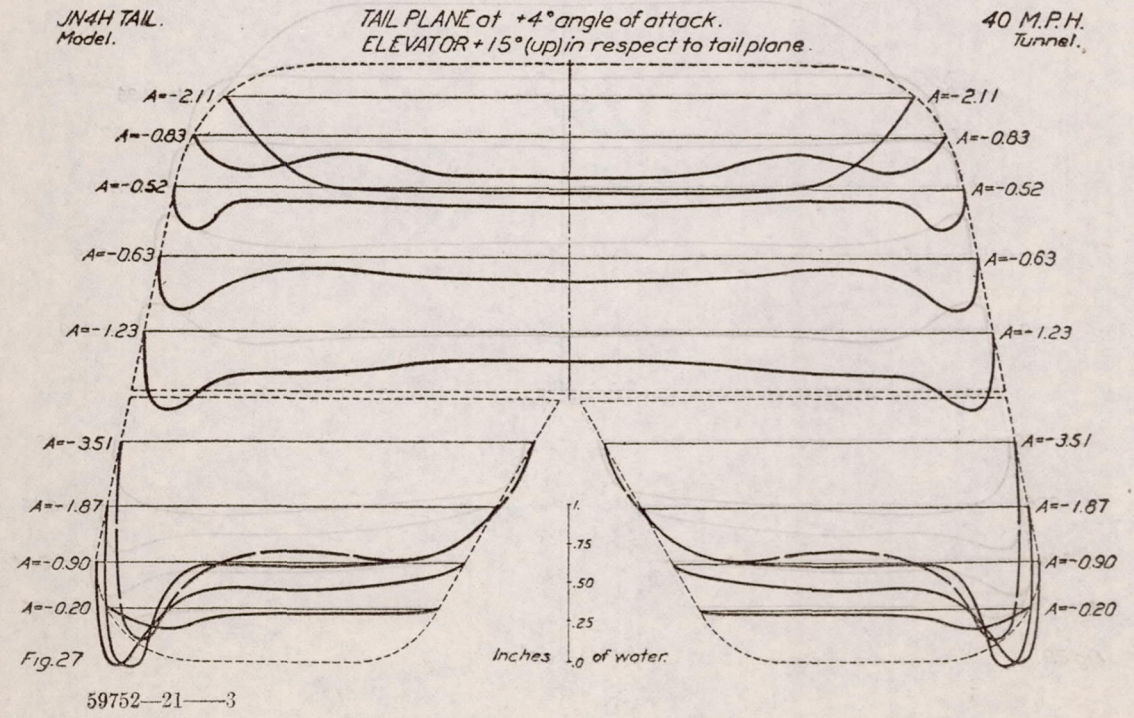
JN4H TAIL.
Model.
TAIL PLANE at +4° angle of attack.
ELEVATOR + 15° (up) in respect to tail plane.
40 M.P.H.
Tunnel.
A=-2.11
A=-0.83
A=-0.52
A=-0.63
A=-1.23
A=-3.51
A=-1.87
A=-0.90
A=-0.20
1.
.75
.50
.25
0
Inches of water.

Fig. 27

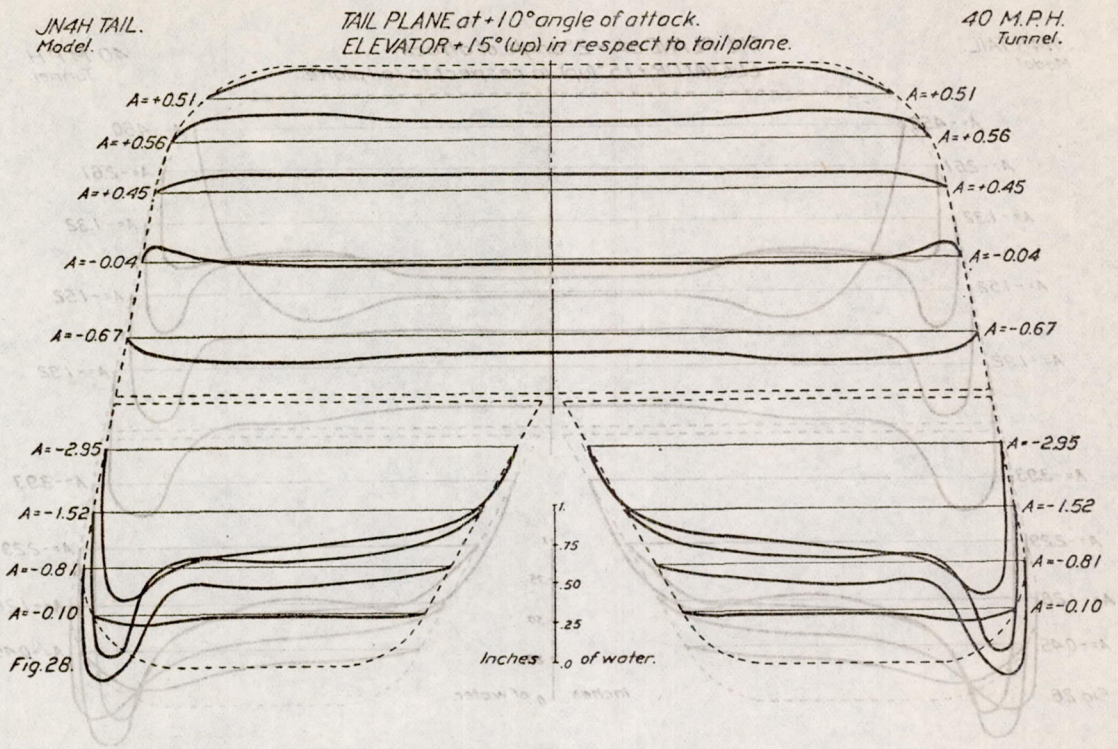
JN4H TAIL.
Model.
TAIL PLANE at +10° angle of attack.
ELEVATOR +15° (up) in respect to tail plane.
40 M.P.H.
Tunnel.
A=+0.51
A=+0.56
A=+0.45
A=-0.04
A=-0.67
A=-2.95
A=-1.52
A=-0.81
A=-0.10
1.
.75
.50
.25
.0
Inches of water.

Fig. 28.

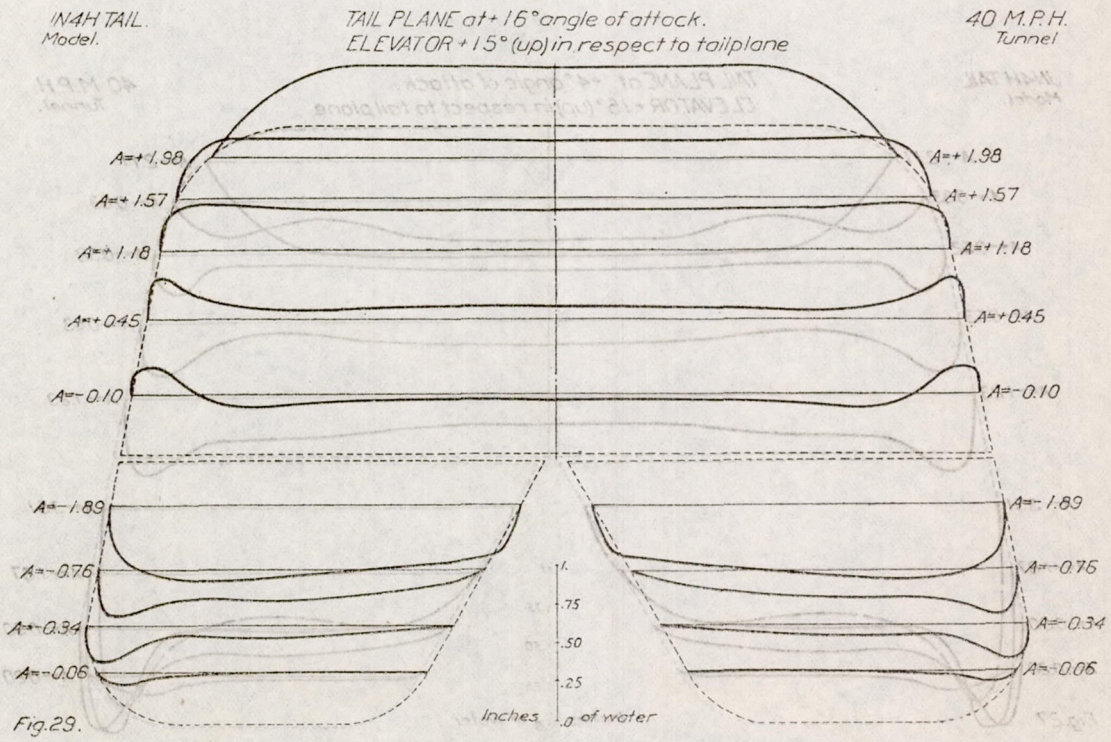
JN4H TAIL.
Model.
TAIL PLANE at +16° angle of attack.
ELEVATOR +15° (up) in respect to tail plane
40 M.P.H.
Tunnel
A=+1.98
A=+1.57
A=+1.18
A=+0.45
A=-0.10
A=-1.89
A=-0.76
A=-0.34
A=-0.06
1.
.75
.50
.25
.0
Inches of water.

Fig. 29.

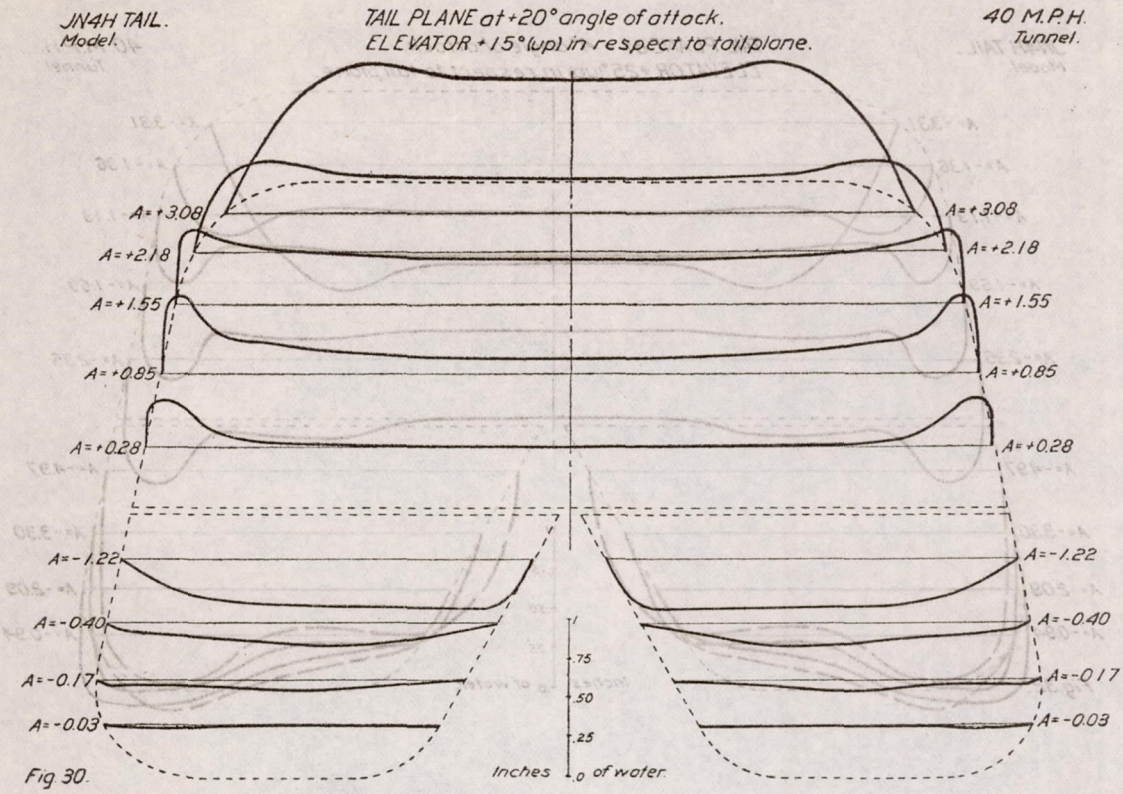
JN4H TAIL.
Model.
TAIL PLANE at +20° angle of attack.
ELEVATOR +15° (up) in respect to tail plane.
40 M.P.H.
Tunnel.
A = +3.08
A = +2.18
A = +1.55
A = +0.85
A = +0.28
A = -1.22
A = -0.40
A = -0.17
A = -0.03
1
.75
.50
.25
0
Inches of water.

Fig. 30.

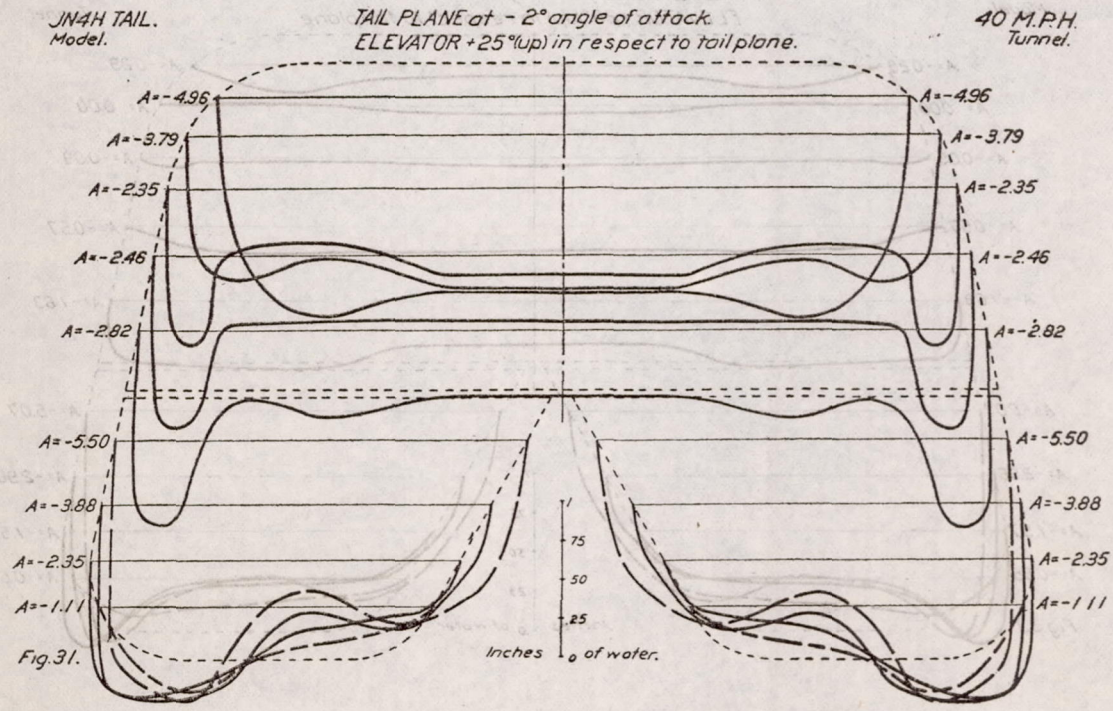
JN4H TAIL.
Model.
TAIL PLANE at - 2° angle of attack.
ELEVATOR +25° (up) in respect to tail plane.
40 M.P.H.
Tunnel.
A = -4.96
A = -3.79
A = -2.35
A = -2.46
A = -2.82
A = -5.50
A = -3.88
A = -2.35
A = -1.11
1
.75
.50
.25
0
Inches of water.

Fig. 31.

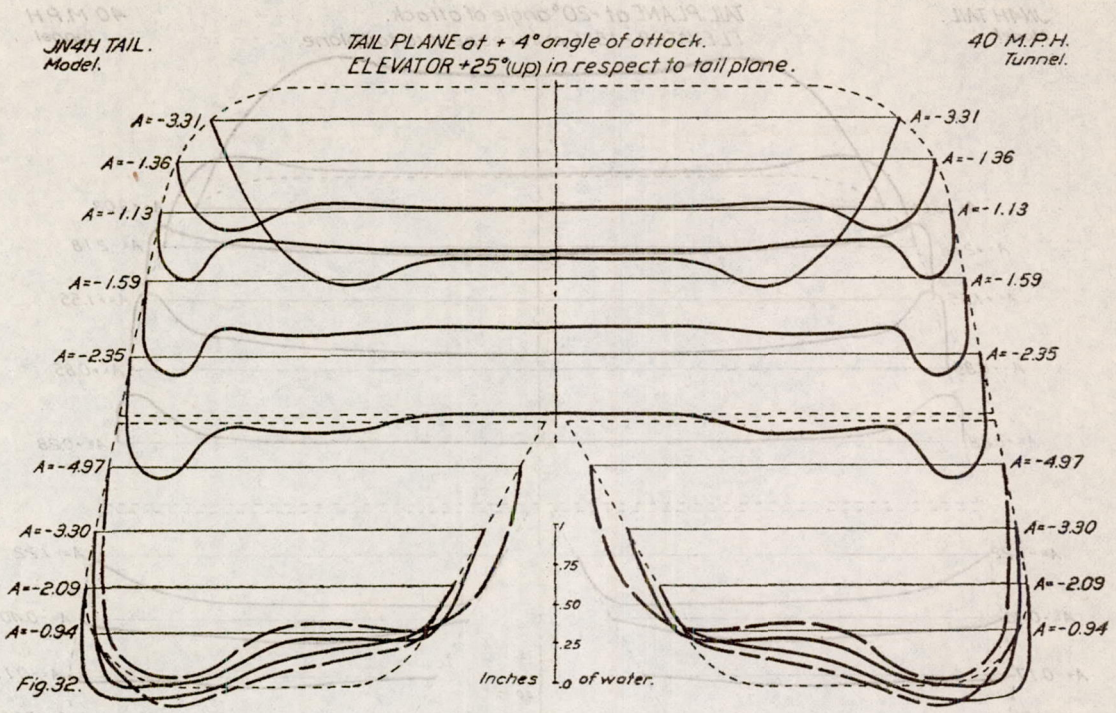
JN4H TAIL.
Model.
TAIL PLANE at + 4° angle of attack.
ELEVATOR +25° (up) in respect to tail plane.
40 M.P.H.
Tunnel.
A=-3.31
A=-1.36
A=-1.13
A=-1.59
A=-2.35
A=-4.97
A=-3.30
A=-2.09
A=-0.94
1
.75
.50
.25
.0
Inches of water.

Fig. 32.

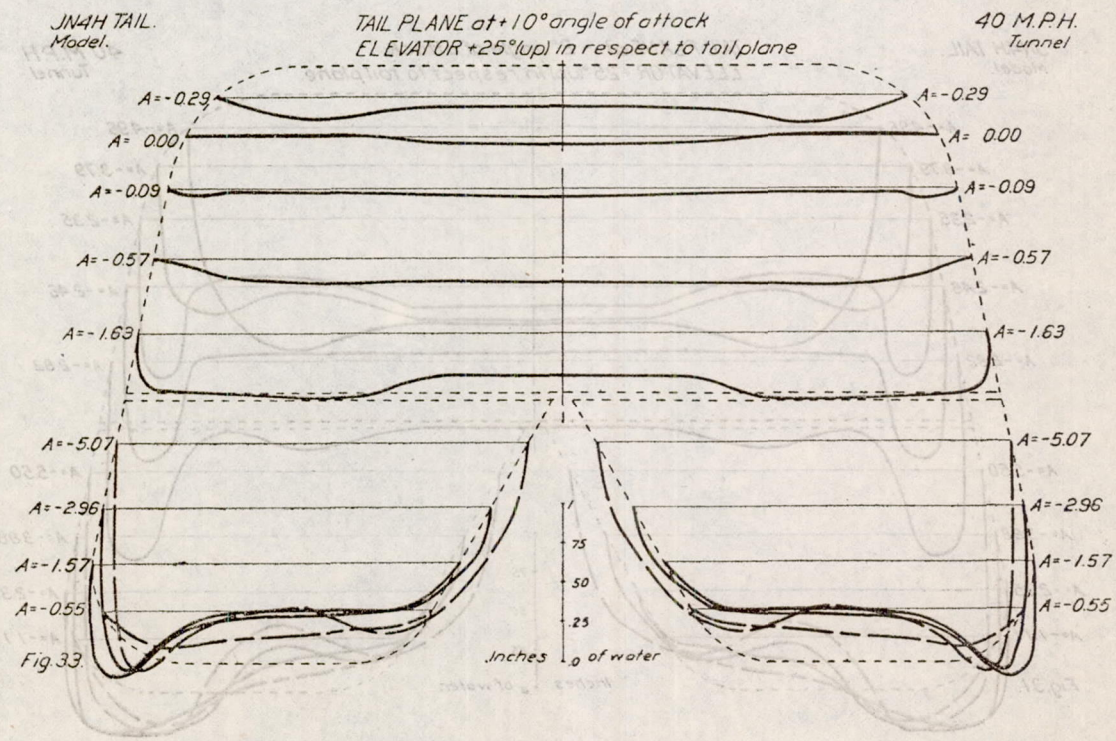
JN4H TAIL.
Model.
TAIL PLANE at + 10° angle of attack
ELEVATOR +25° (up) in respect to tail plane
40 M.P.H.
Tunnel
A=-0.29
A= 0.00
A=-0.09
A=-0.57
A=-1.63
A=-5.07
A=-2.96
A=-1.57
A=-0.55
1
.75
.50
.25
.0
Inches of water.

Fig. 33.

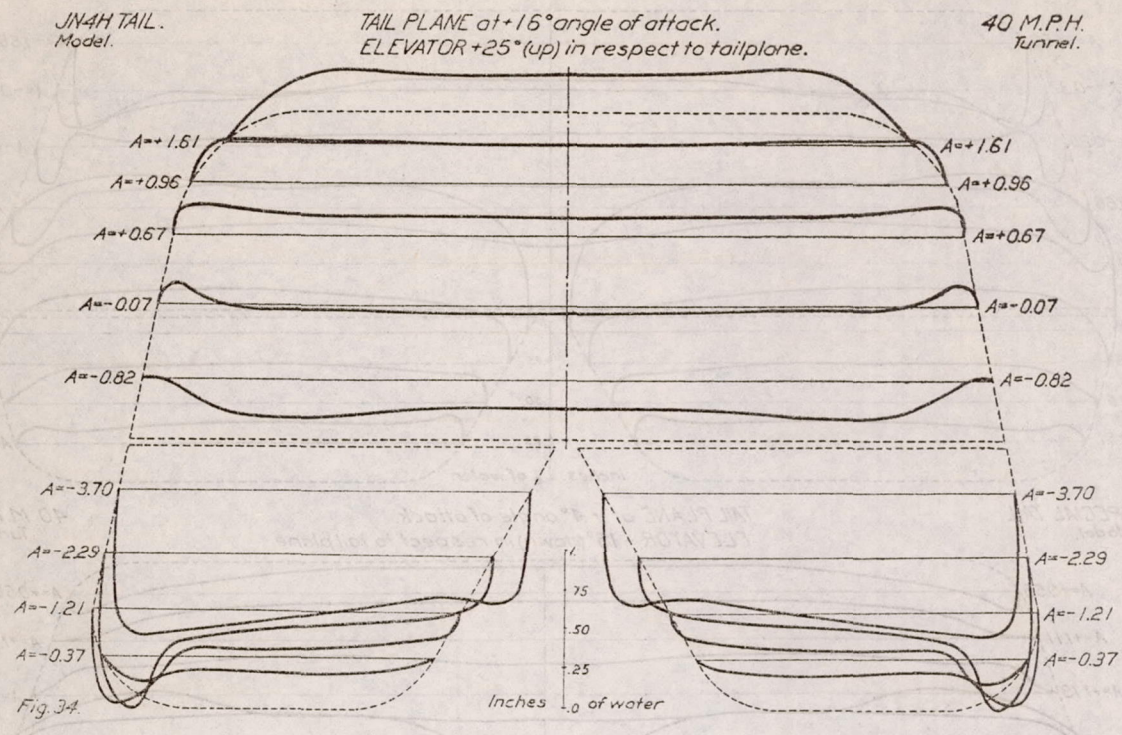
JN4H TAIL.
Model.
TAIL PLANE at +16° angle of attack.
ELEVATOR +25° (up) in respect to tailplane.
40 M.P.H.
Tunnel.
A=+1.61
A=+0.96
A=+0.67
A=-0.07
A=-0.82
A=-3.70
A=-2.29
A=-1.21
A=-0.37
1
.75
.50
.25
.0
Inches of water

Fig. 34.

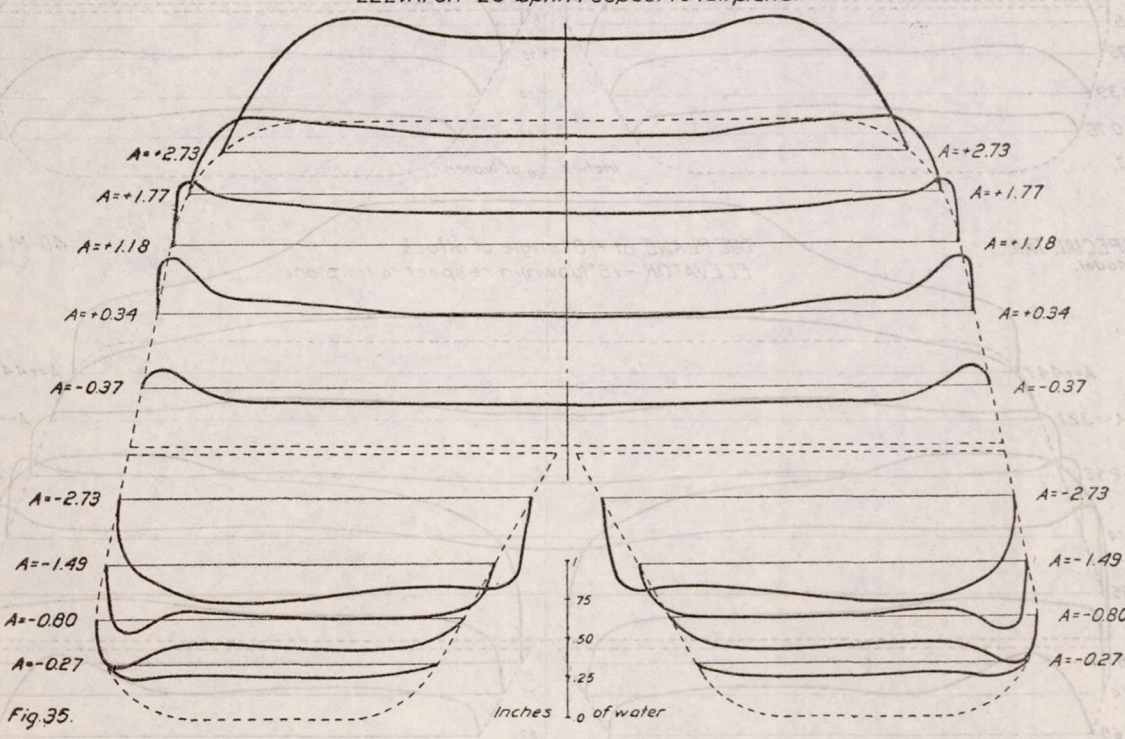
JN4H TAIL.
Model.
TAIL PLANE at +20° angle of attack.
ELEVATOR +25° (up) in respect to tail plane.
40 M.P.H.
Tunnel.
A=+2.73
A=+1.77
A=+1.18
A=+0.34
A=-0.37
A=-2.73
A=-1.49
A=-0.80
A=-0.27
1
.75
.50
.25
.0
Inches of water

Fig. 35.

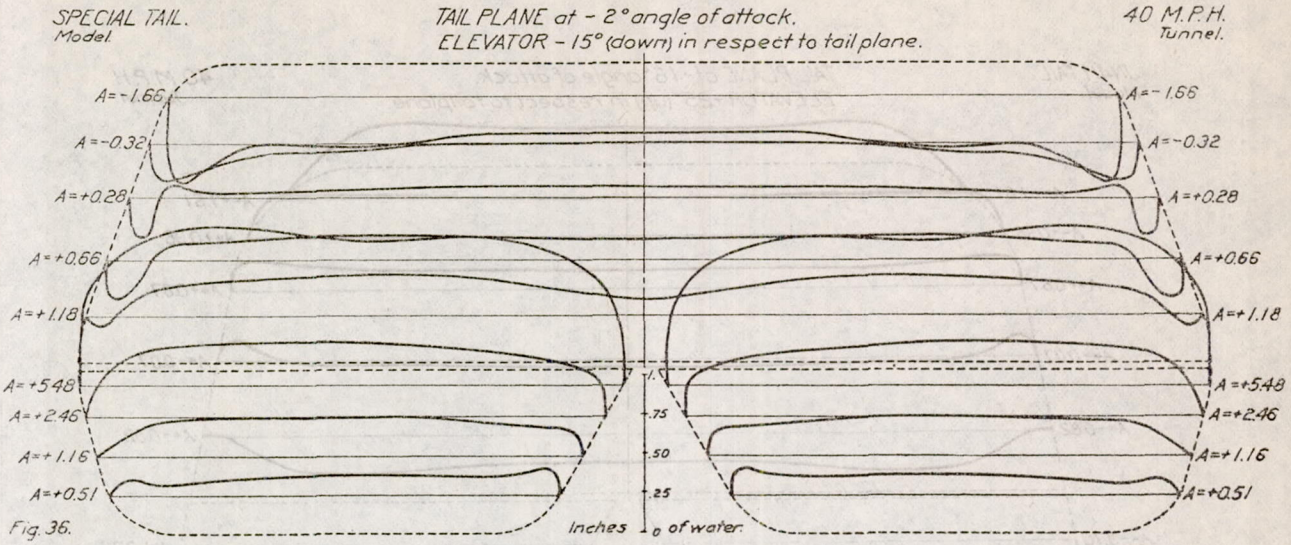

Fig. 36.

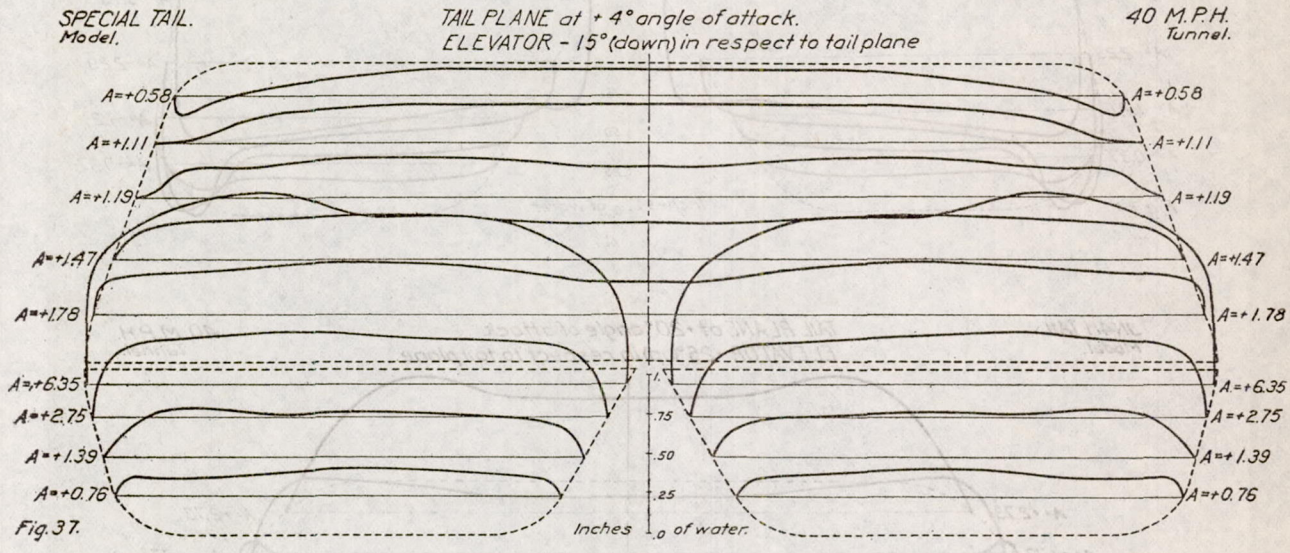

Fig. 37.

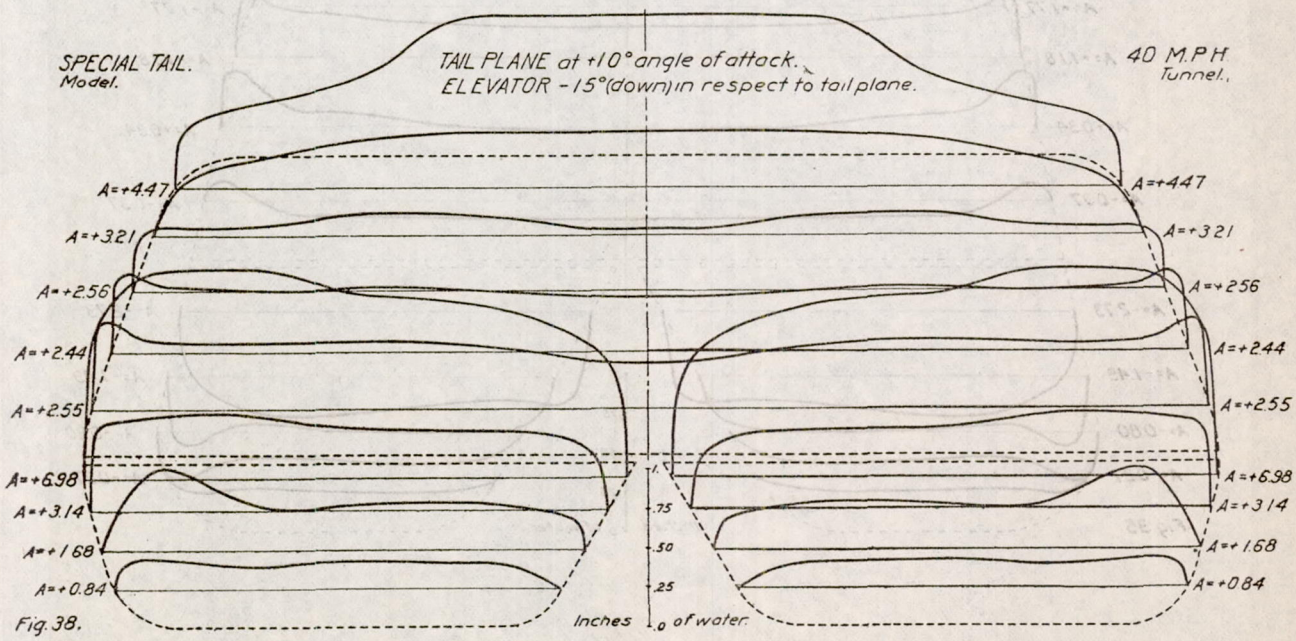

Fig. 38.

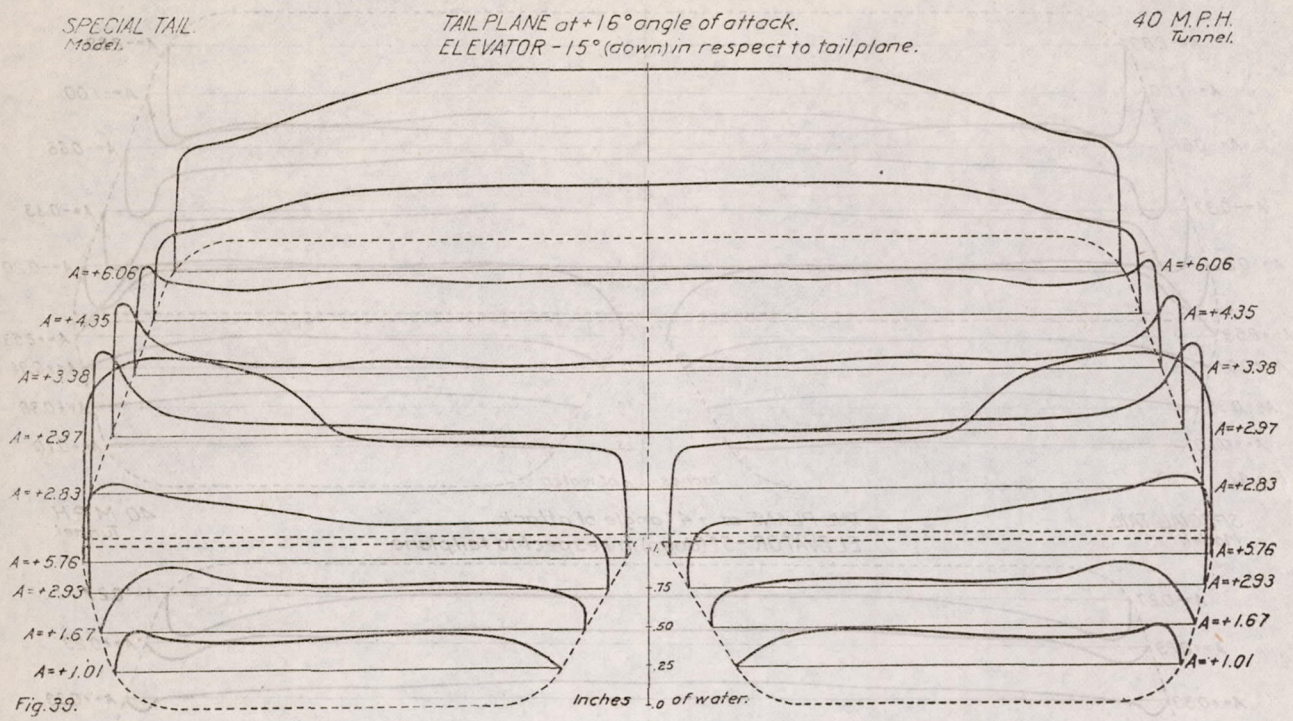
SPECIAL TAIL.
Model.
TAIL PLANE at +16° angle of attack.
ELEVATOR -15° (down) in respect to tail plane.
40 M.P.H.
Tunnel.
A=+6.06
A=+4.35
A=+3.38
A=+2.97
A=+2.83
A=+5.76
A=+2.93
A=+1.67
A=+1.01
1.
.75
.50
.25
.0
Inches of water.

Fig. 39.

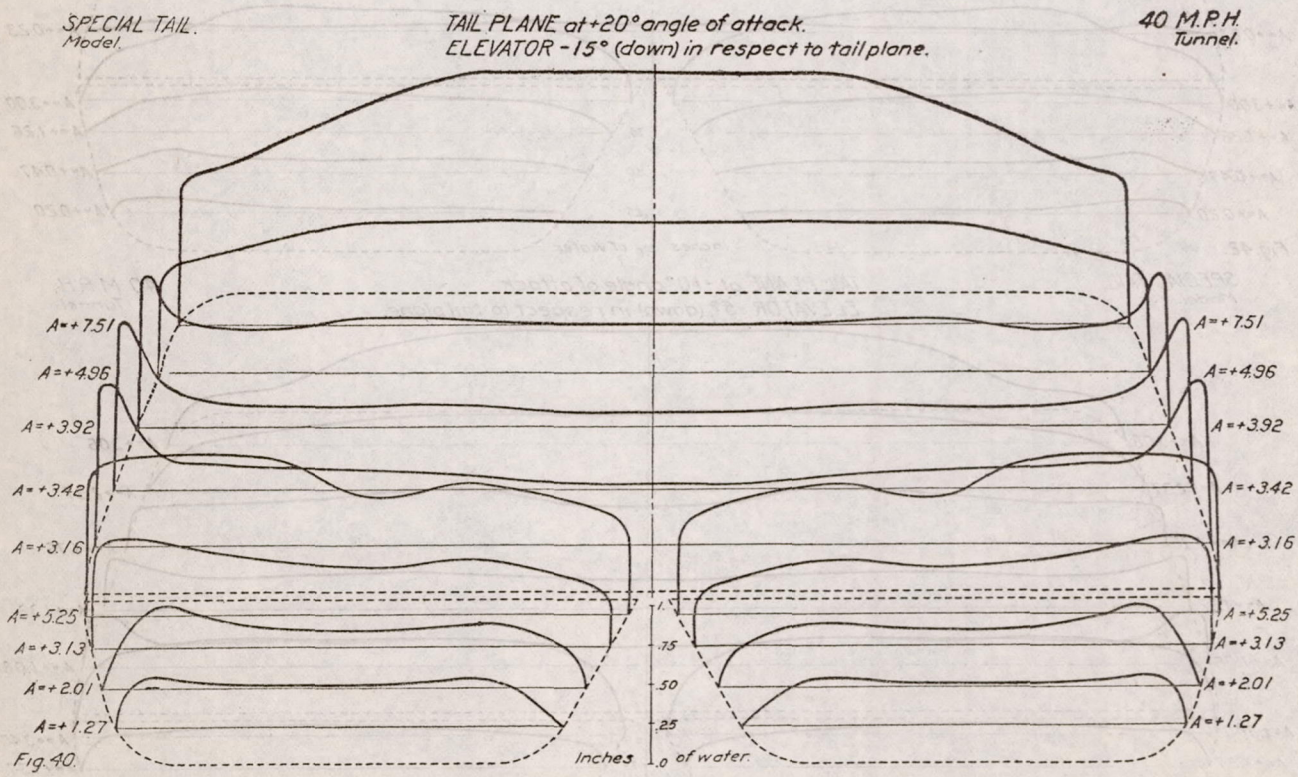
SPECIAL TAIL.
Model.
TAIL PLANE at +20° angle of attack.
ELEVATOR -15° (down) in respect to tail plane.
40 M.P.H.
Tunnel.
A=+7.51
A=+4.96
A=+3.92
A=+3.42
A=+3.16
A=+5.25
A=+3.13
A=+2.01
A=+1.27
1.
.75
.50
.25
.0
Inches of water.

Fig. 40.

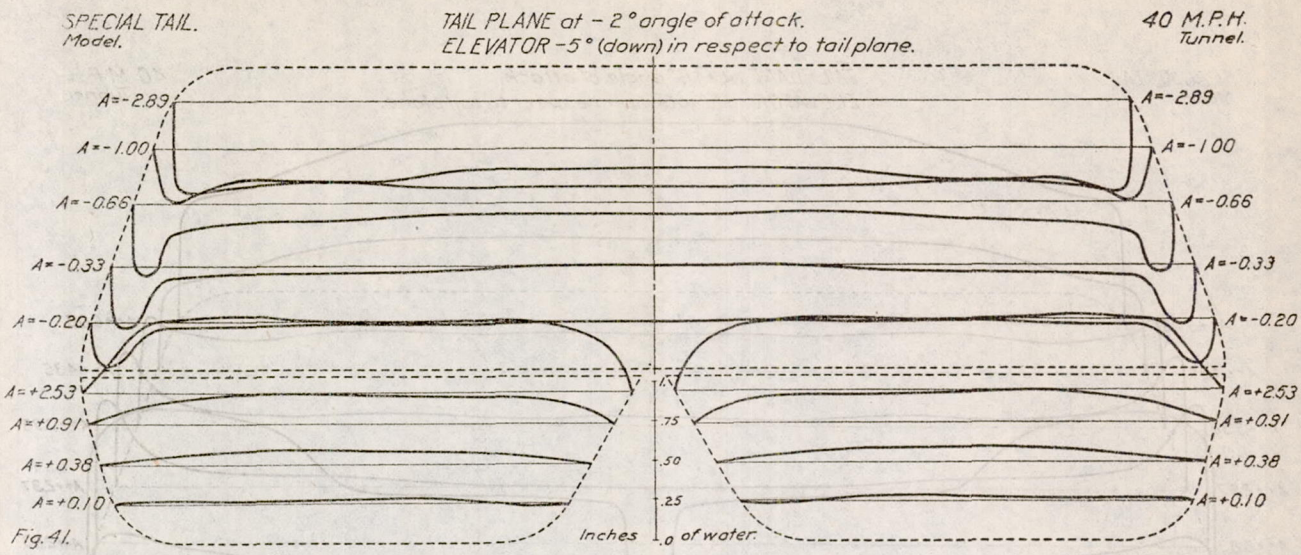

Fig. 41.

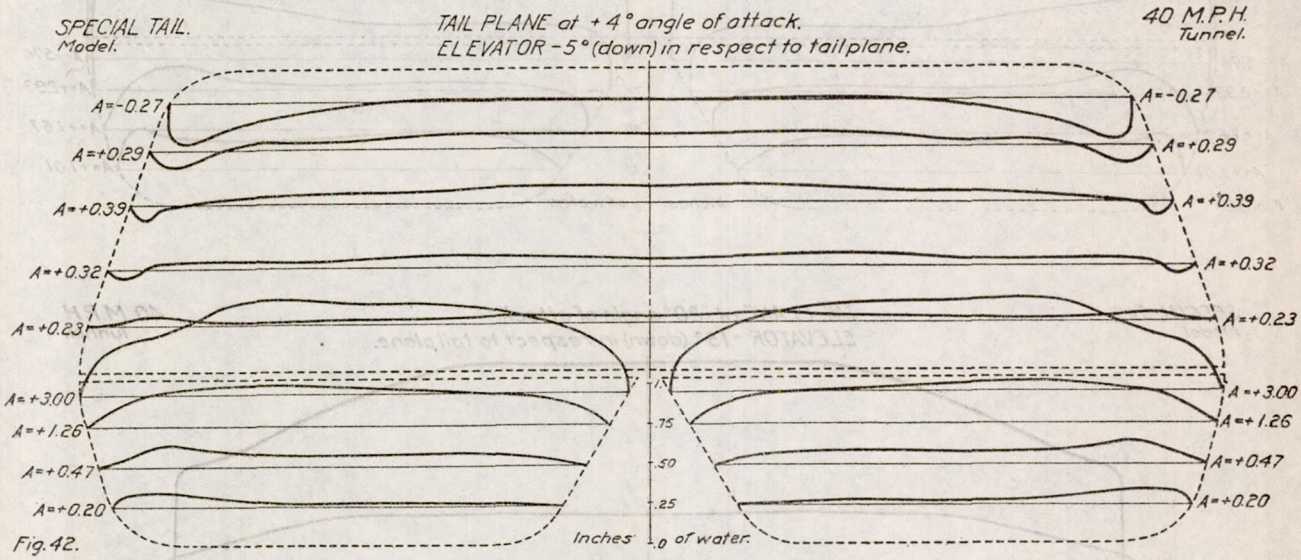

Fig. 42.

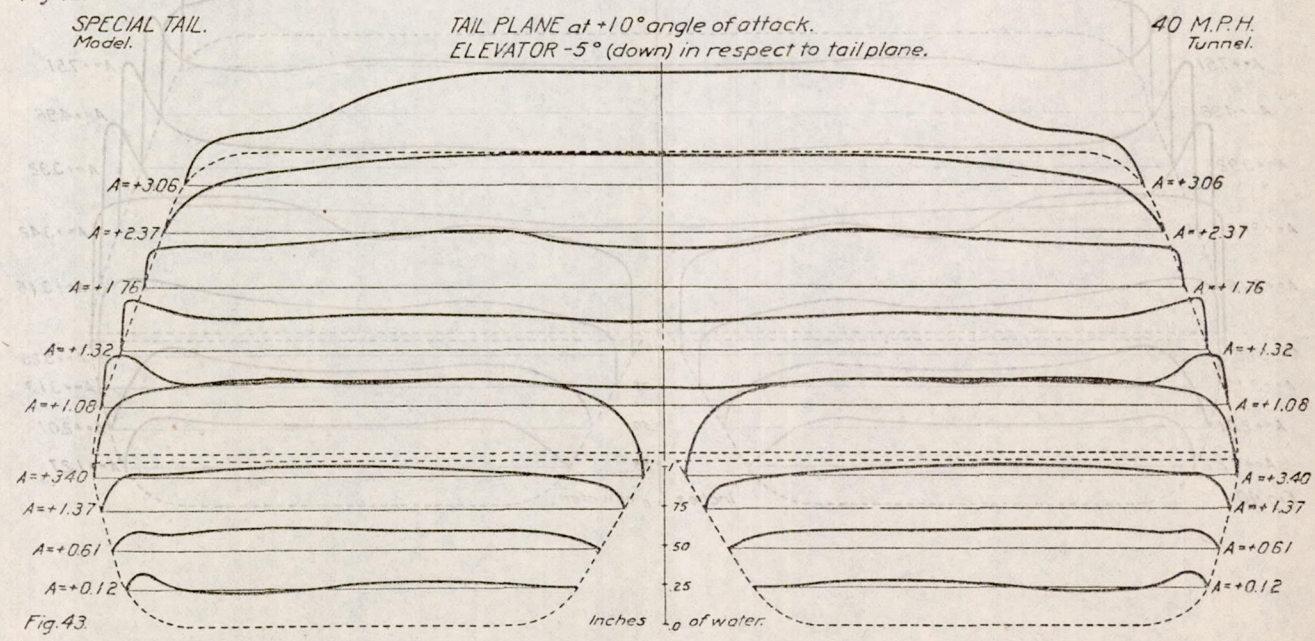

Fig. 43.

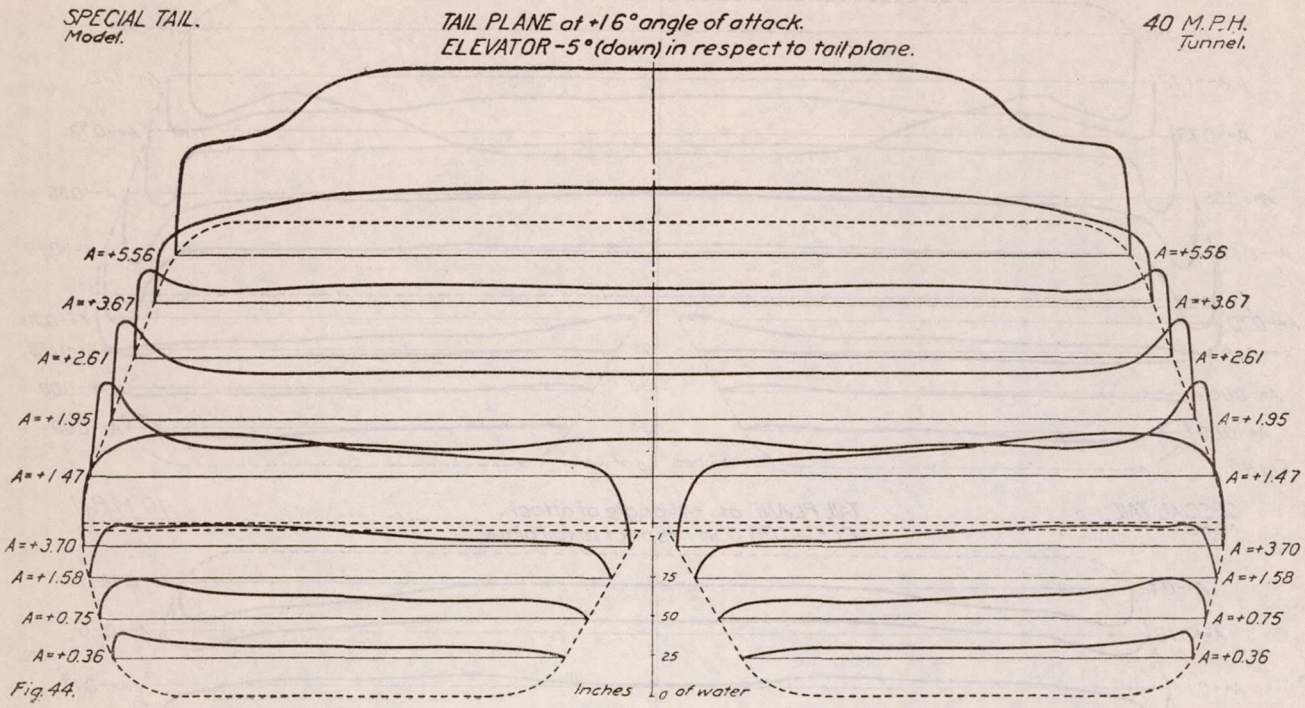
SPECIAL TAIL.
Model.
TAIL PLANE at +16° angle of attack.
ELEVATOR -5° (down) in respect to tail plane.
40 M.P.H.
Tunnel.
A=+5.56
A=+3.67
A=+2.61
A=+1.95
A=+1.47
A=+3.70
A=+1.58
A=+0.75
A=+0.36
1
.75
.50
.25
0
Inches of water

Fig. 44.

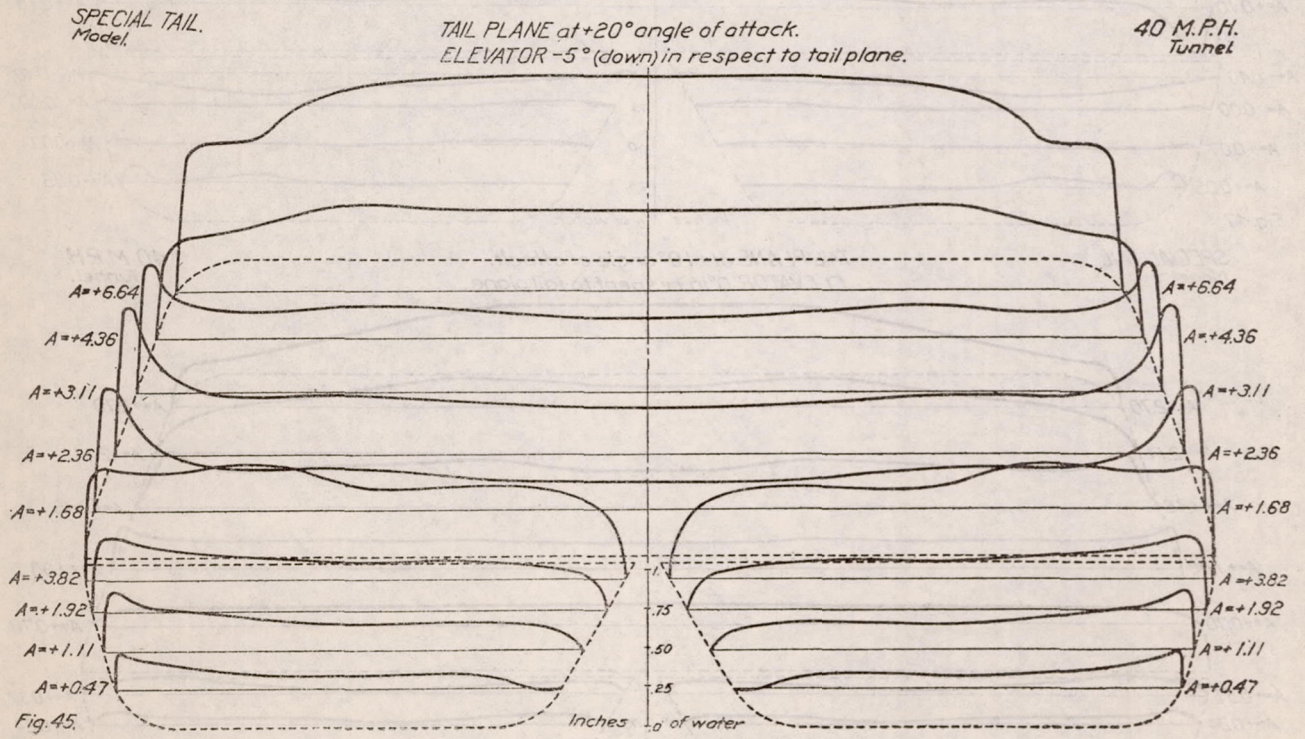
SPECIAL TAIL.
Model.
TAIL PLANE at +20° angle of attack.
ELEVATOR -5° (down) in respect to tail plane.
40 M.P.H.
Tunnel.
A=+6.64
A=+4.36
A=+3.11
A=+2.36
A=+1.68
A=+3.82
A=+1.92
A=+1.11
A=+0.47
1
.75
.50
.25
0
Inches of water

Fig. 45.

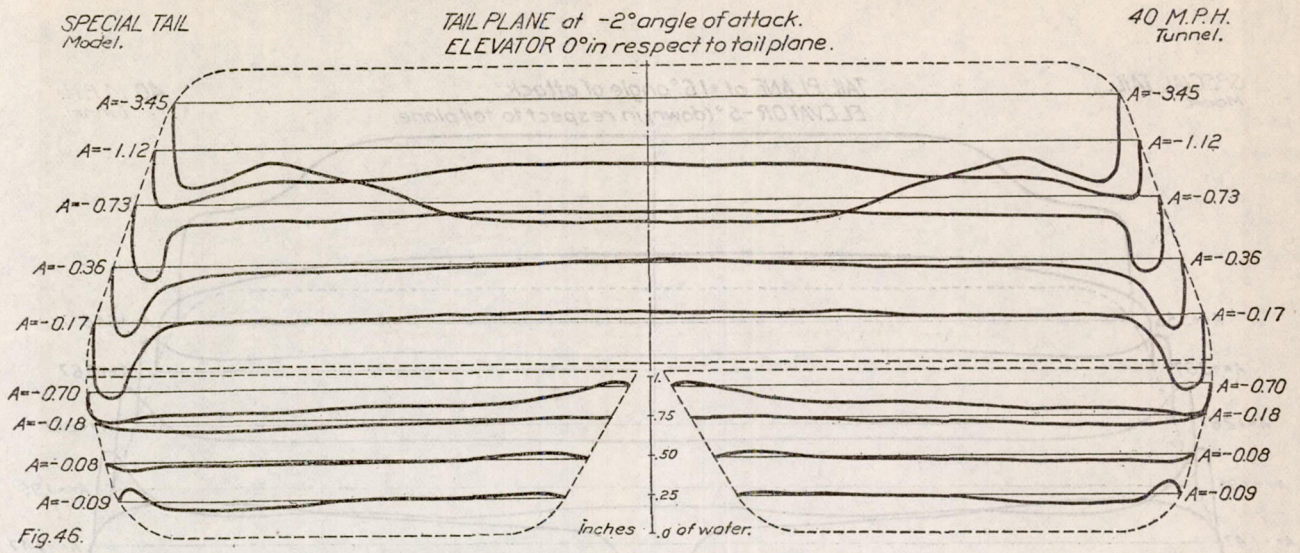

Fig. 46.

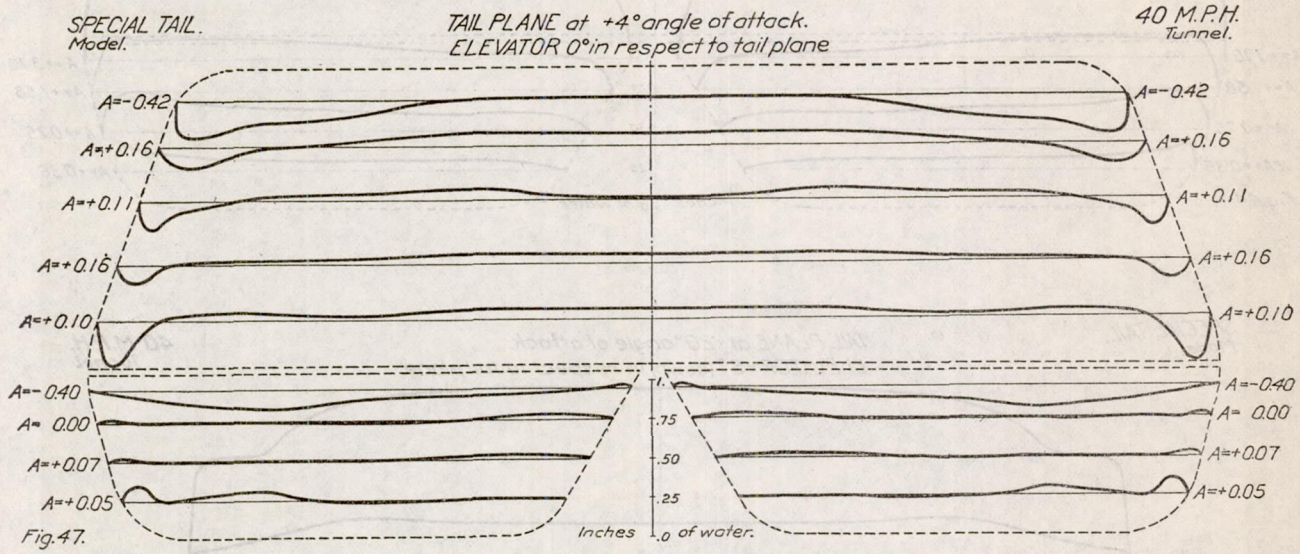

Fig. 47.

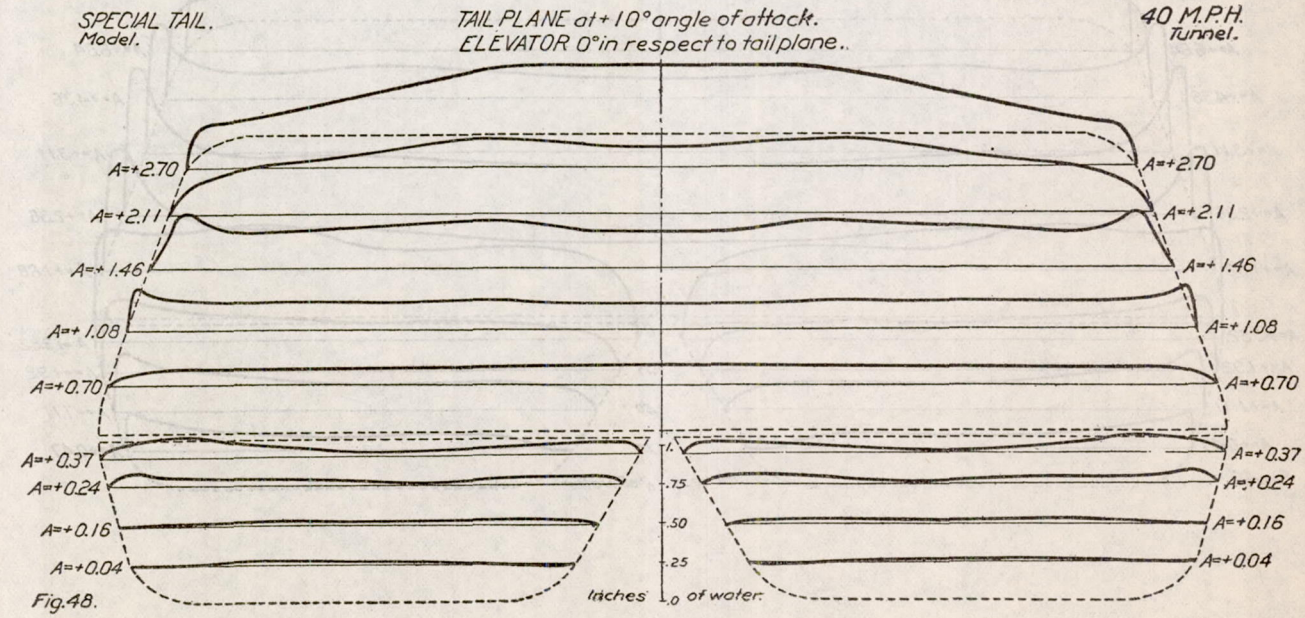

Fig. 48.

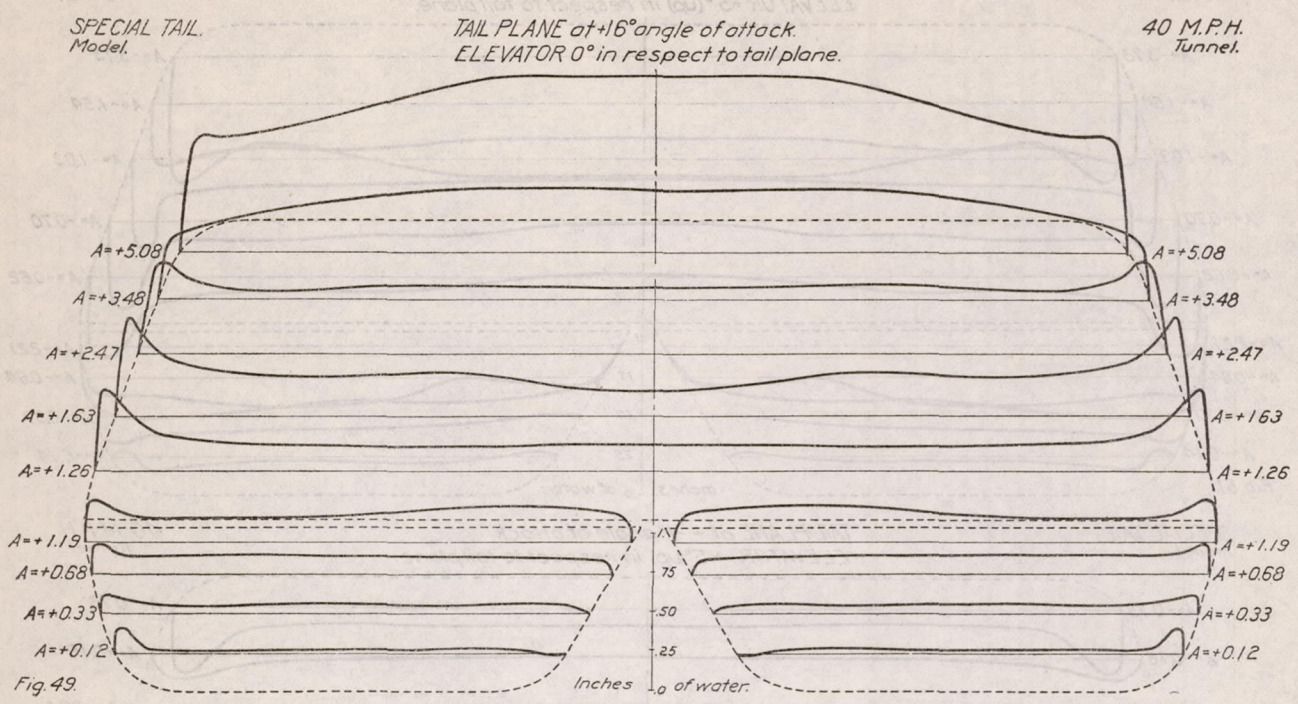
SPECIAL TAIL.
Model.
TAIL PLANE at +16° angle of attack.
ELEVATOR 0° in respect to tail plane.
40 M.P.H.
Tunnel.
A=+5.08
A=+3.48
A=+2.47
A=+1.63
A=+1.26
A=+1.19
A=+0.68
A=+0.33
A=+0.12
1.0
.75
.50
.25
0
Inches of water.

Fig. 49.

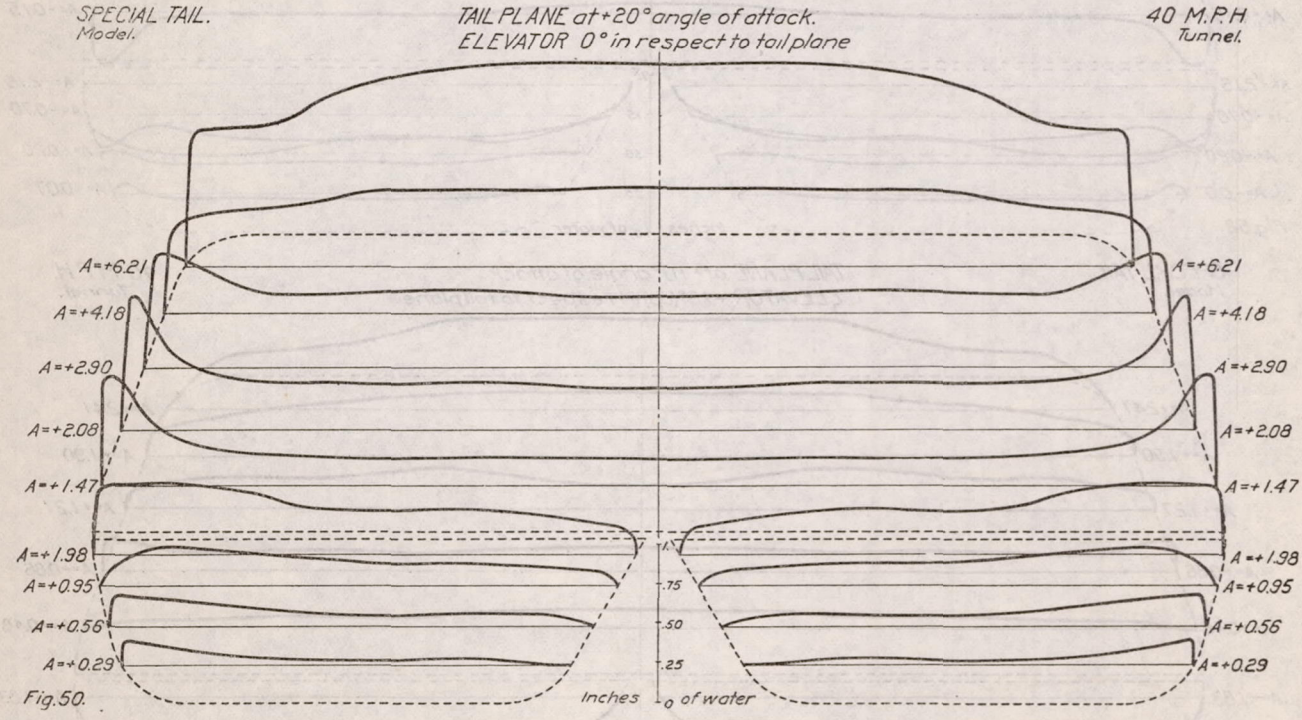
SPECIAL TAIL.
Model.
TAIL PLANE at +20° angle of attack.
ELEVATOR 0° in respect to tail plane
40 M.P.H.
Tunnel.
A=+6.21
A=+4.18
A=+2.90
A=+2.08
A=+1.47
A=+1.98
A=+0.95
A=+0.56
A=+0.29
1.0
.75
.50
.25
0
Inches of water

Fig. 50.

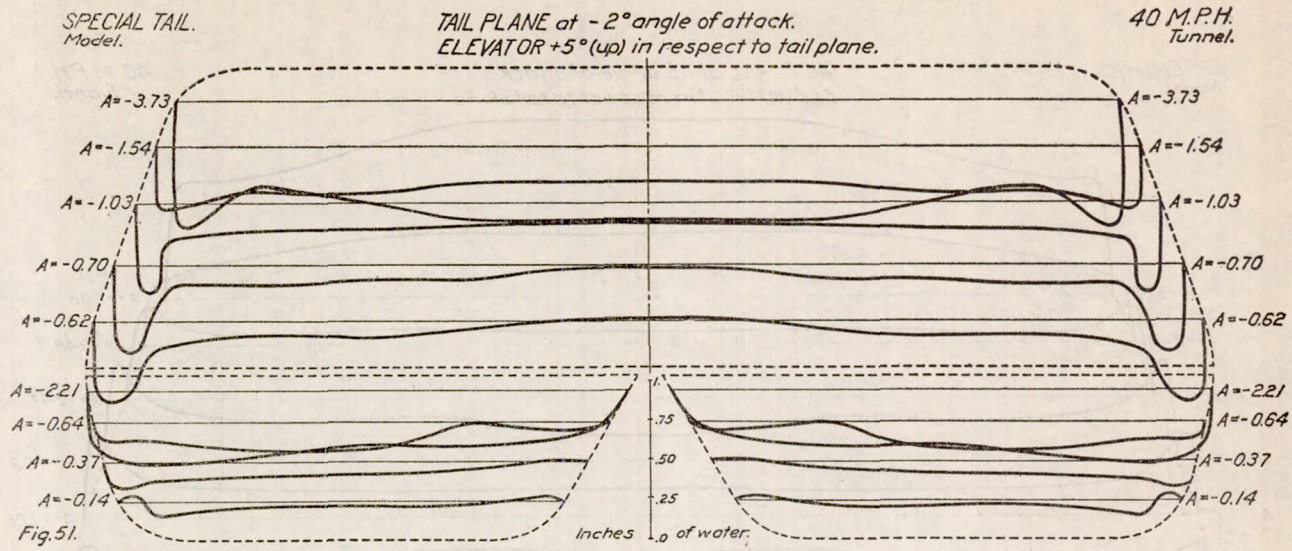

Fig. 51.

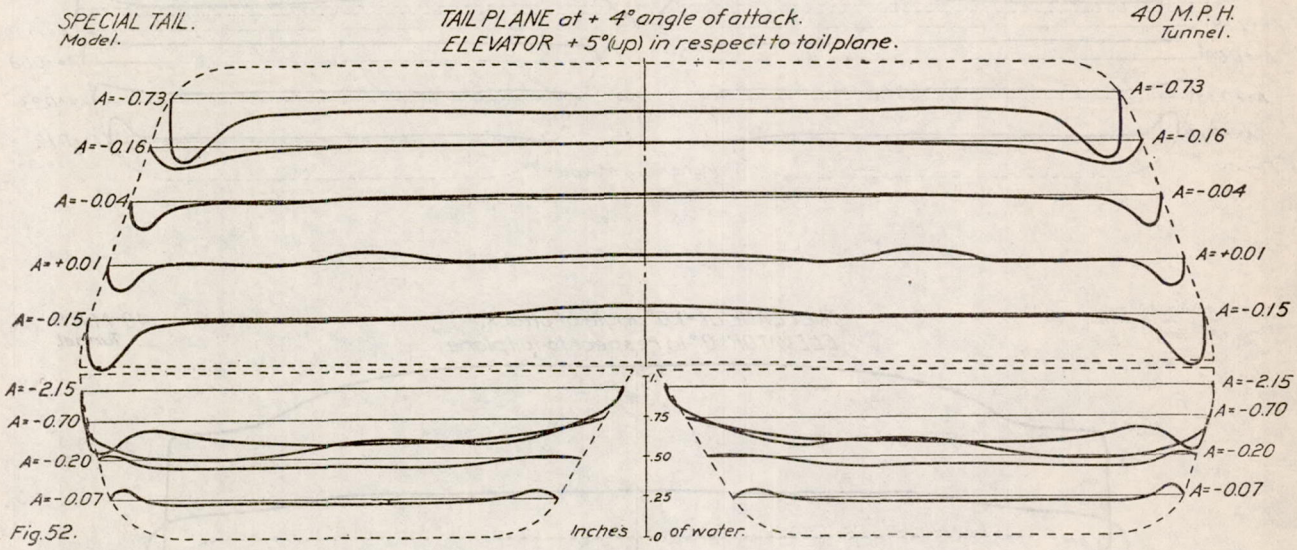

Fig. 52.

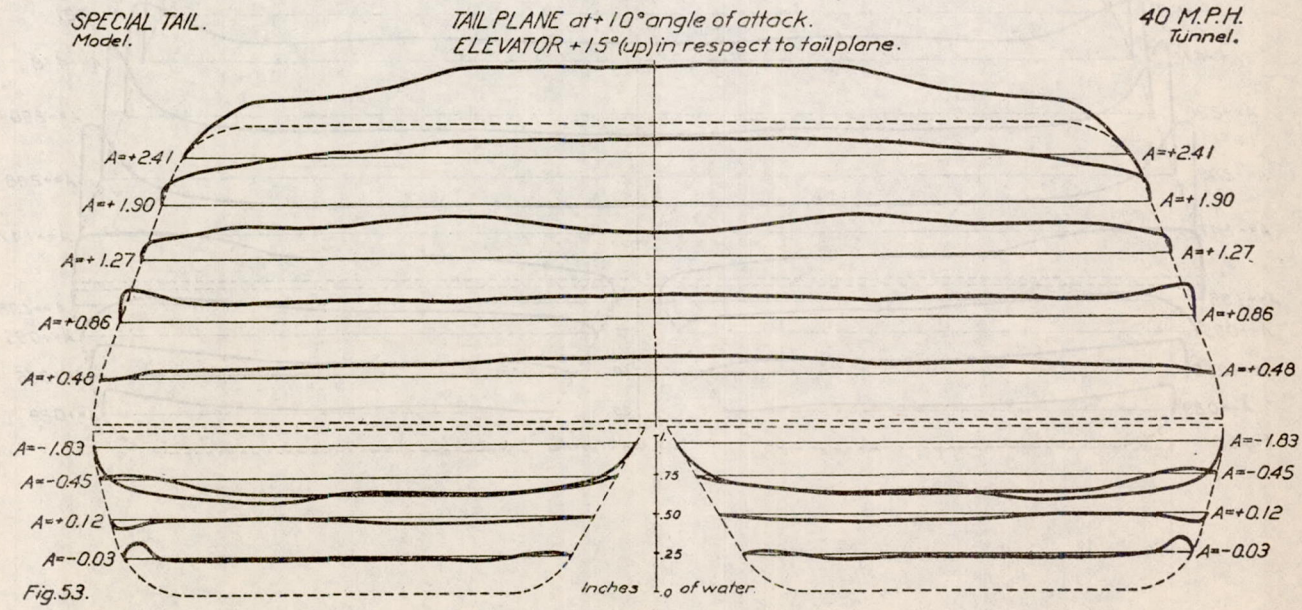

Fig. 53.

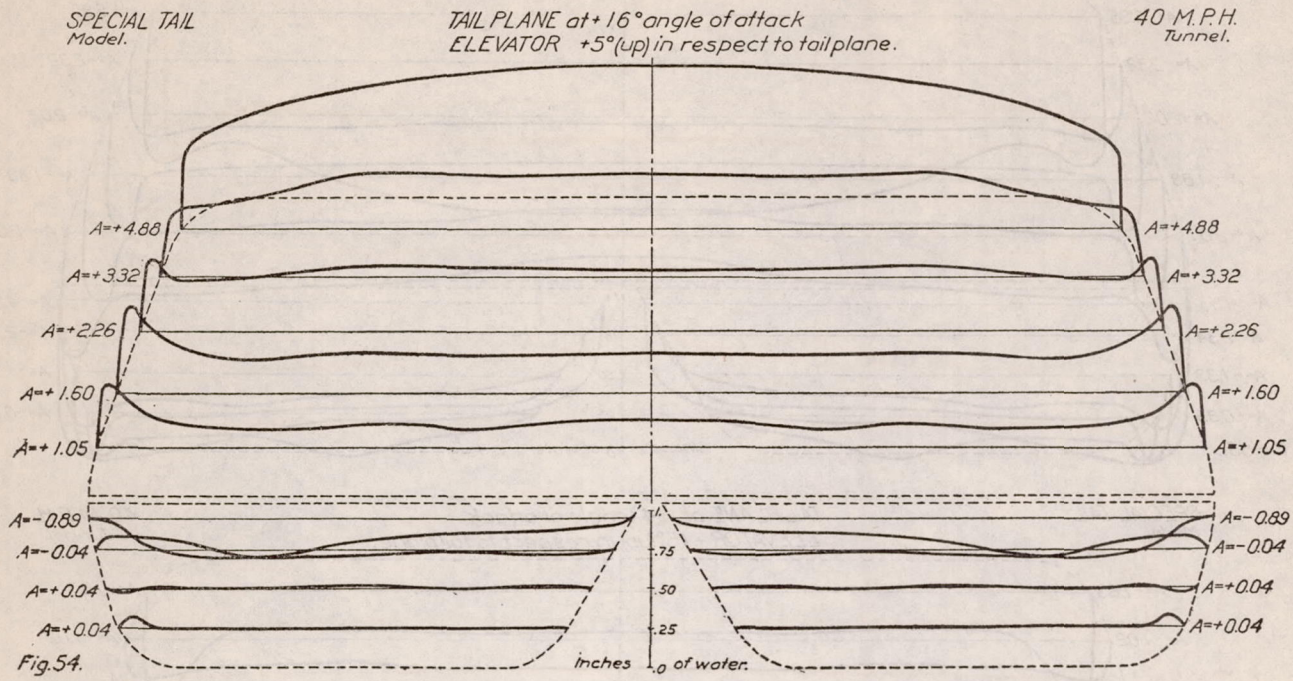
SPECIAL TAIL
Model.
TAIL PLANE at + 16° angle of attack
ELEVATOR +5° (up) in respect to tail plane.
40 M.P.H.
Tunnel.
A=+4.88
A=+3.32
A=+2.26
A=+1.60
A=+1.05
A=-0.89
A=-0.04
A=+0.04
A=+0.04
1.0
.75
.50
.25
0 of water.
inches

Fig. 54.

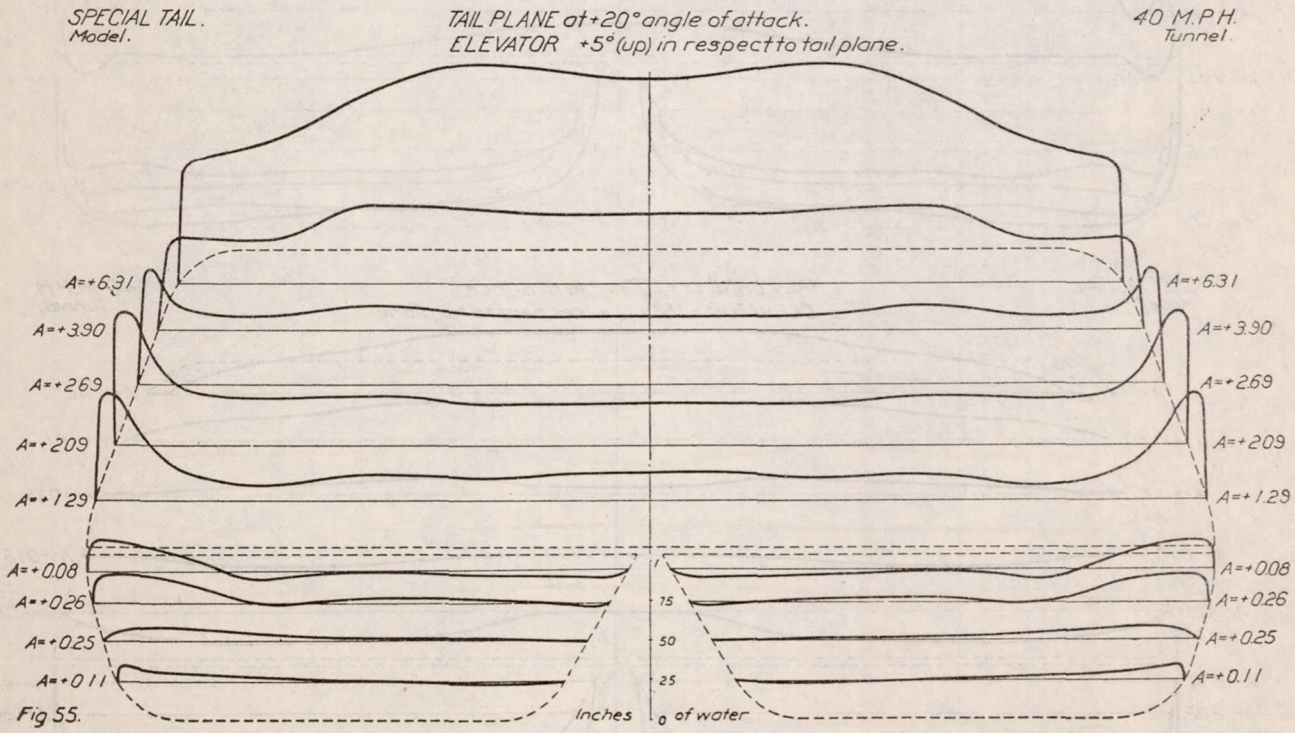
SPECIAL TAIL.
Model.
TAIL PLANE at + 20° angle of attack.
ELEVATOR +5° (up) in respect to tail plane.
40 M.P.H.
Tunnel.
A=+6.31
A=+3.90
A=+2.69
A=+2.09
A=+1.29
A=+0.08
A=+0.26
A=+0.25
A=+0.11
1.0
.75
.50
.25
0 of water
inches

Fig 55.

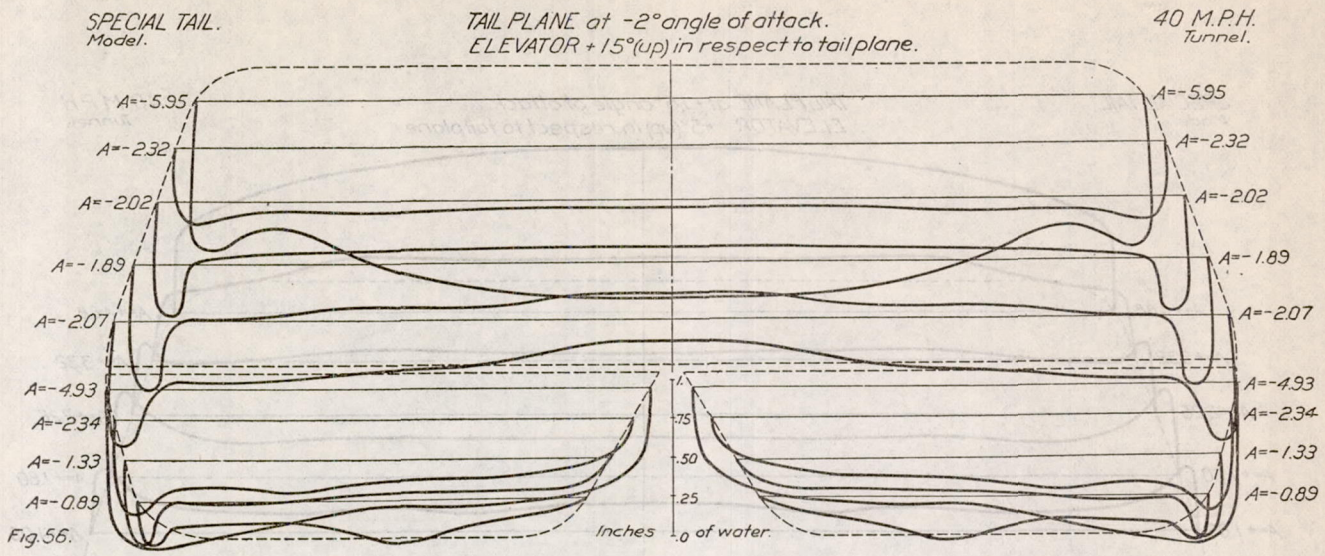

Fig. 56.

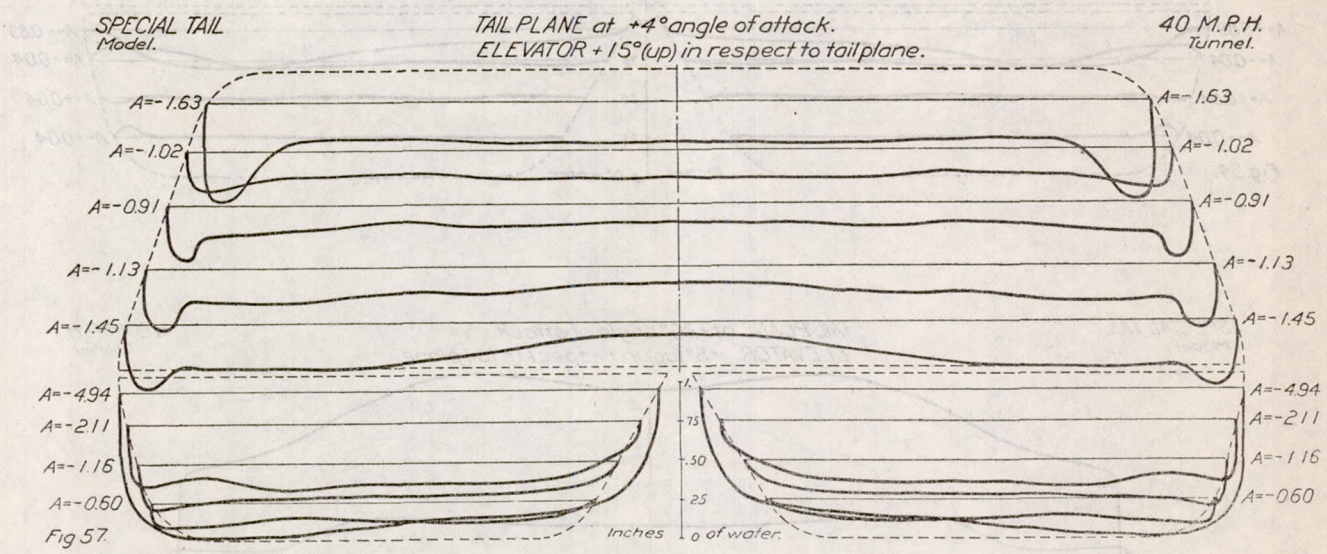

Fig 57.

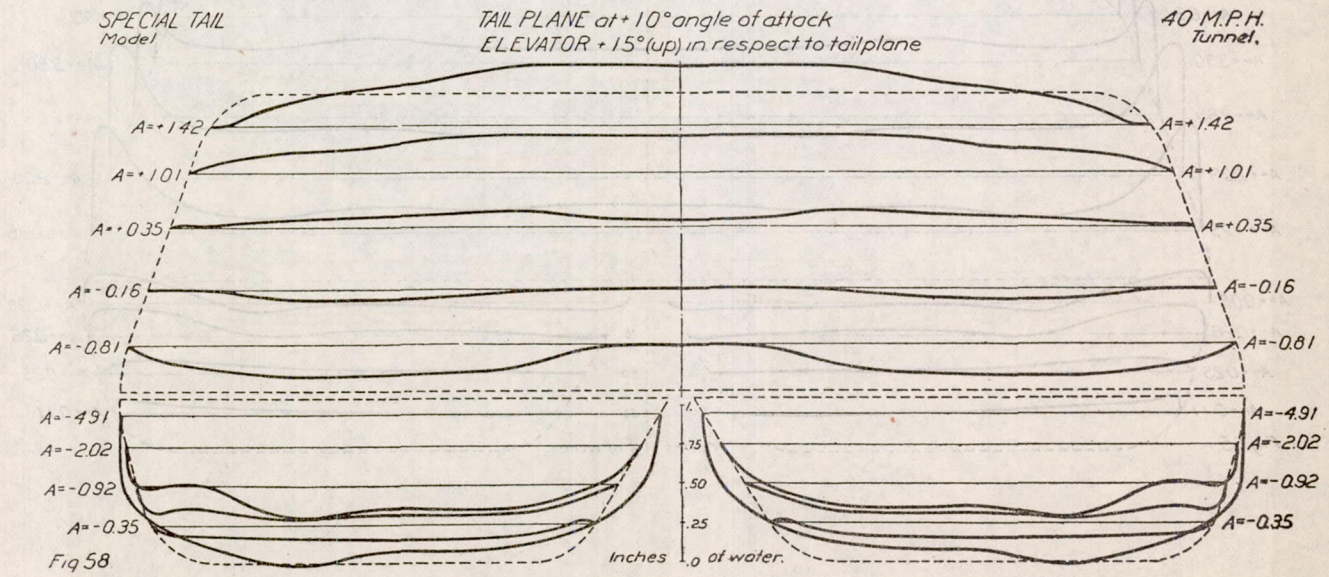

Fig 58

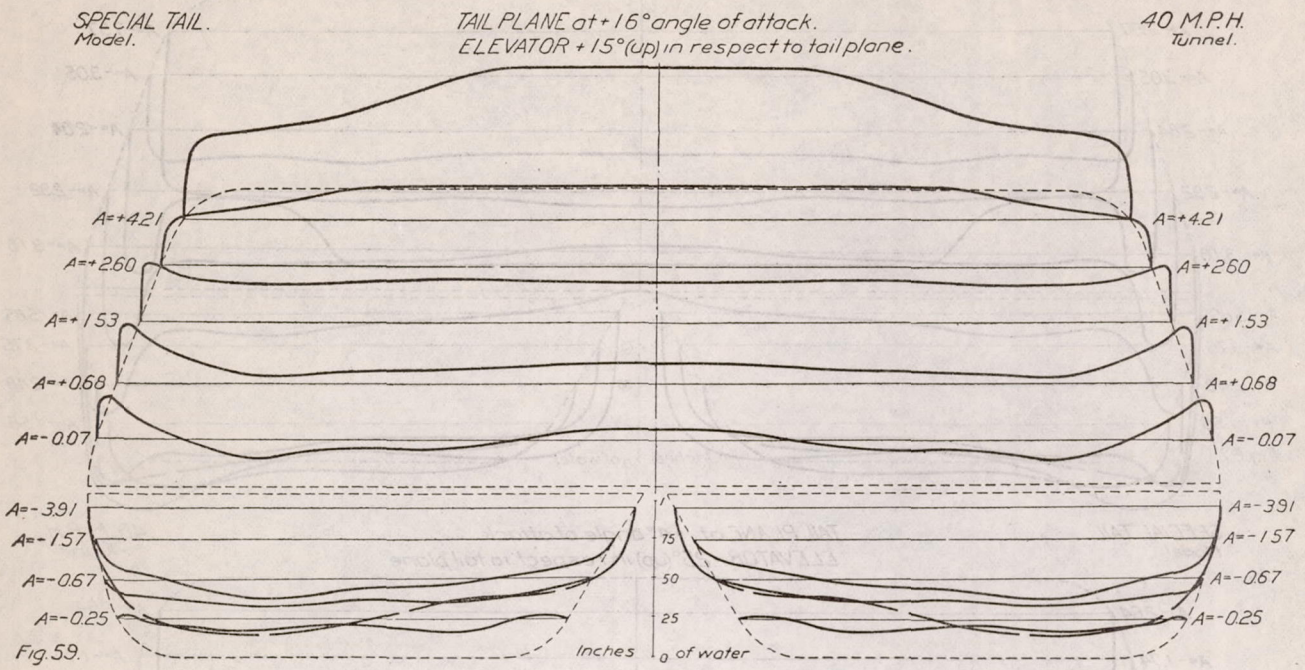
SPECIAL TAIL.
Model.
TAIL PLANE at +16° angle of attack.
ELEVATOR +15° (up) in respect to tail plane.
40 M.P.H.
Tunnel.
A=+4.21
A=+2.60
A=+1.53
A=+0.68
A=-0.07
A=-3.91
A=-1.57
A=-0.67
A=-0.25
A=+4.21
A=+2.60
A=+1.53
A=+0.68
A=-0.07
A=-3.91
A=-1.57
A=-0.67
A=-0.25
1
75
50
25
0
Inches of water

Fig. 59.

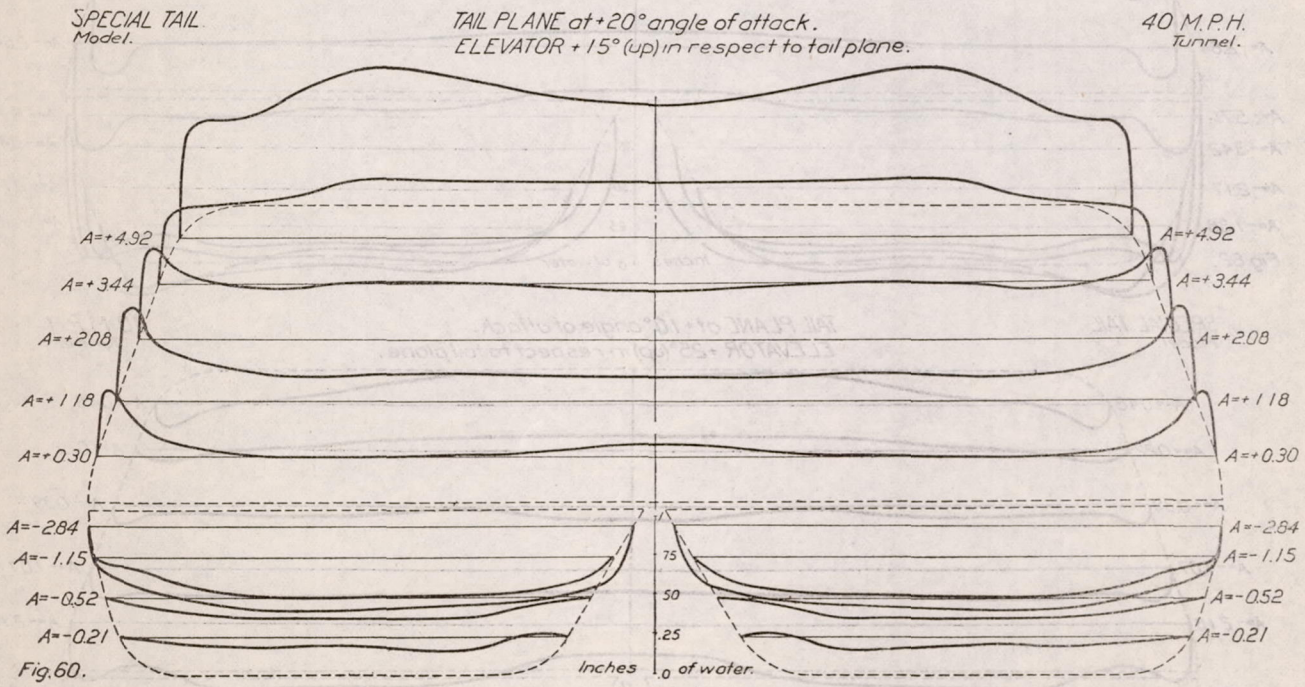
SPECIAL TAIL.
Model.
TAIL PLANE at +20° angle of attack.
ELEVATOR +15° (up) in respect to tail plane.
40 M.P.H.
Tunnel.
A=+4.92
A=+3.44
A=+2.08
A=+1.18
A=+0.30
A=-2.84
A=-1.15
A=-0.52
A=-0.21
A=+4.92
A=+3.44
A=+2.08
A=+1.18
A=+0.30
A=-2.84
A=-1.15
A=-0.52
A=-0.21
75
50
25
0
Inches of water.

Fig. 60.

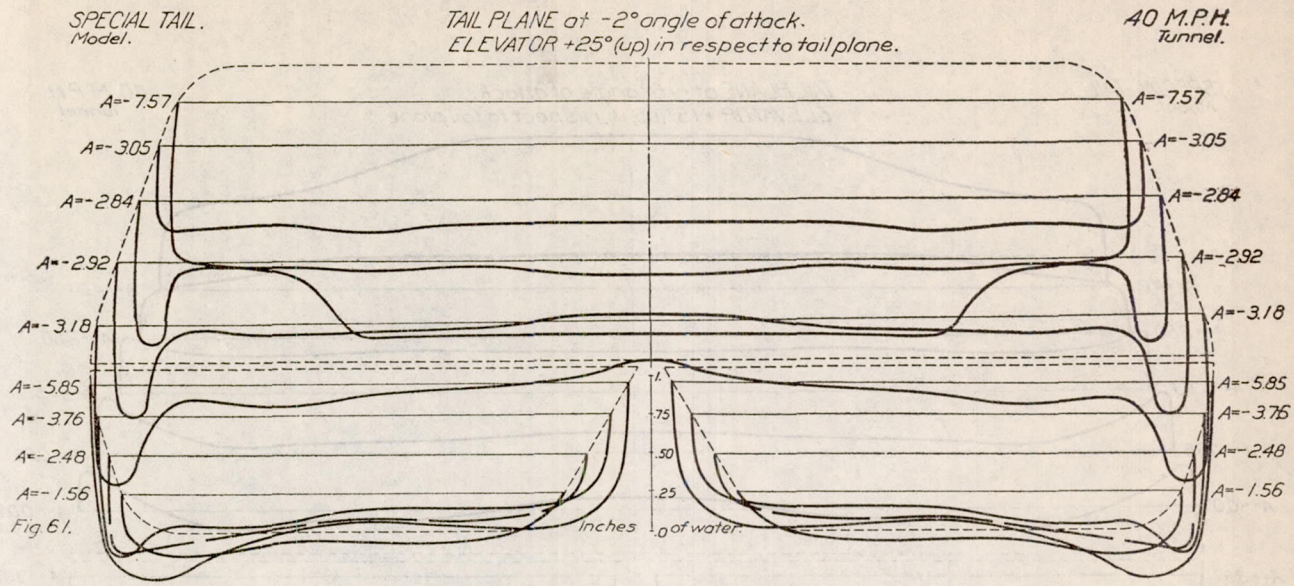

Fig. 61.

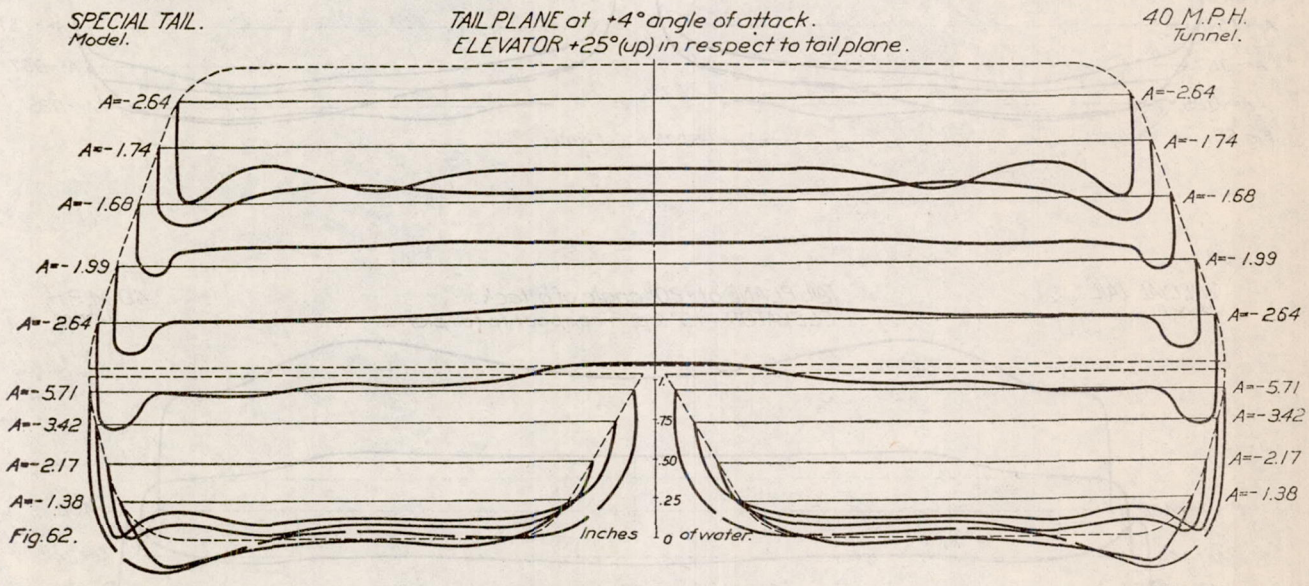

Fig. 62.

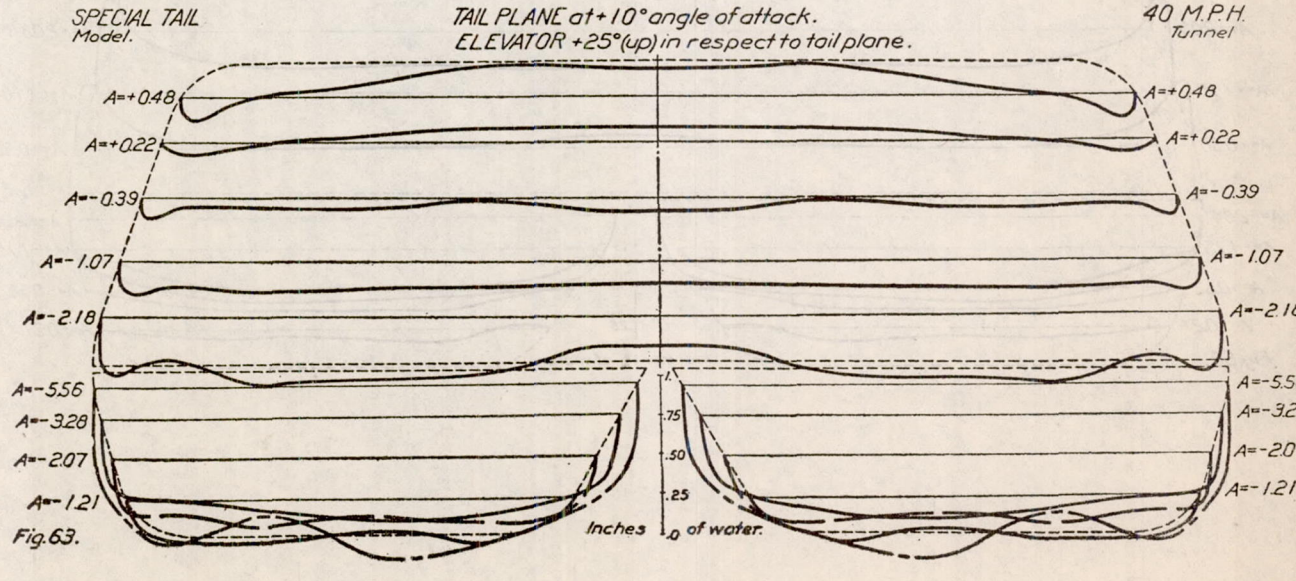

Fig. 63.

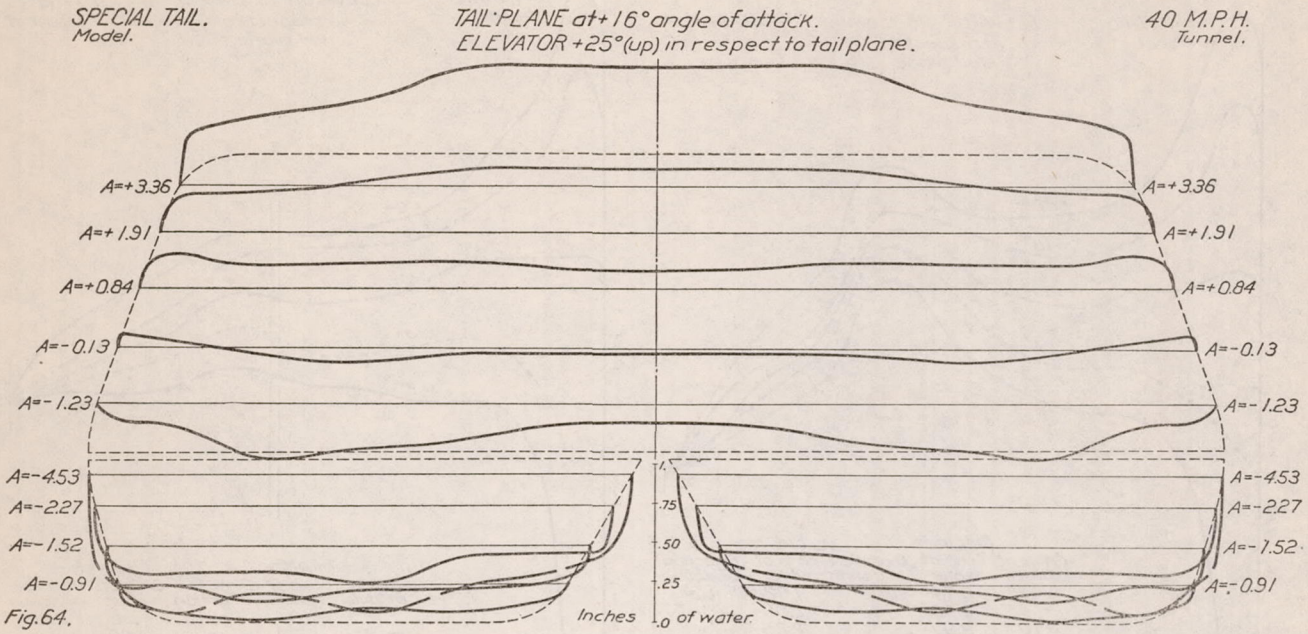
SPECIAL TAIL.
Model.
TAIL PLANE at +16° angle of attack.
ELEVATOR +25° (up) in respect to tail plane.
40 M.P.H.
Tunnel.
A=+3.36
A=+1.91
A=+0.84
A=-0.13
A=-1.23
A=-4.53
A=-2.27
A=-1.52
A=-0.91
1.
.75
.50
.25
.0
Inches of water.

Fig. 64.

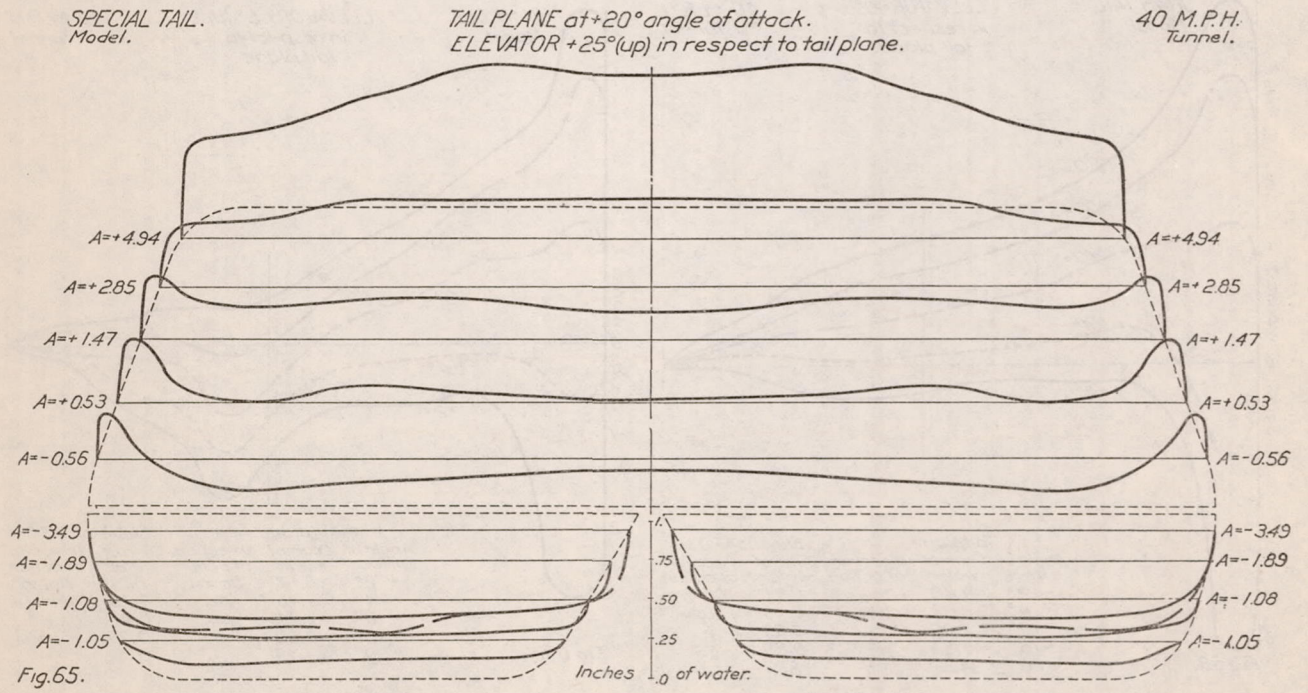
SPECIAL TAIL.
Model.
TAIL PLANE at +20° angle of attack.
ELEVATOR +25° (up) in respect to tail plane.
40 M.P.H.
Tunnel.
A=+4.94
A=+2.85
A=+1.47
A=+0.53
A=-0.56
A=-3.49
A=-1.89
A=-1.08
A=-1.05
1.
.75
.50
.25
.0
Inches of water.

Fig. 65.

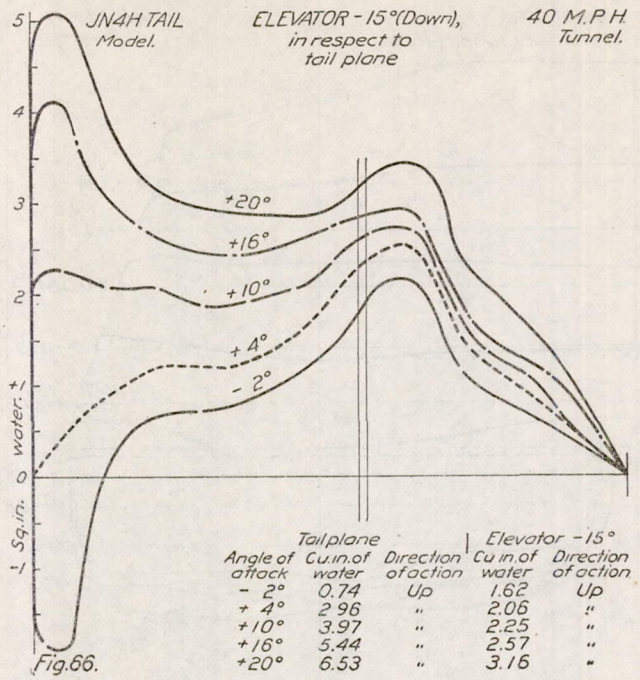

Fig.66.

Angle of attack	Tailplane Cu.in.of water	Direction of action	Elevator -15° Cu.in.of water	Direction of action
- 2°	0.74	Up	1.62	Up
+ 4°	2.96	"	2.06	"
+10°	3.97	"	2.25	"
+16°	5.44	"	2.57	"
+20°	6.53	"	3.16	"

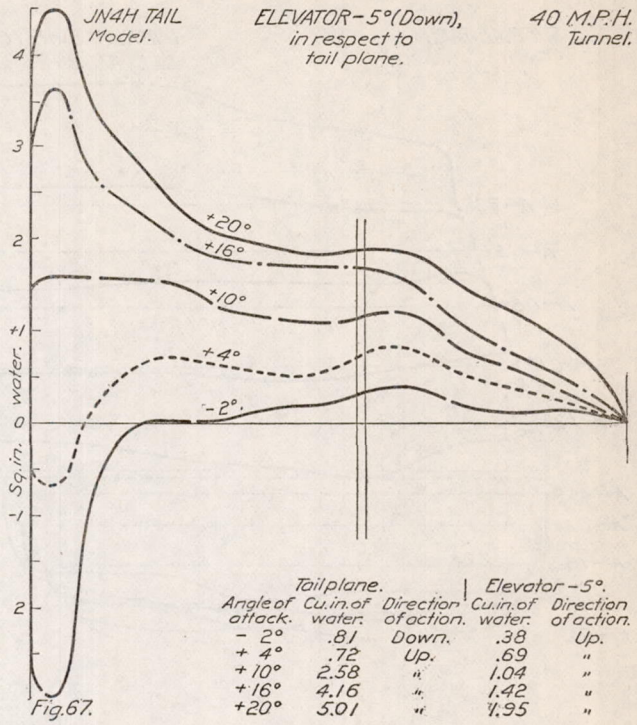

Fig.67.

Angle of attack.	Tailplane. Cu.in.of water.	Direction of action.	Elevator -5°. Cu.in.of water.	Direction of action.
- 2°	.81	Down.	.38	Up.
+ 4°	.72	Up.	.69	"
+10°	2.58	"	1.04	"
+16°	4.16	"	1.42	"
+20°	5.01	"	1.95	"

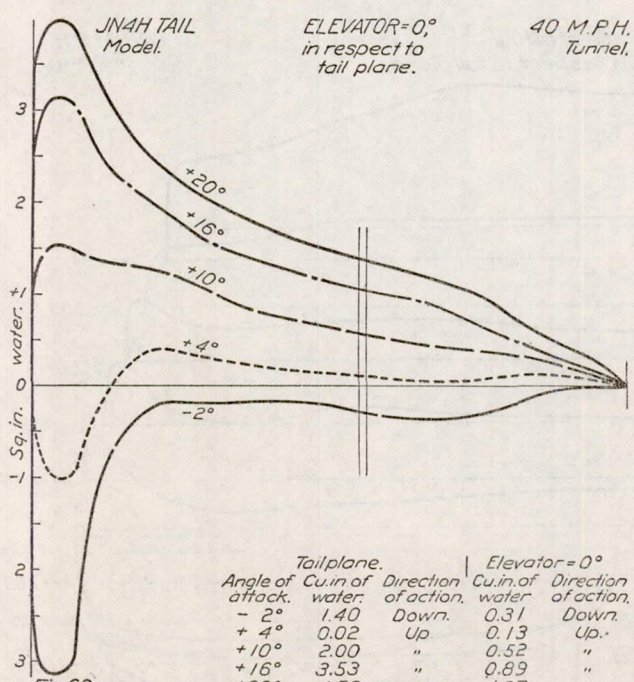

Fig.68.

Angle of attack.	Tailplane. Cu.in.of water.	Direction of action.	Elevator=0° Cu.in.of water	Direction of action.
- 2°	1.40	Down.	0.31	Down.
+ 4°	0.02	Up.	0.13	Up.
+10°	2.00	"	0.52	"
+16°	3.53	"	0.89	"
+20°	4.50	"	1.27	"

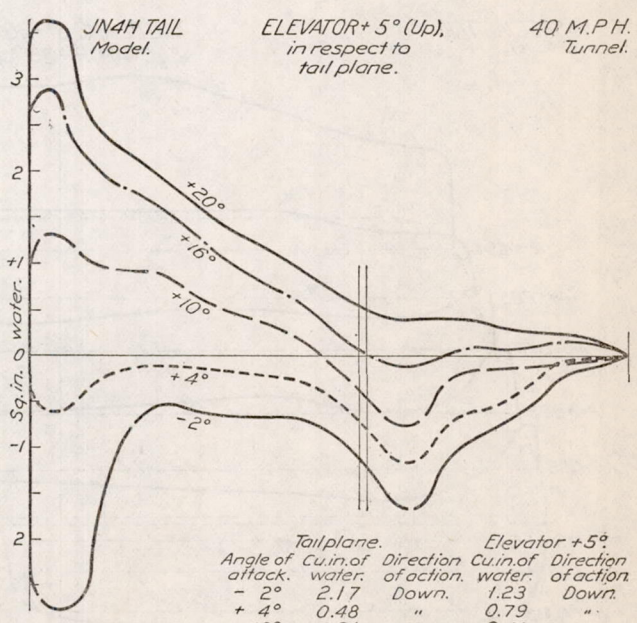

Fig.69.

Angle of attack.	Tailplane. Cu.in.of water.	Direction of action.	Elevator +5° Cu.in.of water.	Direction of action.
- 2°	2.17	Down.	1.23	Down.
+ 4°	0.48	"	0.79	"
+10°	1.21	Up.	0.41	"
+16°	2.62	"	0.09	Up.
+20°	3.49	"	0.50	"

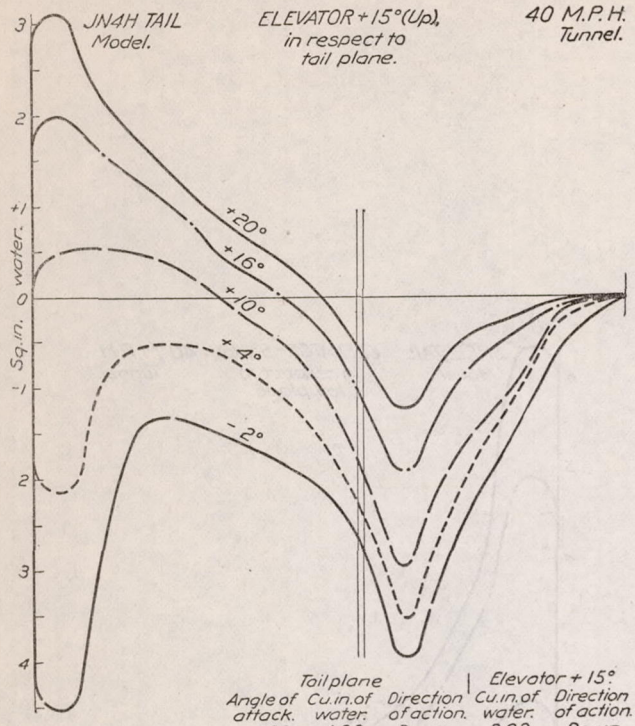

Angle of attack.	Tailplane Cu.in.of water.	Direction of action.	Elevator + 15° Cu.in.of water.	Direction of action.
− 2°	4.29	Down.	2.93	Down.
+ 4°	2.16	"	2.37	"
+10°	0.13	"	1.95	"
+16°	1.41	Up.	1.13	"
+20°	2.38	"	0.67	"

Fig. 70.

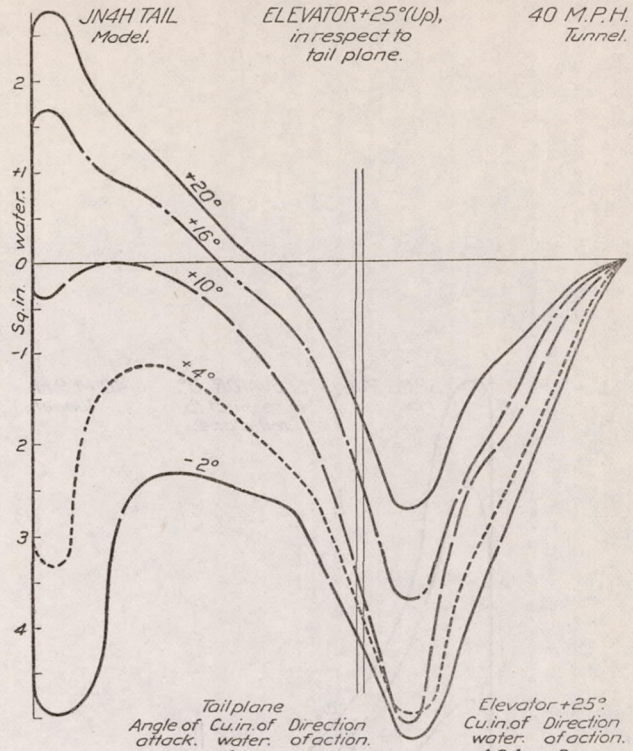

Angle of attack.	Tailplane Cu.in.of water.	Direction of action.	Elevator + 25° Cu.in.of water.	Direction of action.
− 2°	6.12	Down	4.64	Down
+ 4°	3.87	"	4.20	"
+10°	1.55	"	3.61	"
+16°	0.23	Up	2.81	"
+20°	1.00	"	1.99	"

Fig. 71.

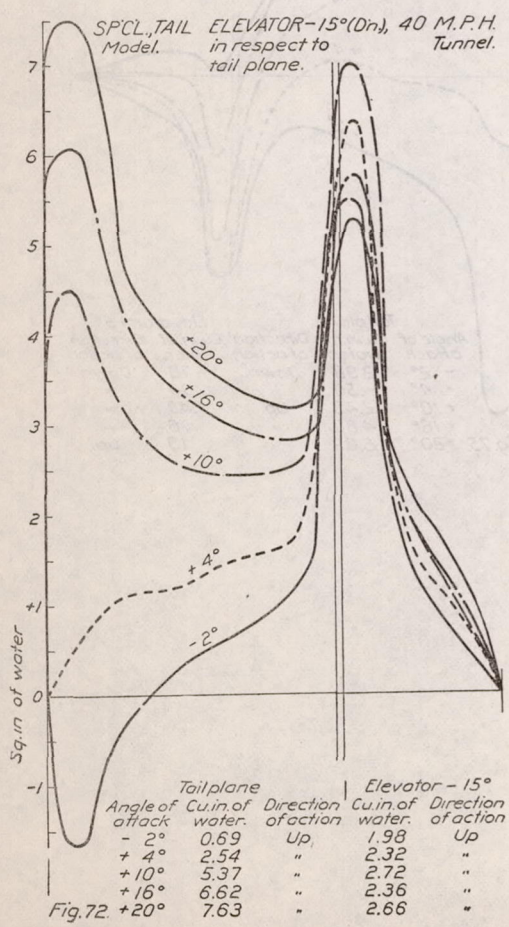

Angle of attack	Tailplane Cu.in.of water.	Direction of action	Elevator − 15° Cu.in.of water.	Direction of action
− 2°	0.69	Up	1.98	Up
+ 4°	2.54	"	2.32	"
+10°	5.37	"	2.72	"
+16°	6.62	"	2.36	"
+20°	7.63	"	2.66	"

Fig. 72.

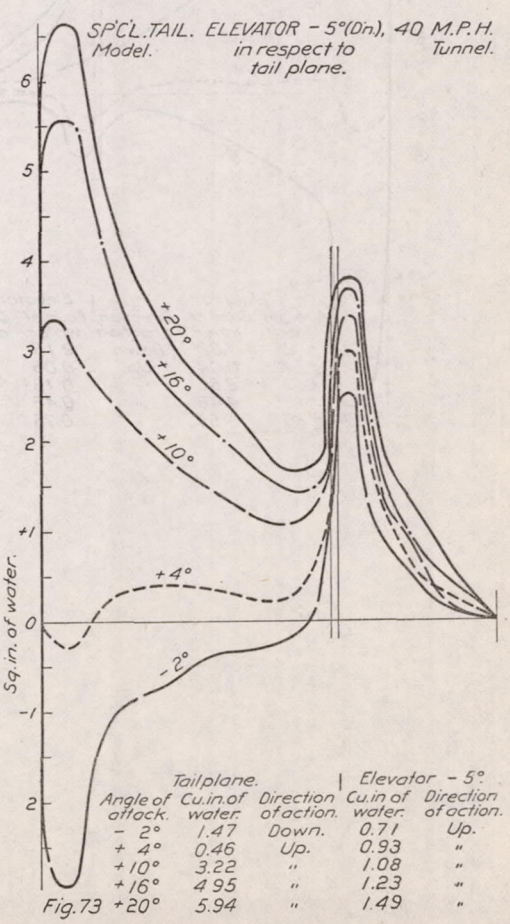

Angle of attack.	Tailplane. Cu.in.of water.	Direction of action.	Elevator − 5° Cu.in.of water.	Direction of action.
− 2°	1.47	Down.	0.71	Up.
+ 4°	0.46	Up.	0.93	"
+10°	3.22	"	1.08	"
+16°	4.95	"	1.23	"
+20°	5.94	"	1.49	"

Fig. 73.

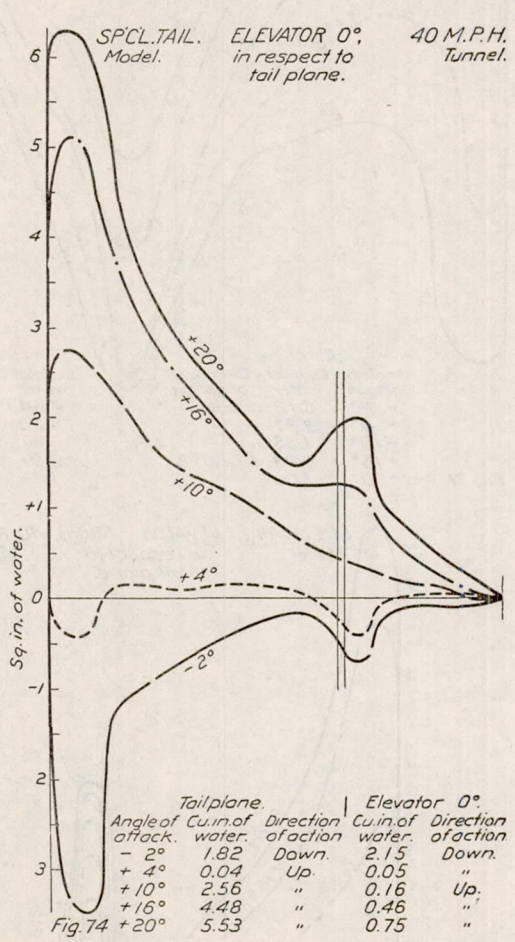

Angle of attack.	Tailplane. Cu.in.of water.	Direction of action	Elevator 0°. Cu.in.of water.	Direction of action
− 2°	1.82	Down.	2.15	Down.
+ 4°	0.04	Up.	0.05	"
+10°	2.56	"	0.16	Up.
+16°	4.48	"	0.46	"
+20°	5.53	"	0.75	"

Fig. 74

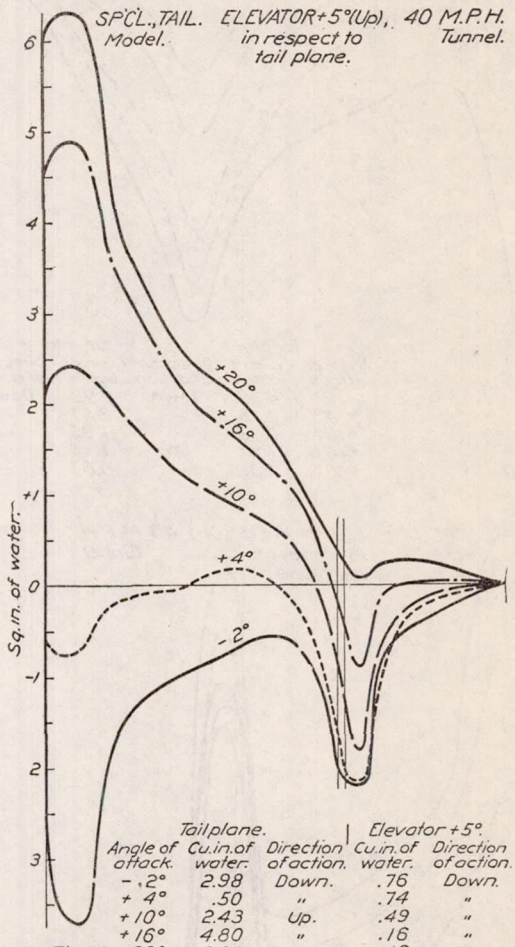

Angle of attack.	Tailplane. Cu.in.of water.	Direction of action.	Elevator +5°. Cu.in.of water.	Direction of action.
− 2°	2.98	Down.	.76	Down.
+ 4°	.50	"	.74	"
+10°	2.43	Up.	.49	"
+16°	4.80	"	.16	"
+20°	6.09	"	.19	Up.

Fig. 75.

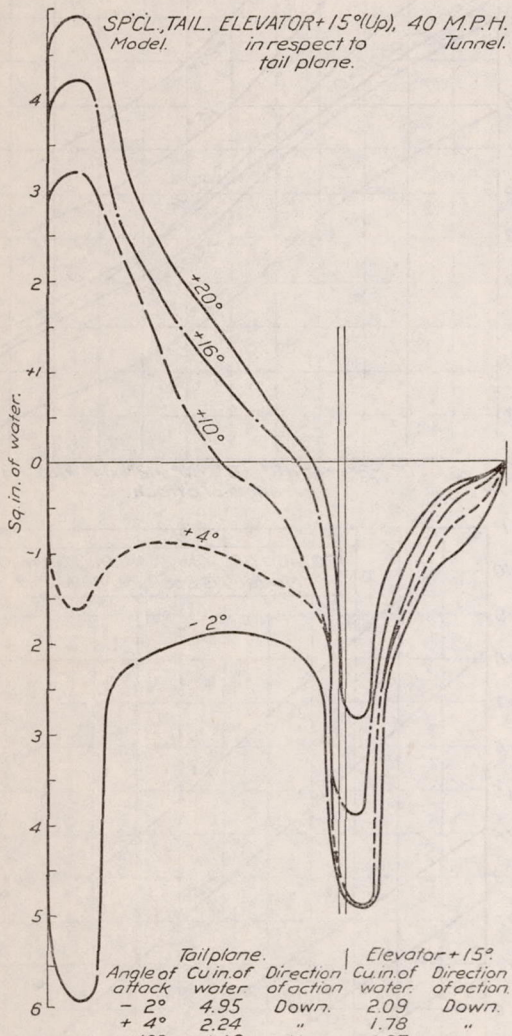

Angle of attack	Tailplane. Cu. in. of water	Direction of action	Elevator +15°. Cu. in. of water.	Direction of action.
− 2°	4.95	Down.	2.09	Down.
+ 4°	2.24	"	1.78	"
+ 10°	1.16	Up.	1.67	"
+ 16°	2.52	"	1.27	"
+ 20°	3.71	"	.93	"

Fig. 76.

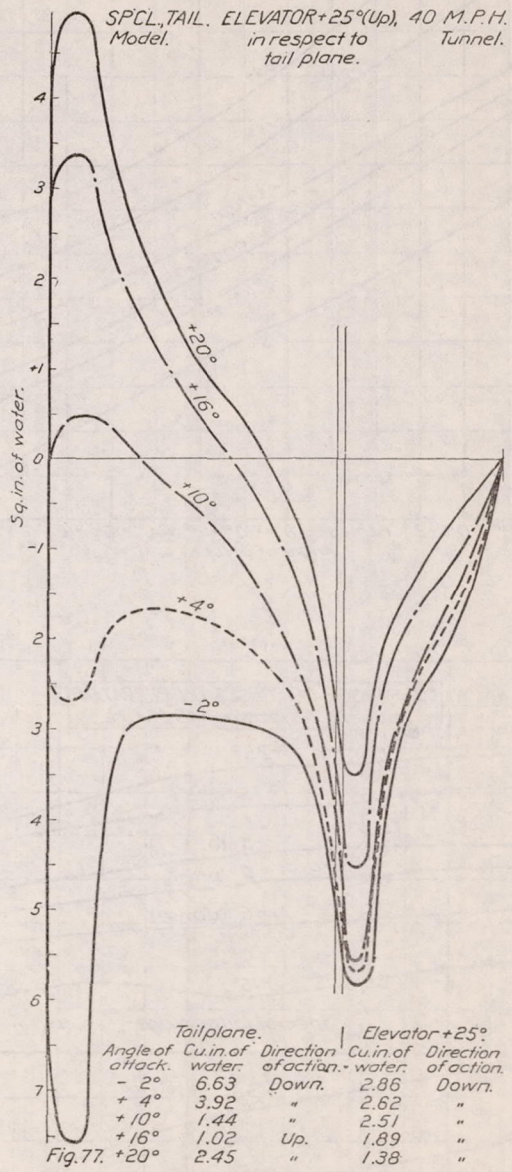

Angle of attack.	Tailplane. Cu. in. of water.	Direction of action.	Elevator +25°. Cu. in. of water.	Direction of action.
− 2°	6.63	Down.	2.86	Down.
+ 4°	3.92	"	2.62	"
+ 10°	1.44	"	2.51	"
+ 16°	1.02	Up.	1.89	"
+ 20°	2.45	"	1.38	"

Fig. 77.

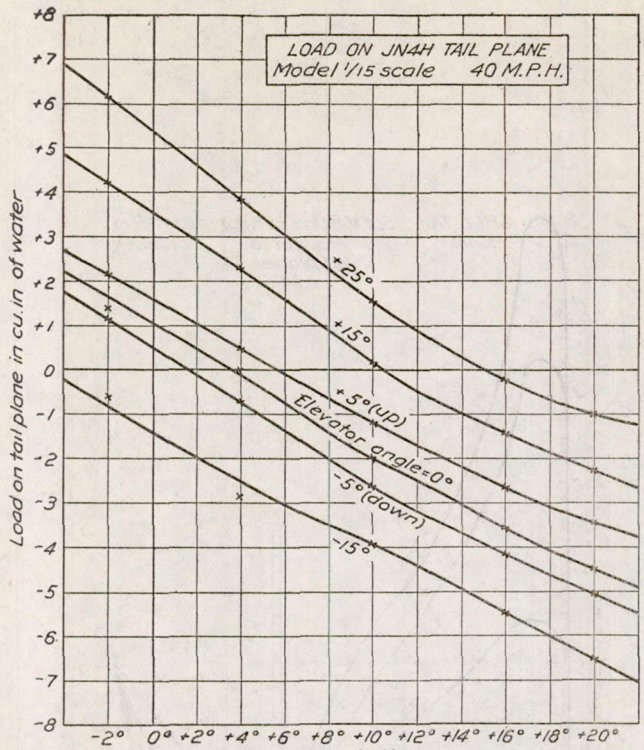

Fig 78

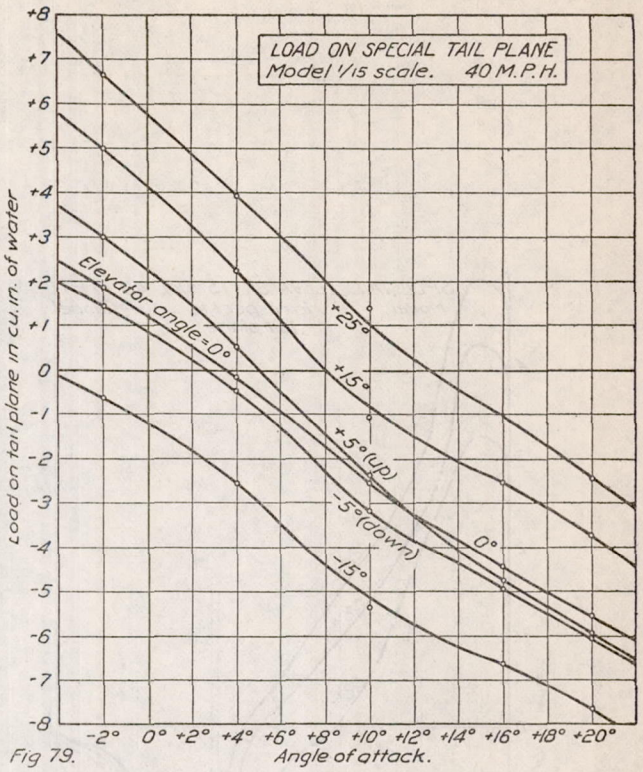

Fig 79.

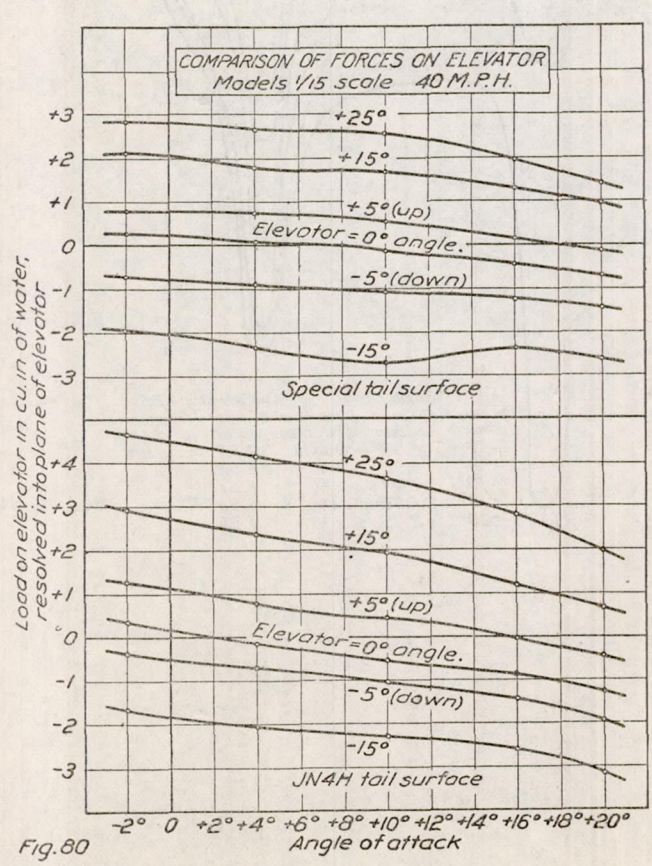

Fig.80

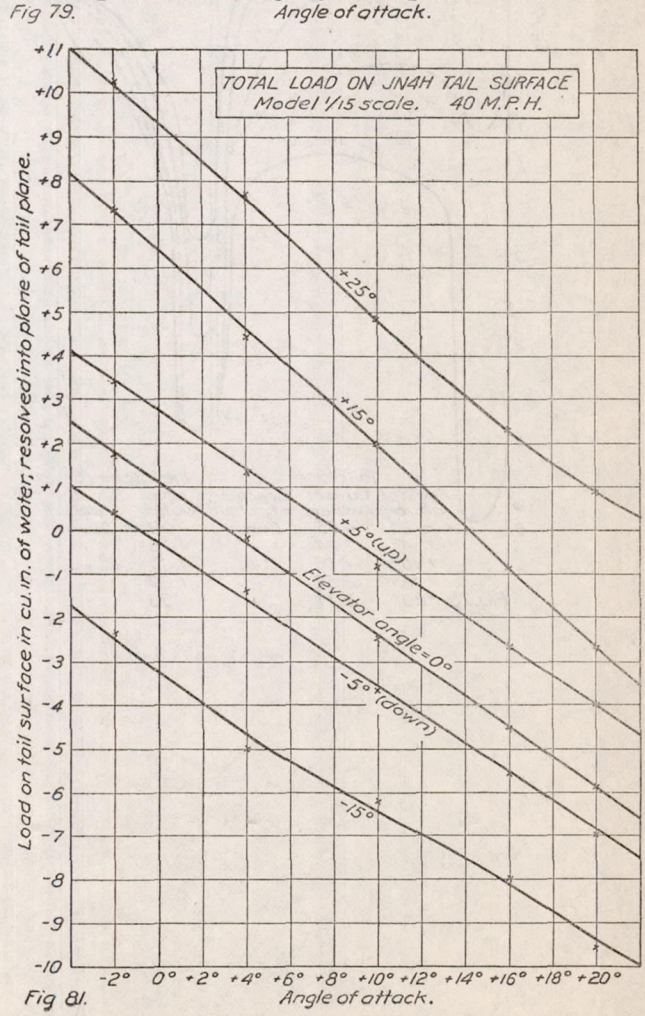

Fig 81.

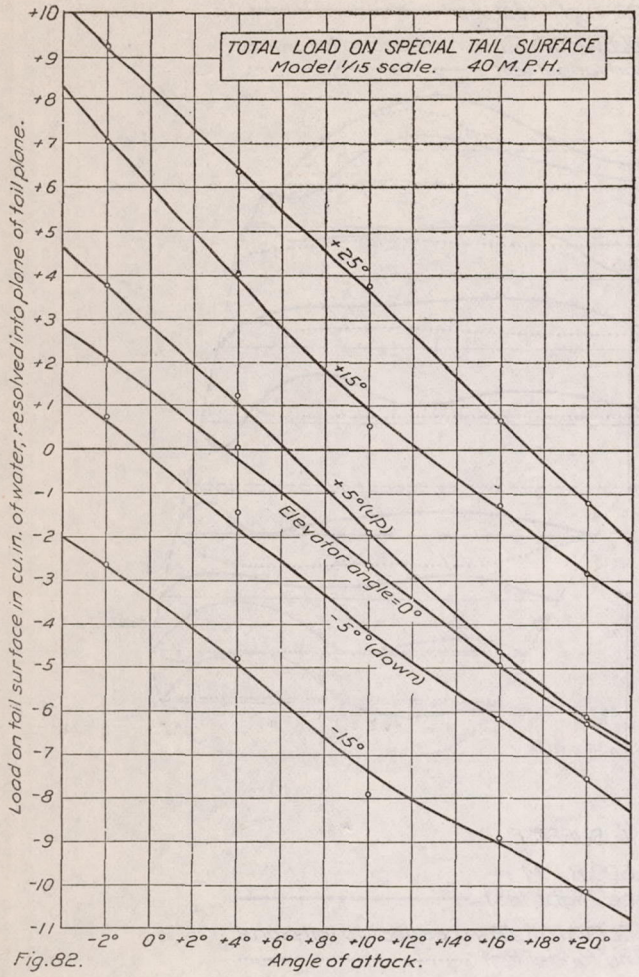

Fig. 82.

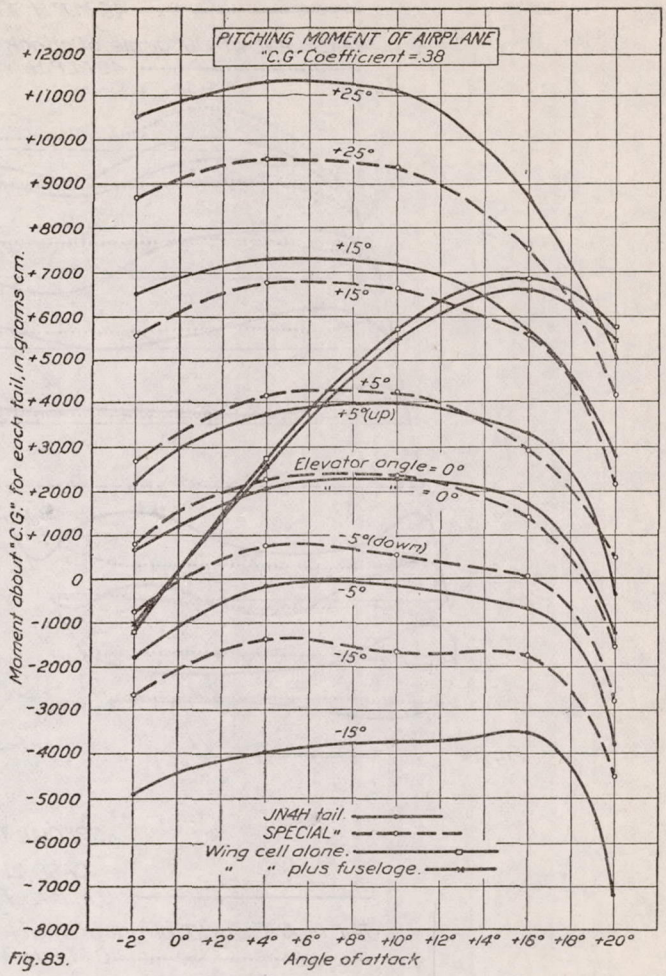

Fig. 83.

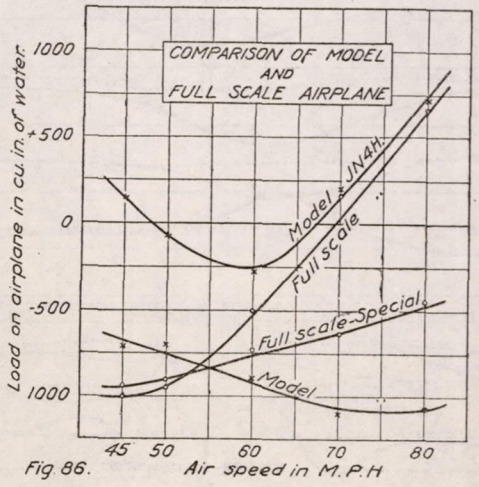

Fig. 86.

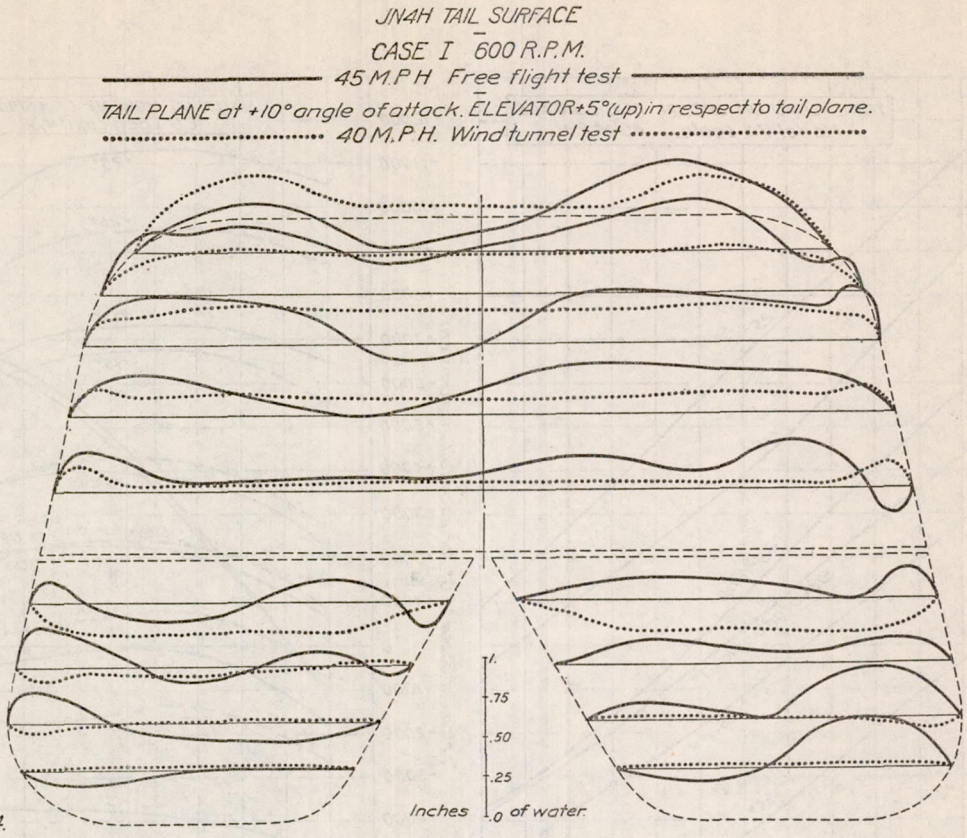
JN4H TAIL SURFACE
CASE I 600 R.P.M.
45 M.P.H Free flight test
TAIL PLANE at +10° angle of attack. ELEVATOR +5° (up) in respect to tail plane.
40 M.P.H. Wind tunnel test
1.
.75
.50
.25
.0
Inches of water.

Fig.84.

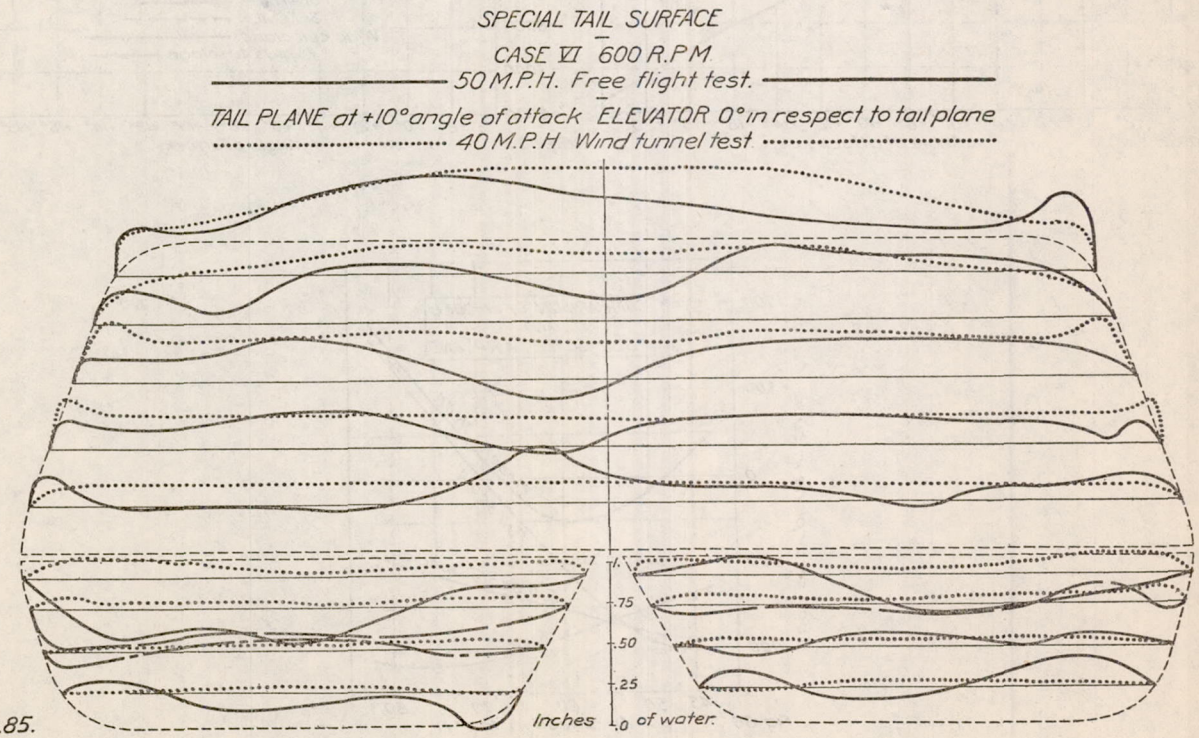
SPECIAL TAIL SURFACE
CASE VI 600 R.P.M.
50 M.P.H. Free flight test.
TAIL PLANE at +10° angle of attack ELEVATOR 0° in respect to tail plane
40 M.P.H Wind tunnel test
1.
.75
.50
.25
.0
Inches of water.

Fig.85.